Design and Development of a Fixture to Study Biaxial Behavior of Materials in Tension

A Thesis Submitted
In partial fulfilment for the award of the degree Of

Masters of Technology
In Mechanical Engineering with specialization in
Computational Design

Submitted By
Rakesh Singla
(2K14/CDN/14)

Under the guidance of
Mr. Vijay Gautam
(Assistant Professor)
DELHI TECHNOLOGICAL UNIVERSITY

Department of Mechanical Engineering
DELHI TECHNOLOGICAL UNIVERSITY
BAWANA ROAD, DELHI-110042
JULY 2016

DELHI TECHNOLOGICAL UNIVERSITY

(Formerly Delhi College of Engineering)

Shahbad Daulatpur, Bawana Road,

Delhi-110042

STUDENT'S DECLARATION

I, **Rakesh Singla,** hereby certify that the work which is being presented in this thesis entitled **"Design and Development of a Fixture to study the Biaxial Behavior of materials under Tensile Forces"** is submitted in the partial fulfillment of the requirement for degree of **Master of Technology (Computational Design)** in Department of Mechanical Engineering at **Delhi Technological University** is an authentic record of my own work carried out under the supervision of Assistant Professor **Vijay Gautam.** The matter presented in this thesis has not been submitted in any other University/Institute for the award of Master of Technology Degree. Also, it has not been directly copied from any source without giving its proper reference.

Signature of Student

This is to certify that the above statement made by the candidate is correct to the best of my knowledge.

Signature of Supervisor

The Master of Technology Viva-Voce examination of Mr. **Rakesh Singla** has been held on ……. and accepted.

Signature of Supervisor **Signature of HOD**

Signature of External Examiner

DELHI TECHNOLOGICAL UNIVERSITY

(Formerly Delhi College of Engineering)

Shahbad Daulatpur, Bawana Road,

Delhi-110042

CERTIFICATE

This is to certify that this thesis report entitled, **"Design and Development of a Fixture to study the Biaxial Behavior of materials under Tensile Forces"** being submitted by **Rakesh Singla (Roll No. 2K14/CDN/14)** at Delhi Technological University, Delhi for the award of the Degree of Master of Technology as per academic curriculum. It is a record of bonafide research work carried out by the student under my supervision and guidance, towards partial fulfillment of the requirement for the award of Master of Technology degree in Computational Design. The work is original as it has not been submitted earlier in part or full for any purpose before.

Vijay Gautam

Assistant Professor

Mechanical Engineering Department

Delhi Technological University

Delhi-110042

ACKNOWLEDGEMENT

First and foremost, praises and thanks to the God, the Almighty, for His showers of blessings throughout my research work to complete the research successfully.

I would like to extend my gratitude to **Prof. R. S. Mishra, Head,** Department of Mechanical Engineering, Delhi Technological University, for providing this opportunity to carry out the present thesis work.

The constant guidance and encouragement received from **Dr. A. K. Agrawal**, M.Tech. Coordinator and Associate Professor**,** Department of Mechanical Engineering, Delhi Technological University, has been of great help in carrying out the present work and is acknowledge with reverential thanks.

I would like to express my deep and sincere gratitude to my research supervisor, **Mr. Vijay Gautam,** Assistant Professor, Department of Mechanical Engineering, Delhi Technological University, for giving me the opportunity to do research and providing invaluable guidance throughout this research. His dynamism, vision, sincerity and motivation have deeply inspired me. He has taught me the methodology to carry out the research and to present the research works as clearly as possible. It was a great privilege and honor to work and study under his guidance. I am extremely grateful for what he has offered me. Without the wise advice and able guidance, it would have been impossible to complete the thesis in this manner.

I am extremely grateful to my parents and family for their love, prayers, caring and sacrifices for educating and preparing me for my future.

RAKESH SINGLA

M.Tech. (COMPUTATIONAL DESIGN)

ABSTRACT

Numerous components during forming operations or in general use, like pressure vessels, structures and sheet metal parts may undergo biaxial state of stress and the tensile properties obtained from the uniaxial tests do not exhibit the true plastic behavior of sheet materials. So, it is important to predict this biaxial behavior of engineering materials before used in actual applications but Biaxial or Multiaxial experimental data is quite limited. Consequently, strength and applications of materials needs extensive testing and necessitates the development of reliable testing methods.

The present work deals with the design of a light weight fixture which is used to characterize the material in biaxial tension. This fixture has been designed for a 50kN universal testing machine. The fixture is an innovative design with optimum size and its weight is optimized by employing high strength steels. Due consideration has been given to factor of safety to avoid the fixture from being fatigued. The fixture distributes equal stress in both directions; however, the ratio of stress in the direction cannot be changed. Only equal stress in each direction can be carried out.

Simulations have been carried out on Ansys® Workbench 15.0 and Abaqus® software environments. The computational results obtained are used to evaluate the performance of the fixture and to analyze stress and strain distributions on cruciform shaped specimen for better understanding of the effects of miniaturization. The simulation work is validated by conducting the uniaxial testing on UTM. Then validated material model is used for biaxial testing simulation of the cruciform specimen.

TABLE OF CONTENTS

LIST OF FIGURES

Chapter 5 RESULTS AND DISCUSSION

LIST OF TABLES

Chapter 1

Introduction

Metals, and in particularly sheet metals are used in a wide range of applications in industry, where main fields of application are packaging (food containers, beverage cans), automotive and aerospace industry. As material costs are a significant part of the costs of manufactured products and most of the products are produced in large numbers, large cost reductions can be achieved by lowering the amount of material used. To lower the material consumption we need to develop the new composite materials which have the less density with higher or at least equal strength.

So now a days there is increase in the popularity of composites materials and AHSS (e.g. dual phase, TRIP) in automotive industry [8-10]. With this recent increase in the popularity of these materials new challenges have arisen. Multi axial loading of these materials, particularly composites, has been quite poorly understood due to anisotropy present in materials. The strength when put under biaxial conditions depends upon the alignment of fibers of the specimen under load. Depending upon the orientation, the biaxial strength can exceed the expected simple uniaxial compressive and tensile tests and it also may be very low.

The ability to accurately capture these effects in continuum models is important for the sheet metal forming industry, in order to carry out these processes as efficient as possible. However, improvements of the numerical tools highly depend on the development of accurate and practical experimental techniques. A testing device for biaxial deformation of sheet metal is such an experimental tool that has been studied by many researchers before. Although several experimental set-ups have been proposed in the literature, most of these designs are not capable of providing information up to the point of fracture.

So my project aims to design a biaxial fixture which can give the results of stress and strain of any material used as specimen under equibiaxial tensile loading conditions.

A definition of anisotropy and biaxial stress is giving, followed by definitions for the working plane, geometrical constraining and properties to measure. Brief description about the terms fixture, biaxial loading, formability, strain paths etc. are also described further:

Anisotropy

Anisotropy is the variation in properties with respect to directions, due to variations in microstructures introduced in forming operations such as rolling. In rolling, the grains are elongated along the rolling direction. As a result, tensile properties differ along different directions.

Definition of Anisotropy Coefficient

Due to their crystallographic structure and the characteristics of the rolling process, sheet metals generally exhibit a significant anisotropy of mechanical properties [1]. The variation of their plastic behavior with direction is assessed by a quantity called Lankford parameter or anisotropy coefficient (**r**). This coefficient is determined by uniaxial tensile tests on sheet specimens in the form of a strip. The anisotropy coefficient (r) is defined by

$$r = \frac{\varepsilon_2}{\varepsilon_3} \tag{1.1}$$

Where ε_2; ε_3 are the strains in the width and thickness directions, respectively.

Eq. 1.1 can be written in the form

$$r = \frac{\ln\frac{b}{b_0}}{\ln\frac{t}{t_0}} \tag{1.2}$$

Where b_o and b are the initial and final width, while t_o and t are the initial and final thickness of the specimen, respectively. As the thickness of the specimen is very small compared to its width (usually by at least one order), the relative errors of measurement of the two strains will be quite different. Therefore the above relationships are replaced by one implying quantities having the same order of magnitude: length and width of the specimen. Taking into account the condition of volume constancy

$$\varepsilon_1 + \varepsilon_2 + \varepsilon_3 = 0$$

the following form of Eq. 1.1 is obtained

$$r = -\frac{\varepsilon_2}{\varepsilon_1 + \varepsilon_2}$$

and Eq. 1.2 becomes

$$r = \frac{-\ln\frac{b}{b_0}}{\ln\frac{l}{l_0} + \ln\frac{b}{b_0}}$$

Where l_0 and l are the initial and final gage length.
Above Eq. can be rearranged as follows:

$$r = \frac{\ln\frac{b}{b_0}}{\ln\frac{l_0 . b_0}{l . b}}$$

This relationship is used in practice for evaluating the anisotropy coefficient [1].

By convention the r-values usually are determined at 20% elongation for the purpose of comparison. Modern tensile testing machines perform instantaneous measurement of the quantities required for evaluating the anisotropy coefficient and calculate it during the test. Values of r at 20% elongation as well as its variation with strain can be determined.

Experiments show that r depends on the in-plane direction. If the tensile specimen is cut having its longitudinal axis parallel to the rolling direction, the coefficient r90 is obtained. The subscript specifies the angle between the axis of the specimen and the rolling direction. The average of the r-values obtained for different directions in the plane of the sheet metal represents the so-called coefficient of normal anisotropy r_n. Having determined the values of r at specimens cut along

three directions in the plane of the sheet metal (0°, 45°, 90°, respectively), the coefficient of normal anisotropy is obtained from the equation

$$r_n = \frac{r_0 + 2.r_{45} + r_{90}}{4}$$

A measure of the variation of normal anisotropy with the angle to the rolling direction is given by the quantity

$$\Delta r = \frac{r_0 + r_{90} - 2.r_{45}}{4}$$

Known as planar anisotropy.

The normal anisotropy represents the average of anisotropy variation in all directions. The planar anisotropy gives the variation of anisotropy with direction.

The average normal anisotropy value depends on the material structure, grain size, etc. Typically, for HCP materials values are high. Similarly, finer the grains lower is the value of average anisotropy.

MATERIAL	R VALUE
MATERIAL HOT ROLLED STEEL	0.8 to 1.0
STAINLESS STEELS	0.9 to 1.2
ALUMINIUM ALLOYS	0.6 to 0.8
COPPER	0.6 to 0.9

Table 1.1: Material s and their anisotropic values coefficient [1]

Formability of sheet metal in deep drawing can be said to be improved with increase in ductility. However, an increase in planar anisotropy is known to have a negative effect in deep drawing. Higher values of this anisotropy will introduce earing, a variation of the cup height around its wall circumference. In stretch forming the anisotropy parameter seems to

be less significant. In deep drawing, the strain hardening exponent, n seems to be less significant.

Biaxial loading

In the biaxial stress state, forces are working in two directions on an infinitesimal small volume, the third direction is the out of plane direction that is related to the two in plane directions, just like a uniaxial stress state as shown in figure 1.1 on the left. The stresses working on the volume under biaxial stress can be visualized, as shown in figure 1.1 on the right: forces are acting on the four areas perpendicular on the plane, from which the stresses can be computed dividing the force by the area it is acting on.

[5] Strains in a biaxial deformation can then be computed via equations 1.3 to 1.5. Often it is more convenient to measure strains, equations 1.6 and 1.7 are given for calculating stresses from known strains. $\sigma_3 = 0$ as there is no force acting on the plane. These equations are only valid in the elastic regime, whereas in the plastic regime pure biaxial loading only takes place up to localization.

$$\varepsilon_1 = \frac{1}{E}(\sigma_1 - \nu\sigma_2) \tag{1.3}$$

$$\varepsilon_2 = \frac{1}{E}(\sigma_2 - \nu\sigma_1) \tag{1.4}$$

$$\varepsilon_3 = -\frac{\nu}{E}(\sigma_1 + \sigma_2) \tag{1.5}$$

$$\sigma_1 = \frac{E}{(1-\nu^2)}(\varepsilon_1 + \nu\varepsilon_2) \tag{1.6}$$

$$\sigma_2 = \frac{E}{(1-\nu^2)}(\varepsilon_2 + \nu\varepsilon_1) \tag{1.7}$$

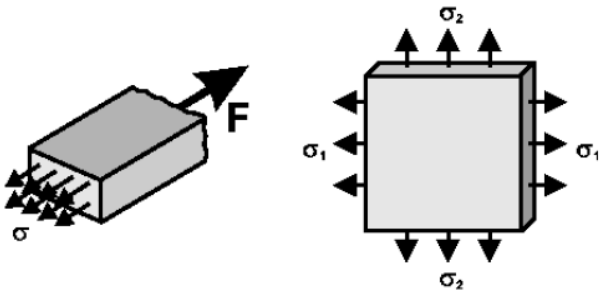

Fig 1.1: Uniaxial and biaxial stress states [33]

A complicating factor in the biaxial case is to determine the area that the forces are acting on, which makes determining stresses σ_1 and σ_2 more difficult than for the uniaxial case. Furthermore, during an actual manufacturing process the biggest problem is determining the plastic response. This cannot be described with a set of equations as given above.

An important observation is that real biaxial loading only occurs up to localization. Due to damage, necking and failure in a material, asymmetry is introduced and the simplified approaches as used in the elasticity regime are not correct anymore. Still the elastic behavior is important, as this is where the final failure mode might be determined.

Formability

This term applicable to sheet metal forming. Formability is the ease with which a sheet metal could be formed into the required shape without undergoing localized necking or thinning or fracture. Sheet metal operations such as deep drawing, cup drawing, bending etc. involve extensive tensile deformation. Therefore, the problems of localized deformation called necking and fracture due to thinning down are common in many sheet forming operations. Anisotropy is a major concern in sheet metal operations. When a sheet metal is subjected to plane strain deformation, the critical strain, namely, the strain at which localized necking or plastic instability occurs can be proved to be equal to 2^n, where n is the strain hardening exponent. For uniaxial tensile loading of a circular rod, the critical or necking strain is given to be equal to n. Therefore, if the values of n are larger, the necking strain is larger, indicating that necking is delayed. In some materials diffuse necking could also happen. Simple uniaxial tensile test is of limited use when we deal with formability of sheet metals. This is due to the biaxial or triaxial nature of stress acting on the sheet metal during forming operations. Therefore, specific formability tests for biaxial testing have been developed, which are appropriate for sheet metals. Loading paths can also be changed by using these new kinds of testing methods.

Forming Limits of Sheet Metal

At the end of the nineteenth century, due to the development of the sheet forming technology, sheet metal formability became a research topic.

Since then, various method for evaluating sheet metal formability have been developed.

Forming limit diagram (FLD)

Forming limit diagram is a very effective way of optimizing sheet metal forming. A grid of circles is sketched on the surface of a sheet metal. Then the sheet metal is subjected to deformation. Usually the sheet is deformed by stretching it over a dome shaped die. Strips of different widths can be taken for the test, in order to induce uniaxial or biaxial stress state. The circles deform into elliptic shapes. The strain along two principal directions could be expressed as the percentage change in length of the major and minor axes. The strains as

measured near necks or fracture are the strains for failure. A plot of the major strain versus minor strain is then made. This plot is called Keeler-Goodwin forming limit diagram.

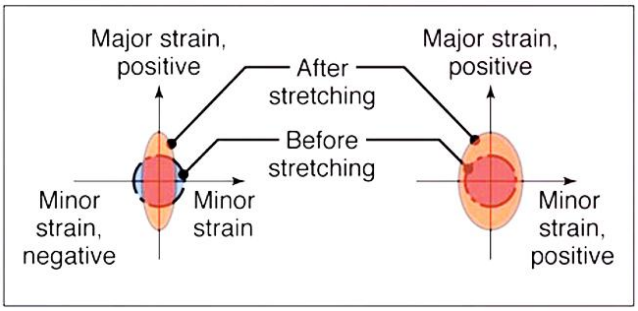

Fig 1.2: Keeler-Goodwin forming limit diagram [3]

This plot gives the limiting strains corresponding to safe deformations. On the other hand, if a circle is drawn on the surface of a spherical balloon and the balloon expanded, the circle becomes a larger circle. This means that both minor and major axes have undergone equal strain. The FLD is generally a plot of the combinations of major and minor strains which lead to fracture. Combination of strains represented above the limiting curves in the Keeler-Goodwin diagram represent failure, while those below the curves represent safe deformations. A typical Keeler-Goodwin diagram is shown below.

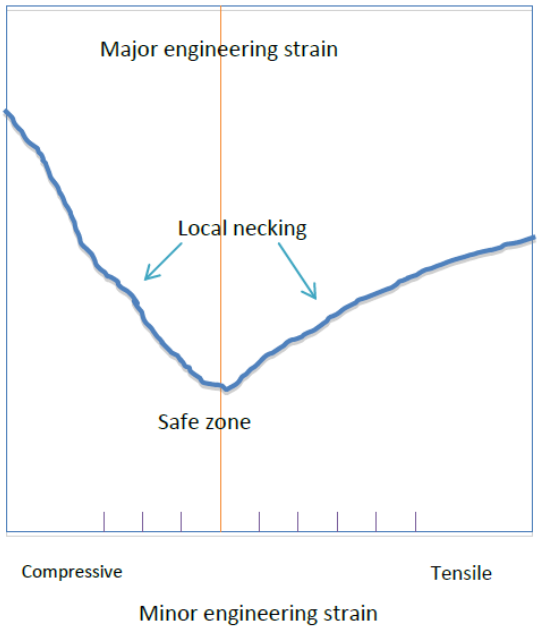

Fig 1.3: Forming limit diagram [3]

The safe zone in which no failure is expected is shown as shaded region. Outside this zone there are different modes of failure represented at different combinations of strains. The

upper part of the safe zone represents necking and fracture. The FLD is based on the assumption that for forming purposes, the maximum deformation is limited by the initiation of unstable deformation, e.g. necking. When forming metal sheets the material is subjected to different strains and strain paths, which have been found to have different maximum allowable deformations.

The maximum values of the principal strains ε_1 and ε_2 can be determined by measuring the strains at fracture on sheet components covered with grids of circles.

Length of major axis of the stretched circle minus diameter of original circle divided by original diameter of circle gives the major strain (engineering strain). Similarly engineering minor strain can be found out. If the minor axis stretches out it represents positive strain. If it shrinks, it is negative strain. By comparing the deformed circles, with original circled we can also predict if the sheet has undergone thinning or not. A larger ellipse is an indication of thinning. After a number of such tests, the forming limit diagram is drawn, between major strain and minor strain. The boundary between safe and failed regions are represented in the forming limit diagram. Any strain represented on the diagram by a point lying above the curve indicates failure. The strain path can be varied by varying the width of the sheet. Different materials have different forming limit diagrams. The higher the position of the curve greater is the formability.

The curves shift upward if the sheet thickness is increased – indicating increase in forming limit. In this diagram, a few straight lines indicating the strain paths are also shown. The vertical line at the center (zero minor strain) represents plane strain. In biaxial strain, both strains are equal. This is represented by the inclined line on right side of the diagram. Simple uniaxial tension is represented on the left side by a line with slope 2:1. This is due to the fact that Poisson's ratio for plastic deformation is ½. Negative minor strain means there is shrinkage. It is better to have negative minor strain because, the major strain for failure will be higher with negative minor strain. Some of the factors which affect the forming limit of a material are: strain rate sensitivity, anisotropy, thickness of the sheet, strain hardening etc. The forming limit curve will be shifted upwards for a thicker sheet.

Today, depending on the kind of limit strains that is measured different types of FLSD's are determined: one for necking and one for fracture, see Fig. 1.4

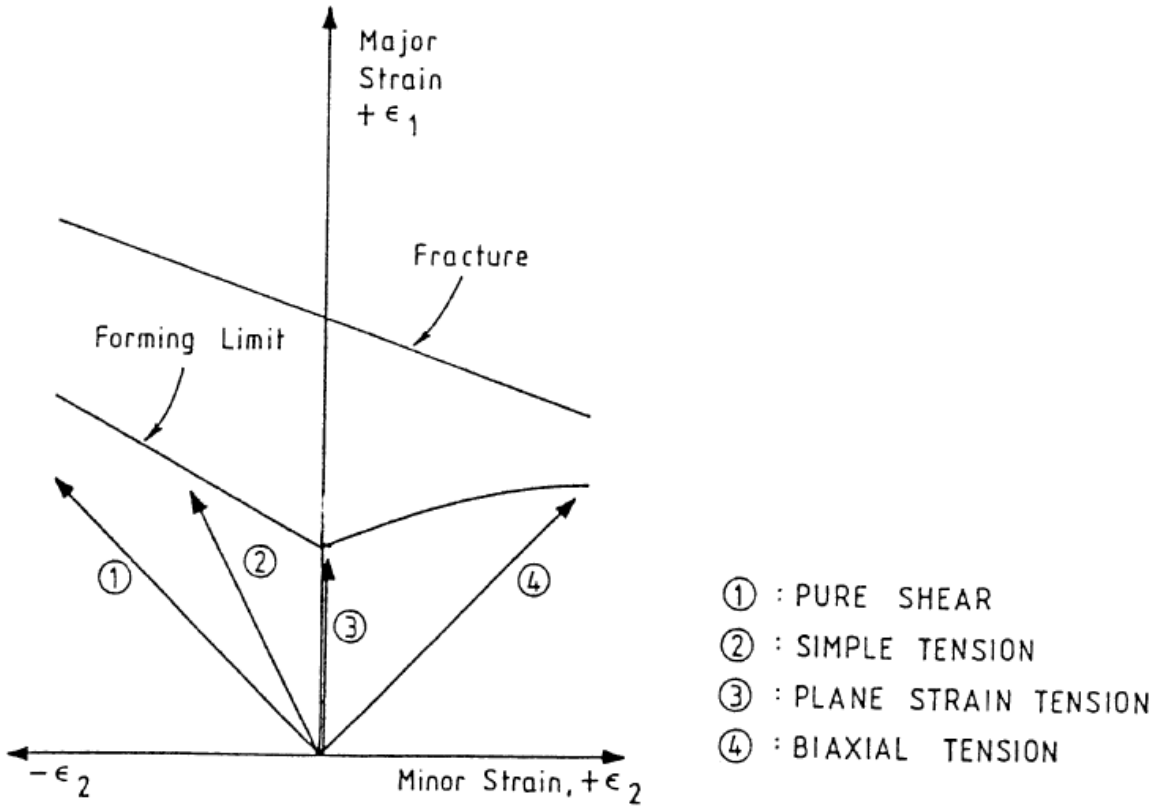

Fig 1.4: Forming limit diagrams for necking and for fracture [5]

On the axes are the strains in the two principle directions in the plane, with the line giving the point of necking for the combination of strains at that point.

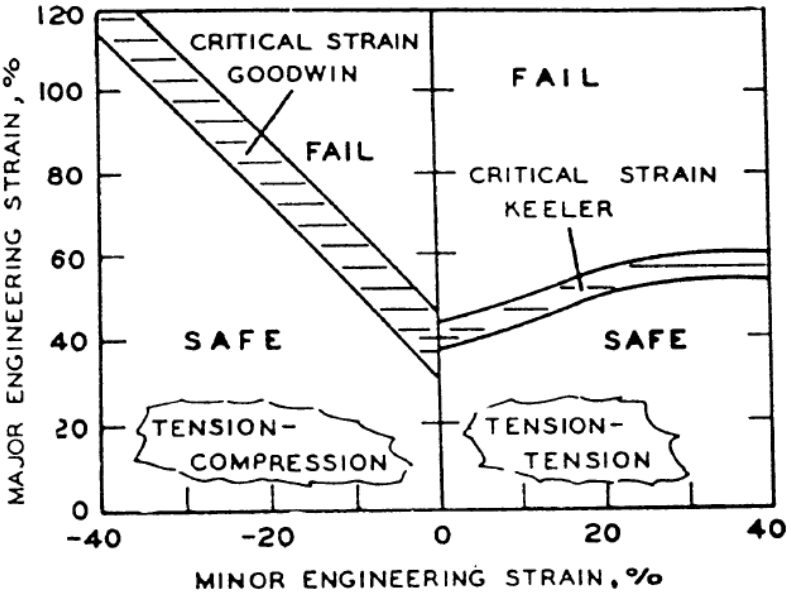

Fig 1.5: Forming limit diagrams [5]

The limits of the FLD are becoming clear when testing a sheet metal under a changing strain path. The figure shows the strain paths up to necking for linear strain paths on an undeformed sheet of metal. The second figure shows where necking starts for a sheet metal that is first deformed under uniaxial tension, and then by biaxial tension. A large increase in formability is found, that was not predicted by the original FLD. When starting with biaxial tension followed by uniaxial tension, a large decrease in formability is found. This effect is stronger for AHSS then for conventional steels, which makes the need for understanding what happens necessary to be able to use the new steels up to full potential. [3, 24] A quite similar concept, but not less sensitive to strain path changes and thus the strain history of the material, is the stress forming limit diagram, as shown in figure 1.3(b). A disadvantage of the stress based forming limit is uncertainty of the computed stresses, which in practice can only be determined from measured or computed strain fields. A FE model could be used to determine these forming stresses, but therefore the used material model should accurately describe the material behavior.

Working plane

Some experimental set-ups test a material in-plane, others out-of-plane, depending mostly on tooling. As out-of-plane testing gives rise to bending, it is preferred to test in-plane. This means stresses and strains are constant over the thickness of the sheet, which makes computing of the stresses and measuring the strains less complicated.

Some studies also show an influence to the forming limit while comparing in-plane and out-of-plane testing. Forming limits up to 6 % higher where found with out-of-plane testing of the same material.

In this project we opted the in-plane loading conditions.

Fixture

Fixtures are strong and rigid mechanical devices which enable easy, quick and consistently accurate locating, supporting and clamping, blanks or specimen and results consistent quality, functional ability and interchange ability.

A fixture can be used in almost any operation that requires a precise relationship in the position of a tool to a work piece.

Need of Biaxial Testing or Motivation

As we know numerous components during forming operations or in general use, like pressure vessels, structures and sheet metal parts may undergo biaxial or multiaxial state of stress. There are many ways to predict the failure of materials under uniaxial loading conditions; however, the tensile properties obtained from the uniaxial tests do not exhibit the true plastic behavior of sheet materials. However multi axial experimental data is quite limited. As a result, strength and applications of materials requires extensive testing and necessitates the development of reliable testing methods.

As there is extensive increase in demand of high strength alloys a number of composite materials are developing day by day so study the failure behavior of composites under multiaxial loading because of their inherently anisotropic structure is also necessary.

With advances in theoretical understanding, numerical capability, it is now possible to create fixtures that can allow us to predict the strength of materials under multiaxial loads. Experimental data however, still causes problem in comparison of theoretical data. Theoretical data is used for homogenized techniques that can be re-evaluated and compared repeatedly, thereby not allowing further study or understanding.

Many believe that the best solution is through long-term effort that can support numerical predictions with experimental data. Among these, carrying out a biaxial stress experiment in σ_1- σ_2 stress plane is the most difficult to conduct.

Objective

The challenges that have grown due to the increased use of composite materials and AHSS in new designs, leads to the goal of this project. This is the development of an experimental methodology to deform a sheet metal specimen under biaxial tension. The need for such a methodology to analyze stress strain relationship under biaxial loading is obvious. The data obtained with such a test method can then be used to predict damage evolution and thus in the future make better FE-modelling possible for designing or redesigning the products.

Such a set-up can then be used in future to study and characterize new materials, as developed by the industry.

Strategy

Working towards a suitable test method, various known methods for testing under biaxial loading are studied. The literature survey in chapter 2 is meant to provide better understanding of the problem and different set-ups.

Design of fixture is discussed in chapter 3. Material selection for the fixture is described then How the fixture will work under loading, types of joints, relative motion of each link with respect to another, kinematics parts are described

The further studying of the most promising set-up is done numerically in chapter 4. The model and the Finite Element Analysis are being discussed in this chapter 4. Different material models, different loading conditions are also described with the help of images.

The results of numerical work are discussed in chapter 5. The numerical and experimental results are compared in order to find limitations and possible future improve ments.

Need of Biaxial Testing or Motivation

As we know numerous components during forming operations or in general use, like pressure vessels, structures and sheet metal parts may undergo biaxial or multiaxial state of stress. There are many ways to predict the failure of materials under uniaxial loading conditions; however, the tensile properties obtained from the uniaxial tests do not exhibit the true plastic behavior of sheet materials. However, multi axial experimental data is quite limited. As a result, strength and applications of materials requires extensive testing and necessitates the development of reliable testing methods.

As there is extensive increase in demand of high strength alloys a number of composite materials are developing day by day so study the failure behavior of composites under multiaxial loading because of their inherently anisotropic structure is also necessary.

With advances in theoretical understanding, numerical capability, it is now possible to create fixtures that can allow us to predict the strength of materials under multiaxial loads. Experimental data however, still causes problem in comparison of theoretical data. Theoretical data is used for homogenized techniques that can be re-evaluated and compared repeatedly, thereby not allowing further study or understanding.

Many believe that the best solution is through long-term effort that can support numerical predictions with experimental data. Among these, carrying out a biaxial stress experiment in σ_1- σ_2 stress plane is the most difficult to conduct.

Objective

The challenges that have grown due to the increased use of composite materials and AHSS in new designs, leads to the goal of this project. This is the development of an experimental methodology to deform a sheet metal specimen under biaxial tension. The need for such a methodology to analyze stress strain relationship under biaxial loading is obvious. The data obtained with such a test method can then be used to predict damage evolution and thus in the future make better FE-modelling possible for designing or redesigning the products.

Such a set-up can then be used in future to study and characterize new materials, as developed by the industry.

Strategy

Working towards a suitable test method, various known methods for testing under biaxial loading are studied. The literature survey in chapter 2 is meant to provide better understanding of the problem and different set-ups.

Design of fixture is discussed in chapter 3. Material selection for the fixture is described then How the fixture will work under loading, types of joints, relative motion of each link with respect to another, kinematics parts are described

The further studying of the most promising set-up is done numerically in chapter 4. The model and the Finite Element Analysis are being discussed in this chapter 4. Different material models, different loading conditions are also described with the help of images.

The results of numerical work are discussed in chapter 5. The numerical and experimental results are compared in order to find limitations and possible future improvements.

Chapter 2

Literature Survey

In the last decades several scientists have studied methods to deform sheet metal under complex strain paths, including punch tests [17,18,19 & 20], bulge pressure tests [11,13,14 & 15], viscous pressure forming (VPF) tests [12], biaxial compression tests [33 & 35] or cruciform tests [37,38,40 & 41].

Many techniques and shapes for specimen have been used to produce these stress conditions. They can be classified into two categories [33]:

(i) Using single loading system

(ii) Using independent loading systems.

In the second category, the two systems are completely independent machines to achieve the purpose. However, these often mean doubling the cost of the machine. The availability of space, flexibility in design and independent calibration of both systems often require great amount of work and capital on the researcher's part.

Independent systems do allow for numerous configurations based on the design and positioning of the loading systems, including angle of force, and magnitude in relation to each other.

The first option is much more acceptable in terms of cost, calibration time, and the time taken, including the limitations of space in the research laboratory, etc.

Currently the most used method for determining FLCs in the industry is by using punch tests, which are known to overestimate the maximum allowable strains [3]. As the exact amount of the overestimation of cannot be exactly determined, an unknown error in the resulting FLD makes a relatively large safety margin (up to 10 %) is applied to the maximum allowable strains when using the material in a forming process. This means more material will be used to make a safe structure or product, leading to higher costs. This chapter will first describe several properties of the biaxial testing set-ups that will be used in the following sections to compare the different set-ups. The set-ups to be discussed are the

punch test, the bulge test, the cruciform tensile test and the Marciniak test, with a study of the workings of each set-up and recent developments.

Bulge Test

The bulge test is a well described experimental set-up for biaxial loading, where pressure is used to deform a specimen. The set-up consists only of a pressure chamber and clamping mechanism. The bulge test is mostly used for testing thin films, as bending stresses can be neglected for that case. The pressure can be build up by a gas, a fluid or even a flowing polymer.

D. W. A. REES (1995) [14] presented a theoretical analysis of plastic flow of metallic thin sheets at the top of elliptical bulge formed through a die by applying normal pressure. The bulge was formed by subjecting the underside of the disc to oil pressure from a controller graduated in increments of 100 psi to a maximum of 3000 psi (gauge pressure).

J liu et al. (2000) [12] evaluated the sheet formability by **VPF (Viscous pressure forming)** dome test. They proposed an approach to determine the formability of thin sheet metal plates in stretching (multi axial strain) using a critical damage value concept in aggregation with FE simulations. In their process they used a highly viscous semi solid medium pumped under high pressure into the cavity. . And concluded that the formability of the sheet stretching with VPF is greater than that of the sheet stretched with a hemispherical solid metal punch. Because In the VPF process, friction effects are very small at the sheet & media interfaces. Consequently, there is no strain localization. So sheet is stretched more uniformly and superior formability is achieved.

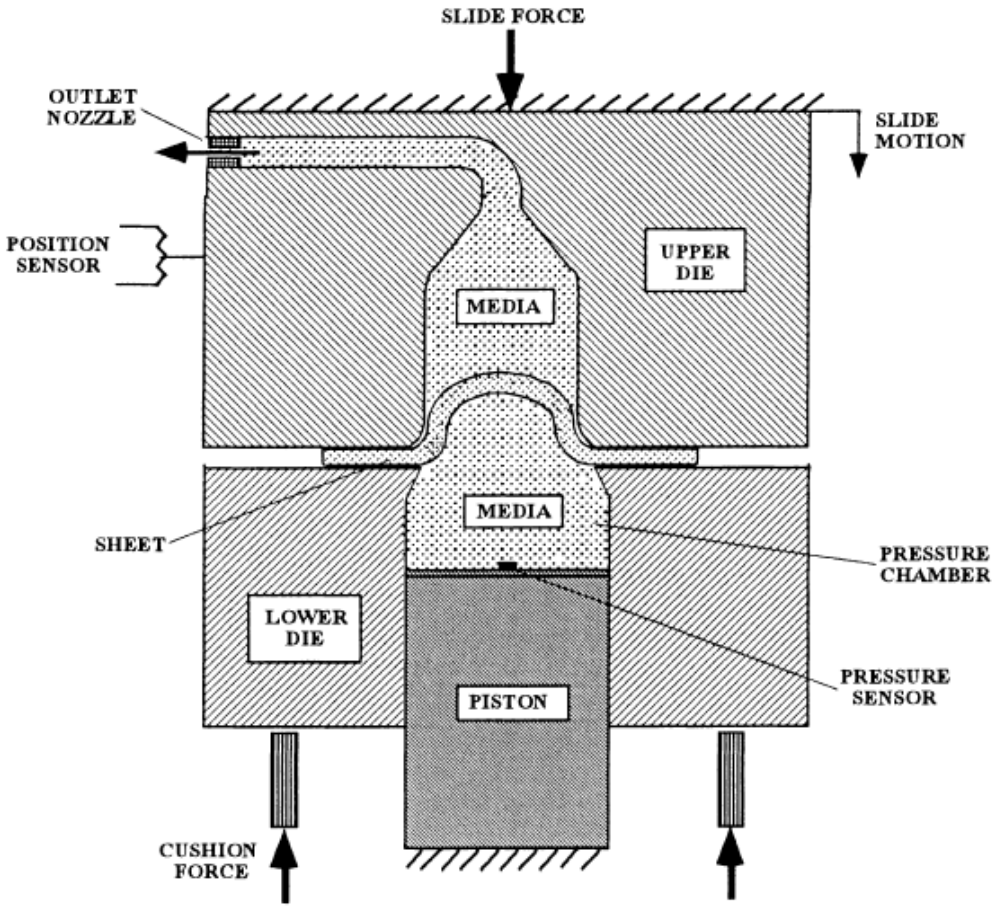

Fig 2.1: Sketch of the VPF dome test tooling.

Gerhard Gutscher et al. (2004) [11] discussed the use of the **viscous pressure bulge (VPB)** test for determination of flow stress under biaxial state of stress.

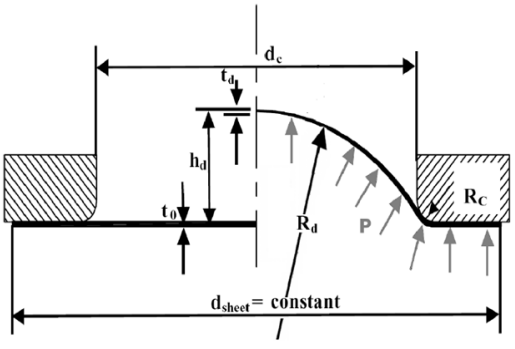

Fig 2.2: Geometry of Bulge Test

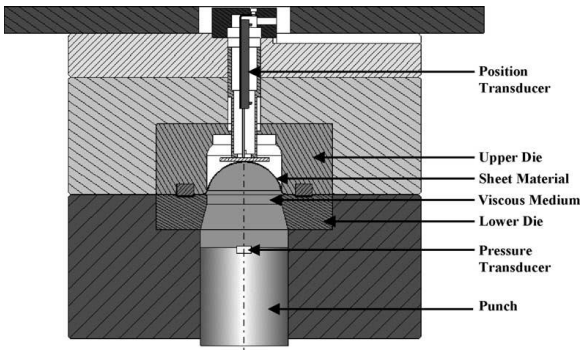

Fig 2.3: Sketch of tooling used in the VPB test.

In figure 2.2, a simple bulge test set-up is shown, with the most important properties visualized being t_0 and t_d, the initial and final thickness of the sheet, d_{sheet} the diameter of the sheet, d_c the diameter of the die cavity, h_d the height of the dome and R_C the radius of the die edge. R_d is the radius of the bulge in a circular set-up. R_d is divided in two values R_1 and R_2 for an elliptic bulge, with the two radii relating to the bulge radius in the principle directions.

The use of viscous material instead of fluid as a pressure medium has made the VPB test simple and easy to evaluate the formability of sheet metals. The use of a viscous material as a pressure medium, however, has a disadvantage. At high deformation velocities, the viscous material is strain rate dependent. Therefore, the pressure readings do not represent purely the hydrostatic pressure but also include the "stiffening" or the pressure increase of viscosity of the viscous material with strain rate. At low deformation speeds, as used here, this effect is negligible.

Josef Kana et al. (2015) [15] proposed a methodology for Measuring Material Mechanical Properties of very thin Metal Foils (up to 0.05 mm of thickness) Using Bulge Test Method. The design of the whole device was all remade, pressure measurement was significantly improved, new control and evaluation software was introduced. First modification they introduced was the use of air as pressurizing medium in place of mostly used oil or water. The second one was use of laser for specimen displacement measurement.

Fig 2.4: Testing Device

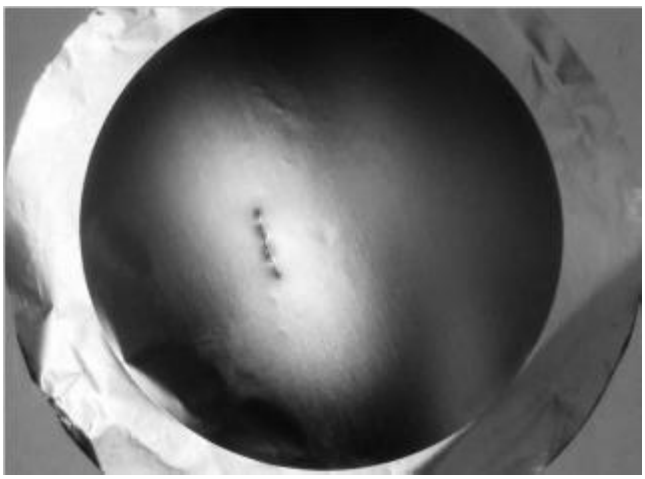

Fig 2.5: Al 0.013 mm.

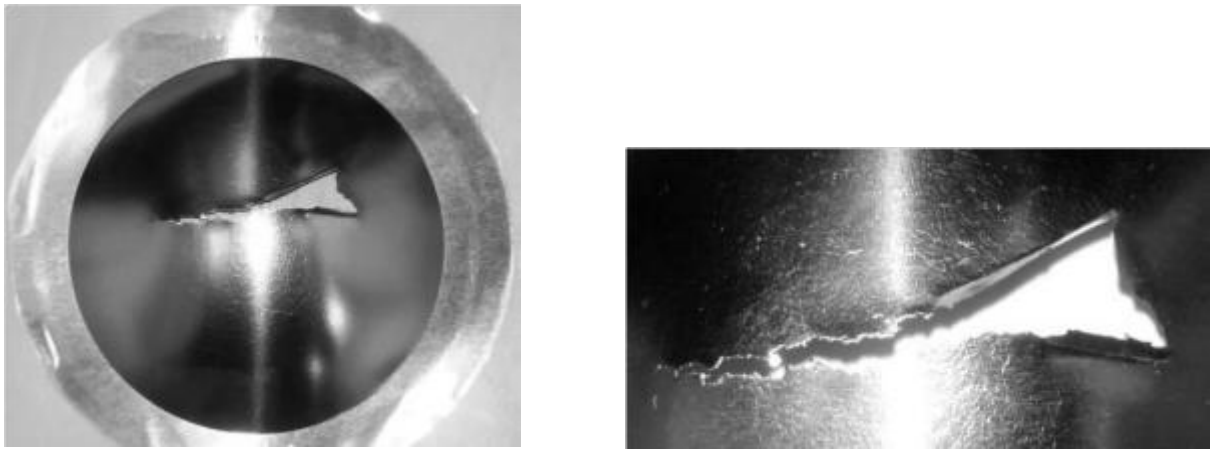

Fig 2.6: Al 0.05 mm, crack detail.

This method was limited by a maximum pressure up to 1 MPa as there were reasons of safety as well as specimens were torn in such a high pressure that they were too damaged to undergo further analysis. This limitation did not have technical or theoretical reasons but only safety and practical ones.

Advantages and Disadvantages of Bulge Test [33]

An advantage of the bulge test is the absence of contact (and therefore friction) in the area of interest, which makes the analytical solution less complex. There are no geometrical constraints due to the tooling or the geometry of the specimen.

Some disadvantages of the bulge test include the large height difference between the deformed and undeformed specimen, making it di-cult to use lens systems for online and in-situ measurements (e.g. imaging correlation analysis). Moreover, only strains in the "1 > 0 and "2 > 0 region can be determined, as the sheet needs to be clamped over the whole outer region to prevent the pressurizing air or fluid from escaping.

The high pressure also leads to uncontrollable neck and crack propagation, because of the force controlled nature of the experiment. Necking and fracture might occur in a split second, with no tools available to measure the phenomenon. The high pressure needed in a miniature set-up might even prove to be a problem to reach in a conventional set-up without the use of a large hydraulic system or polymer as pressure body.

Punch test

Gerard Quaak (2008) [33] A second, somewhat similar approach, is the use of a punch to deform sheet metal under many strain paths, including biaxial tension. Several standardized tests are available (e.g. Keeler, Nakazima and Hasek tests) as described by Banabic [3]. Although all these tests are used to determine the same material properties, there are several differences.

An advantage of the punch test is its ability to undergo various strain paths, all of them up to necking and fracture. Many ideas to achieve different strain paths have been proposed and will be brief discussed. Changing the strain path during a test is practically impossible

Punch Stretching Test

This test was first proposed and used by Keeler himself. It consists of stretching a specimen (2) clamped between a blank-holder (3) and a die (4) using a spherical of elliptical punch, see Fig. 2.7. The strain path is mainly varied by using specimens of different width; is can also be varied by varying the punch radius and the lubricant. Instead of using rectangular specimens Hasek [20] applied specimens with circular recesses.

Keeler Test [17]

This test consists in the use of punches having different radii in order to vary the stress state, see Fig. 2.8. Disadvantages of the test are the large amount of experimental work; only the positive section of the forming limit curve is obtained, and the shape and position of the forming limit is influenced by the punch radii.

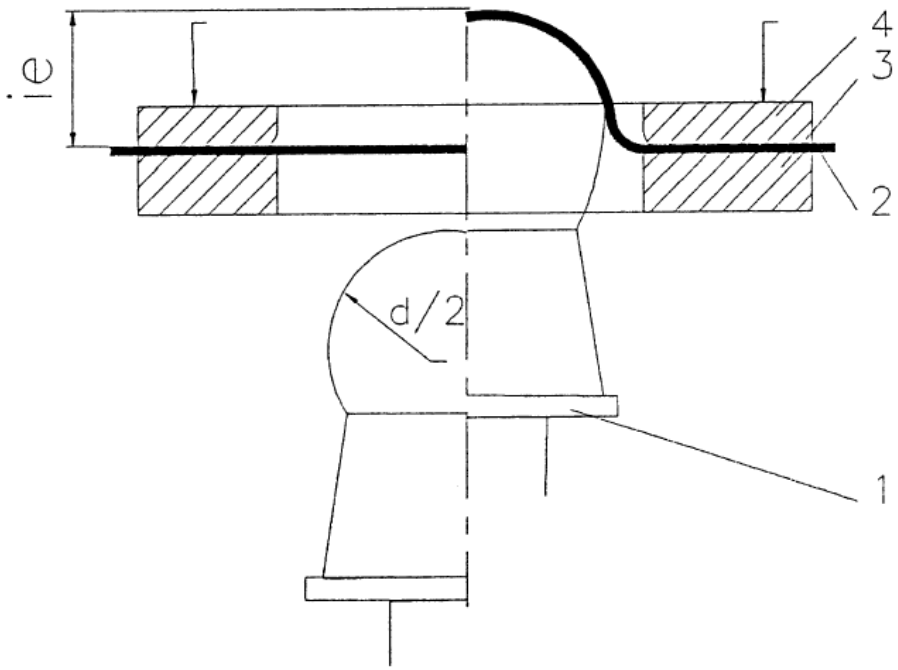

Fig 2.7: Schematic layout of the punch stretching test

The Keeler test uses punches of different radii to vary the strain path of the tested sheet metal specimen, introducing different strain paths due to geometry and friction variations. The specimens are the same for every test, which makes the test easy to prepare. The different punch shapes, as shown in figure 2.3, make the test more time consuming if a larger part of the FLC is to be determined. The test can only determine the positive part of the FLC, $\epsilon 1 > 0$ and $\epsilon 2 > 0$.

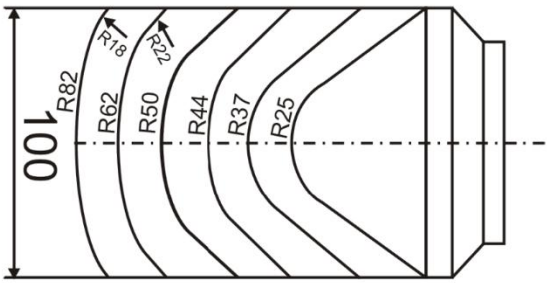

Fig 2.8: Punches used in the Keeler test

An alternative where the same specimen, but only one type of punch are used, is the Hecker test. In this case the amount or type of lubricant is varied, which gives different strain paths. For this test again only the positive part of the FLC can be found. [3]

Hecker Test [18]

In this test only one type and size of punch and specimen is needed whereby the friction regime is varied by varying the lubricant for obtaining different strain paths. A disadvantage is that only the positive region of the forming limit curve is determined.

Hasek Test [20]

In order to avoid wrinkling of the specimens Hasek proposed (fig 2.9) the use of circular specimens with recesses of different radii, see Fig. 2.9. This requires an increased amount of work for manufacturing the specimens.

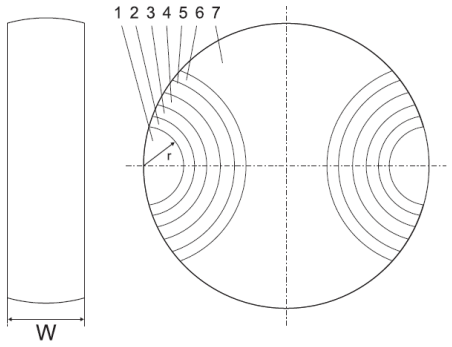

Fig 2.9: Shape of the specimens used in the Hasek test

Nakazima Test [19]

The test consists of drawing rectangular specimens having different widths using a hemispherical punch and a circular die, see Fig. 2.10. By varying the width of the specimen and the lubricant one may obtain both the positive and the negative domain of the FLD curve.

Advantages of the test are the simplicity of the tools, the simple shape of the specimens and the possibility of covering the entire domain of the FLDs. Disadvantages are the possibility of wrinkling and errors of measurement caused by the curvature of the punch.

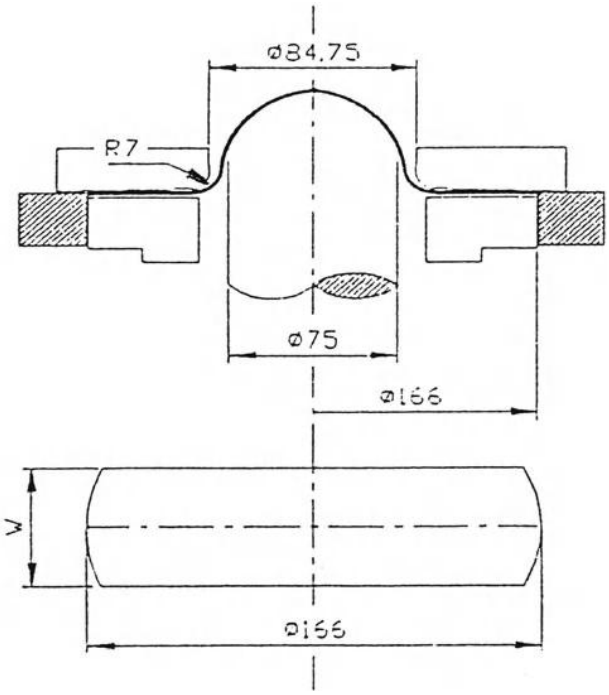

Fig 2.10: Schematic layout of the Nakazima testing device

In the industry the **Nakazima test** (or sometimes the similar Hasek test) is most often used to determine material properties. For both tests a simple hemispherical punch and a circular die are used, while the shape of the specimen determines the strain path. Especially for the Nakazima test both tooling and specimen are relatively simple. The Nakazima specimen, as shown in figure 2.10, only differ in width W. Strain paths for "1 > 0 can be found with this test.

The main disadvantages apart from those due to friction are possible wrinkling and measurement errors caused by the curvature of the punch. Specimens proposed by Hasek (figure 2.9) can be used if wrinkling is a problem. The advantages and disadvantages are the same as for the Nakazima test. The advantage of avoiding wrinkling is countered by the extra work needed to manufacture the specimen.

Tooling influence

The test methods as shown up to here have different regimes they can be used for, as shown in figure 2.5. This clearly shows the limits of the uniaxial tension test, the bulge test and Keelers test. It also shows how different tests can lead to different results, mainly because of differences in tooling and deformations because of that.

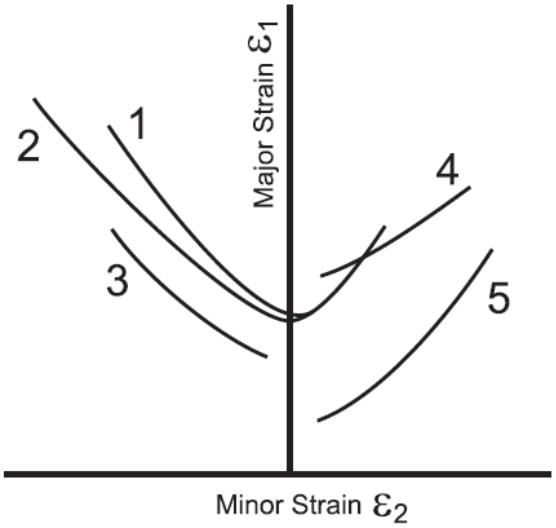

Fig 2.11: FLDs established using different testing methods

1 Hasek; 2 Nakazima; 3 uniaxial tension;

4 Keeler; 5 hydraulic bulge test

Comparison of Different Tests

In addition to the above described methods there are some other tests but their use is limited to a reduced number of strain states (Myauchi test using shearing, Marciniak test [24, 25] using sheet torsion etc.). Hasek [20] published a systematic study of the influence of the testing method upon the obtained FLDs. The key results are summarized in Fig. 2.11
From the tests described above, the following ones are be recommended: Marciniak test or hydraulic bulge test for eliminating friction; uniaxial test if simplicity is sought for; Nakazima test for covering a great variety of strain paths.

Effect of sheet thickness

Another observation is sheet thickness influencing the results in all set-ups, caused by differences in bending stresses. Both Raghavan [6] and Banabic [1] show arising FLC for thicker sheets, showing how a thicker sheet, with more material to flow, is leading to higher forming limits. This is observed for both in-plane and out-of-plane testing and can therefore not be described as a pure bending effect. More likely is the presence of an edge effect, leading to stiffening of the surface of the sheet and leading to earlier fracture in thin sheets as there is less material in the center to distribute the stresses introduced by deformation.

Besides using sheet of higher quality, the most common solution for the success of difficult sheet metal forming processes is to increase the sheet thickness.

The influence of sheet thickness on the FLD is characterized by the following relationships:

- The FLD for necking depends on sheet thickness;
- As the thickness rises, the curve rises on the plot $(\varepsilon_1; \varepsilon_2)$;
- The influence is high for pure expansion and vanishes for pure compression;
- Between the two, the influence of the thickness on the limit strain at necking

$(\Delta\varepsilon_3 / \Delta e)$ increases linearly with the ratio $\varepsilon_1 / \varepsilon_2$;

- Along a linear strain path the rise of the FLD is proportional to the increase of thickness but this influence vanishes above a critical value.

The engineer can decide if an unsuccessful forming process may be improved by increasing the sheet thickness. This is especially important if the stress acting during the forming process is tensile in both principal directions.

Marciniak test

An alternative punch test was proposed by Marciniak and Kuczynski [25], resulting from their theory on loss of material stability under biaxial tension, which manifests itself by a groove running perpendicular to the largest principle stress. They showed how their hypothesis about local strains concentrating in this groove could experimentally be verified with a set-up as shown in figure 2.12.

The idea behind the Marciniak test is it simply converting a vertical force into a biaxial force in the horizontal plane. This is done by a flat punch deforming a test specimen indirectly via a washer sheet with a central hole. The hole expands radially as the punch moves in and because of friction the tested sheet of metal expands with the washer. The radial friction forces in the contact region between washer and sheet also prevent the sheet from fracturing near the rounded edge of the punch, with the largest strains found in the flat central part of the specimen. The central part is now uniformly balanced, biaxially loaded, with no contact in the area, allowing failure to occur anywhere in this region.

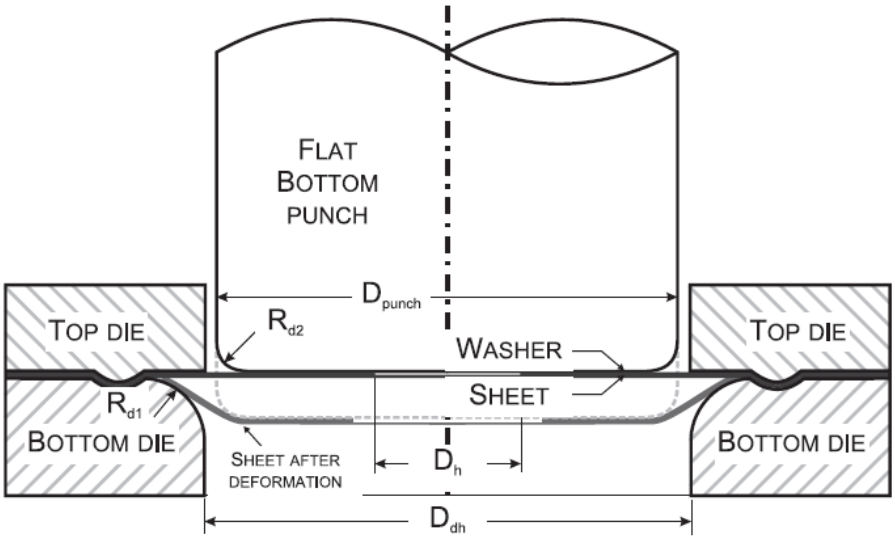

Fig 2.12: Marciniak test setup schematic

In 1977 Tadros and Mellor [40] expanded the theory of Marciniak and Kucznski [25] by adding different tooling shapes. They proposed using elliptical shaped tooling, resulting in various biaxial loads from pure biaxial to aspect ratios of 1:7. They give results for several materials, for some the test set-up works, for others like brass 70/30 it does not. Further research by Mellor showed different damage behavior up to fracture for brass. [40]

As different punch geometries are a costly method for testing, other options to achieve different strain paths have been investigated. One method in particular seems to have potential and is described by Raghavan [6] as a simple technique to generate in-plane forming limits. His proposal, based on earlier work by Gronostajski and Dolny [23], differs from the others by the use of different specimen and washer geometries. With this combination, compared to earlier methods, a wide range of strain paths can be prescribed.

D Banabic [1]

In deep-drawing with a flat bottom punch tearing of the part usually occurs at the connection between the bottom and the cylindrical wall. In order to produce the tearing at the planar bottom of the cup, Marciniak proposed [24] to use a hollow punch and an intermediate part having a circular hole placed between punch and work piece, see Fig. 5.29. The abstention of different strain paths is ensured by using punches with different cross sections (circular, elliptical, rectangular). The advantage of this test is that tearing appears at the planar bottom of the part thus eliminating the errors of measurement caused by a curvature. Disadvantages are the complex shapes of punch and die and the limitation of the test to the positive domain of the forming limit curve. In order to overcome these drawbacks, the test can be modified by using specimens and intermediate parts having different shapes, see Fig. 2.13. By varying the radius of the recesses the entire domain of the FLD is obtained using only one ring punch.

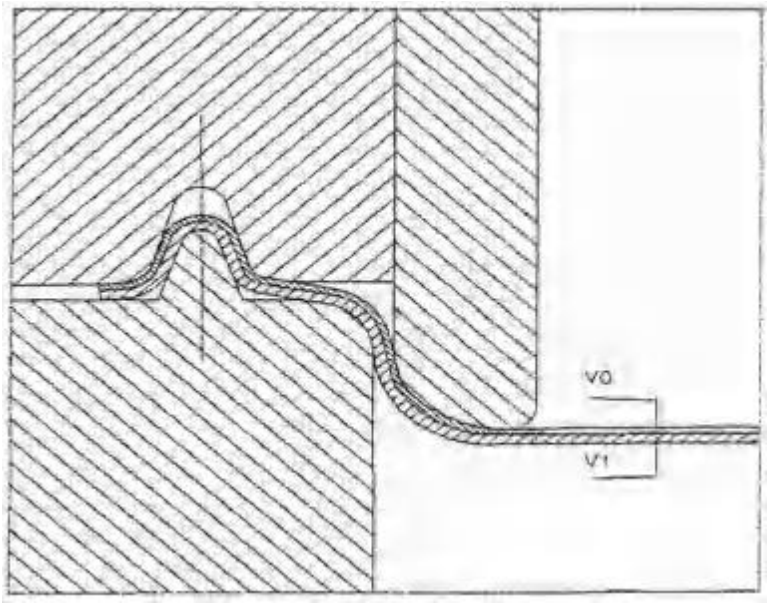

Fig 2.13: Schematic layout of the device used in the Marciniak test

Young-Woong Lee et al. (2004) [32] investigated the response of thin clamped plates subjected to static punch indentation experimentally, analytically and numerically to determine the beginning of fracture. The plots of force–penetration and locations of fracture initiation in the static punch indentation tests were compared with finite-element simulations and analytical approximations showing good agreement. Objective of their work was determination of the beginning of fracture of thin plates with three different thicknesses and three different sizes of hemi-spherical punches.

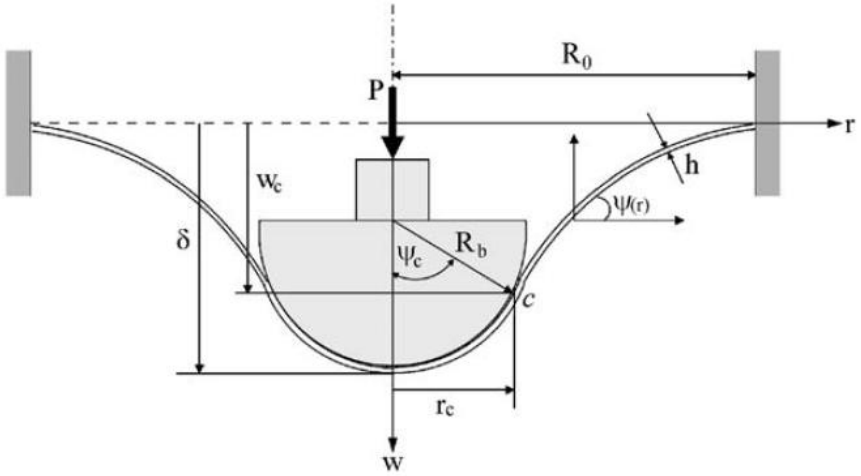

Fig 2.14: Geometry of a clamped thin plate loaded quasi-statically by a hemispherical punch.

And they calibrated the experimental data by performing uniaxial tensile test with finite-element simulations.

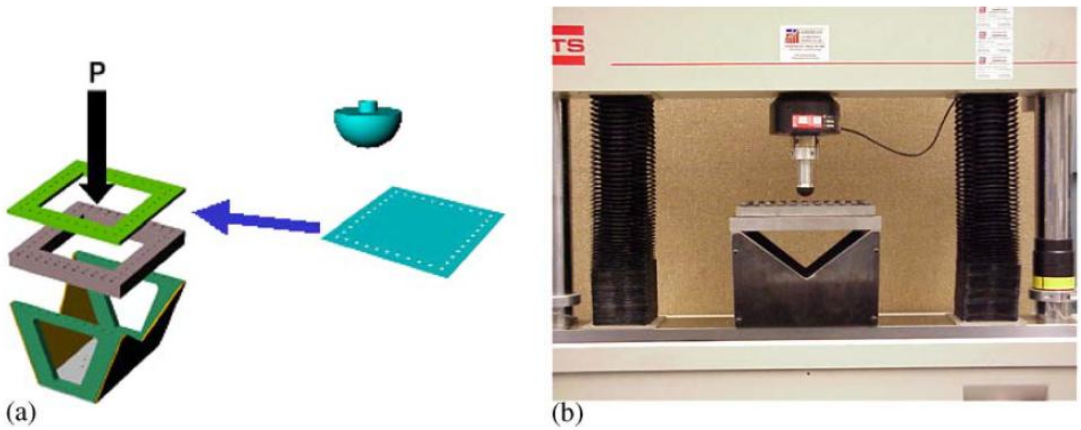

Fig 2.15: Notional test fixture and completed design: (a) schematic fixture and (b) test photo.

J Y Jeon et al. (2015) [22] presented a procedure to predict fracture toughness of steel material Using small punch test and FEA damage analysis. Tensile properties was determined by setting the constitutive equations. And validated by comparing the test data of small punch test with FEA results applying the determined tensile properties.

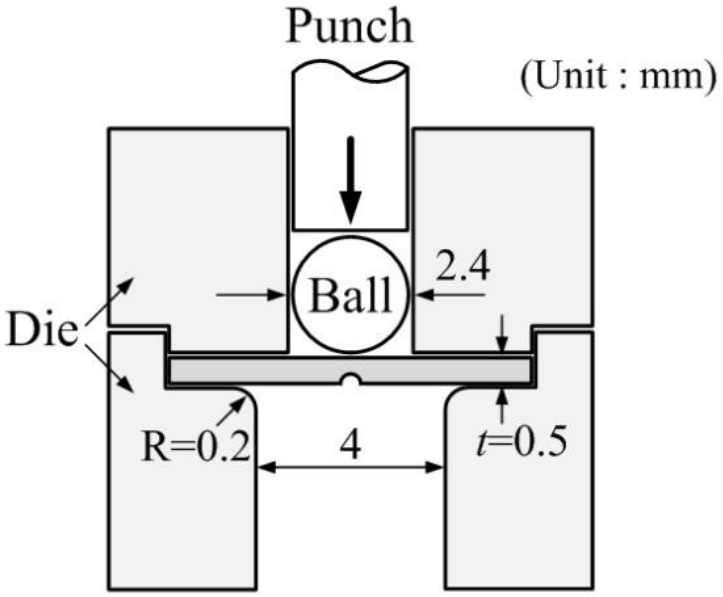

Fig 2.16: Notched small punch test set up

The material was assumed to follow the constitutive equations below:

$$\sigma = E\varepsilon \qquad \text{for} \quad \varepsilon \leq \varepsilon_y$$

$$\sigma = \sigma_y + K(\varepsilon_p)^n \qquad \text{for} \quad \varepsilon \geq \varepsilon_y$$

Where

E elastic modulus ε Total strain

ε_p Plastic strain ε_y Yield strain

M. Coleman et al. (2016) [21] in the current investigation Small Punch (SP) tensile tests were carried out on IN713 Cat room temperature and 650 °C in an air environment under stroke control at a rate of 0.02 mm/s. The fracture surface examination and microstructure characterization as well as detailed Texture analyses were performed using Scanning

Electron Microscopy (SEM) and Electron Backscatter Diffraction (EBSD). Finite Element (FE) analysis of the SP test was also implemented to investigate the role of stress state on the local deformation. It was evident that microstructure parameters such as grain morphology and original texture existed in the disc were the most influential factors in governing the deformation texture in mixed columnar/equiaxed (transition) disc microstructure.

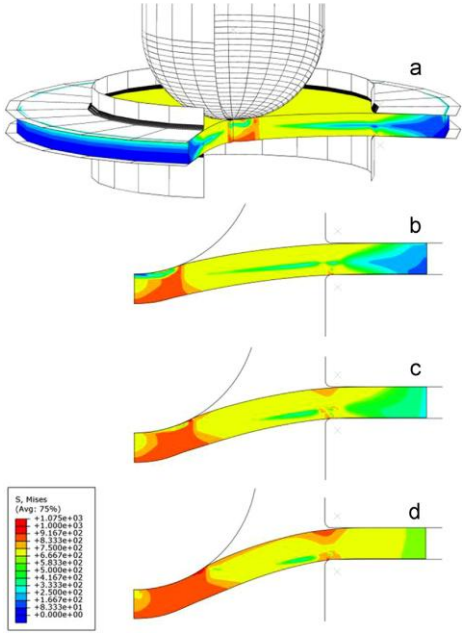

Fig 2.17: Evolution of von-Mises stress during SP test with punch displacements of (a) 0.25mm, (b) 0.5mm, (c) 0.75mmand, (d) 1.0mm.

Advantages and Disadvantages of Punch Test [33]

Punch indentation of thin sheets is a well-established technique to determine the biaxial stresses and forming limit diagram (FLD). An advantage of the punch test is its ability to undergo various strain paths, all of them up to necking and fracture.

The biggest disadvantage of the punch test is the presence of contact, as this both gives rise to geometrical constraints and adds friction to the problem.

Overestimation of fracture strains

A disadvantage of the punch test is the overestimation of acceptable strains, mainly because of tooling introduced geometrical constraints on necking behavior.
An effect found in punch tests, mainly due to friction, is localizing of the neck away from the center of the specimen. A second problem is that the punch test does not allow diffuse necking of the material, leading to larger formability [38]. This happens as the material on top of the punch sticks to the punch, resulting in lower strains. Depending on the shape of the punch, the test method and the lubrication this determines where the material fails and under what strain path. For most punch tests this behavior is unwanted, but tests like Keelers are partly based on this principle. A test with a hemispherical punch and varying lubrication states can be used to determine failure from pure biaxial strain paths (in the center) to almost pure stretching.

Specimen Design

One of the challenging task in biaxial testing is the design of testing specimen. The shape of specimen can vary from simple metallic sheets, cylindrical tubes to little complex cruciform type shapes with extra cuts and grooves. In biaxial testing of the sheet metal cross-shaped (cruciform) specimen is used generally.

The shape design of the cruciform testing specimen is the main difficulty that limits application for the cruciform biaxial tensile test. Although specimens of the cruciform type shapes have been studied quite extensively but no standard geometry exists. The lack of standard cruciform specimen geometry makes it difficult to compare the test results from different research laboratory. Different biaxial tests have been done in parallel to finite element simulations in an attempt to attain an optimum cruciform specimen design.

In designing a specimen, it is of great importance to have the majority of deformation at the center section of the specimen and to avoid stress concentrations in other regions of the specimen.

Yong et al. (2002) [32] presented a paper about design of a cruciform biaxial tensile specimen. According their study the main problem was that stress was not coming to the

central part. Because the arms are always under uniaxial tensile stress and the central part of the specimen is under biaxial tensile stress state. And as the deformation capacity of metal sheet under uniaxial tensile state is far smaller than that under biaxial tension state. So the rupture regularly occurs on the arms of cruciform specimen.

There have been a number of methods employed to prevent this in a cross shaped specimens. The three main methods are the (i) cut type, (ii) reduced section type and (iii) strip and slot type.

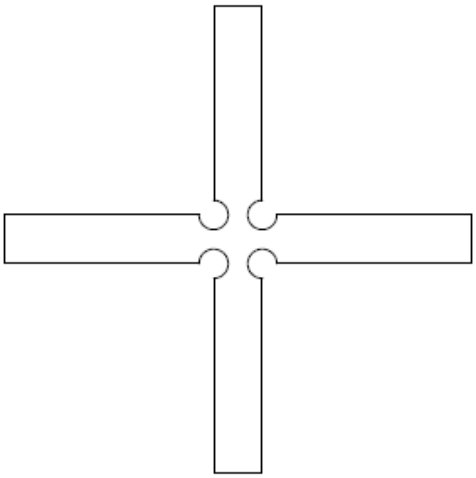

Fig 2.18: Cut type

The cut type uses large radii at the corner sections of the specimen to cause an increase in the deformation at the center section of the specimen.

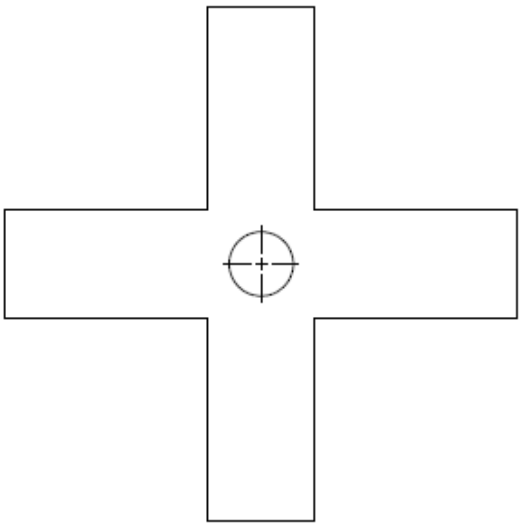

Fig 2.19: Reduced section type

From the cross-section of the reduced section, presented in fig, 2.19 the specimen is reduced in thickness to increase the deformation at the center.

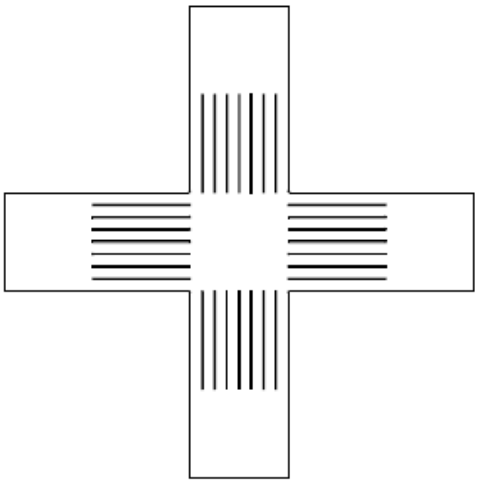

Fig 2.20: strip and slot type

The strips used in the strip and slot-type specimen reduce the effect of load sharing on the arms. These slits made in each arm, were found to be very effective in causing uniform strain distribution within the gauge section, allowing the biaxial stress components in the gauge section to be easily identified without assuming the effective cross-sectional area.

A Smits. et al. [30] proposed a paper “Design of a cruciform specimen for biaxial testing of fiber reinforced composite laminates” in 2005. They used an in-plane biaxial testing device consisting four independent servo hydraulic actuators.

Fig 2.21: in-plane biaxial testing device

This paper mainly focused on design of cruciform specimen. For finding a suitable geometry for biaxial testing the combination of FEA simulations and experiments were performed on different cruciform geometry types (mainly 4) using the digital image correlation technique for full field strain measurements.

The images of principle strains in all four geometries of cruciform specimens by FEA and digital images are:

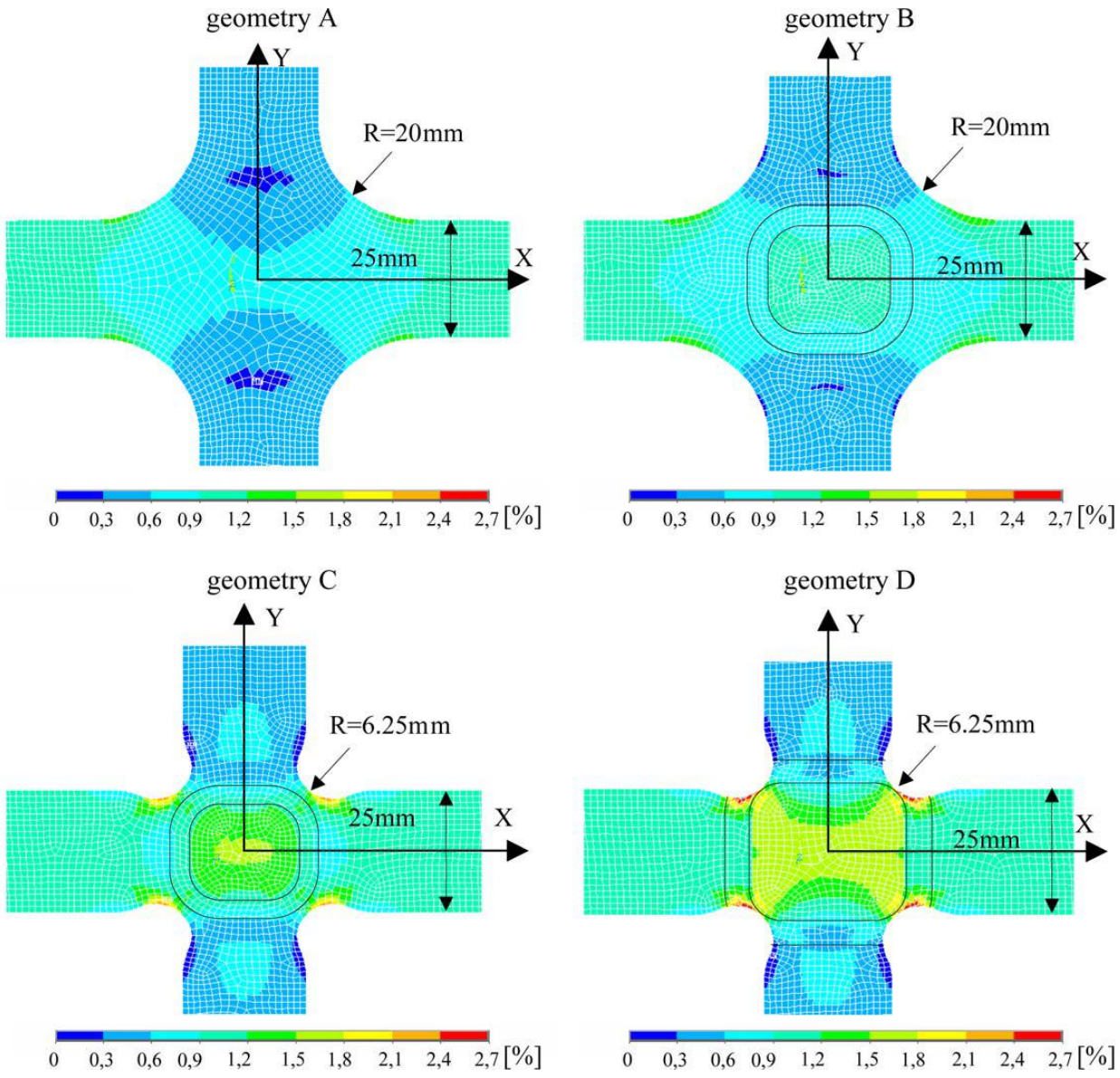

Fig 2.22: Finite element results of the first principal strain for four cruciform geometries.

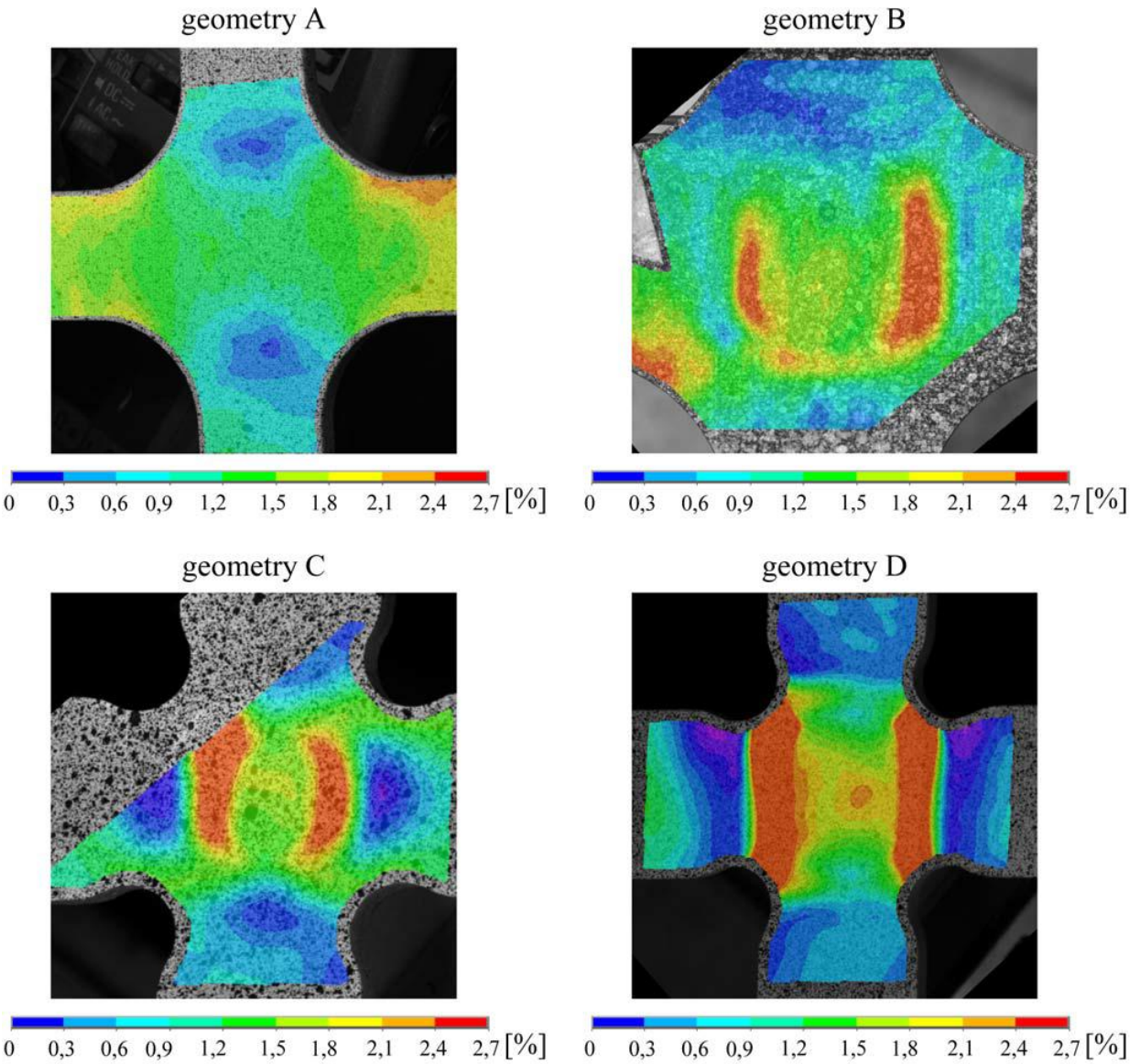

Fig 2.23: Digital image correlation results of the first principal strain for four cruciform geometries.

In geometry A, failure occurs in the arms. To relocate this failure to the center, first a thickness reduction in the center of the specimen was made, which is shown in geometry B. This resulted in an increased principal strain in the center. Subsequently the corner geometry was changed as shown in geometry C. This resulted in high strains and possible failure of the specimen in the center. Changing the geometry of the corners was necessary, because the fibers at ±45 degrees carried the load from one arm to a perpendicular one,

which resulted in unloading of the center of the specimen. In geometry D, a larger thickness reduction area was used. The strain variation over the most loaded axis of the milled zone was examined for each geometry, by finite element simulations and experiments. A higher strain was found in the experiments in the transition zone between the full thickness and the thickness reduced area compared to the finite element predictions. This difference may be eliminated in a more detailed model with a smooth thickness reduction. Geometry C showed the most uniform distribution of strains, both in the simulation and in the experiments. To determine which geometry is the best, also experimental biaxial failure data was obtained. The highest failure strains were found for geometry C, which indicates that this is the most optimal specimen. Failure started at the corners between the two arms for all geometries, but for geometry B and C the complete biaxially loaded test zone was damaged.

R Vos (2007) [27] performed FEA simulations (finite element package Marc/Mental 2005) on number of cruciform specimen designs to find an optimized specimen shape for biaxial testing. The used material was interstitial free (IF) steel, thickness of 0.7 mm. Young's modulus of 45 GPa and a Poisson's ratio of 0.29.

In this work effect of various factors on the specimen were studied (e.g. effect of arm width, corner shape, numbers of arms and thickness reduction)

1. **Effect of arm width**

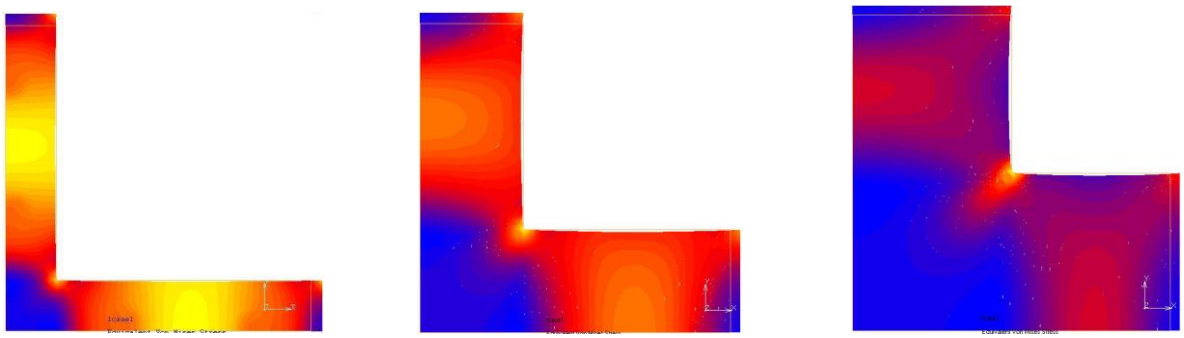

a) Arm width: 10 mm (b) Arm width: 20 mm (c) Arm width: 30 mm

Fig 2.24: Von Mises stress at necking as a function of the arm width

From the results it is concluded that for each width stress localization occurs only in the middle of the arms. There is not significant changes in stress patterns.

2. Effect of corner shape

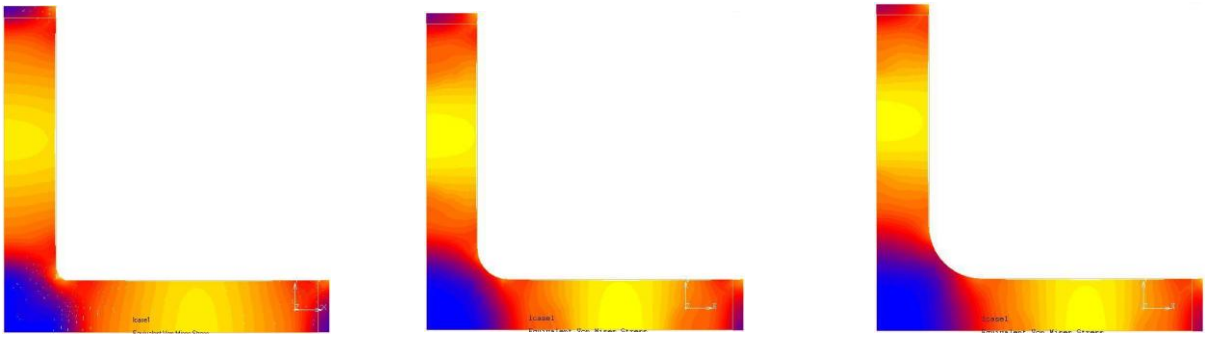

(a) Corner radius: 1 mm (b) Corner radius: 3 mm (c) Corner radius: 5 mm

Fig 2.25: Von Mises stress at necking as a function of the corner radius

The examined geometries with round corners have corners with radii of 1, 3 and 5 mm. The results (Fig. 2.25) show that necking still occurs in the arms, since the radius makes necking near the center less favorable. The only difference between different corner radii is the maximum stress reached in the corners during the stretching of the arms.

These maximum stress values are shown in table 2.1

GEOMETRY	STRESS (MPA)
SHARP CORNER	450
ROUND CORNER RADIUS 1 MM	450
ROUND CORNER RADIUS 3 MM	360
ROUND CORNER RADIUS 5 MM	315

Table 2.1: Maximum values of von Mises stress (MPa) reached in the corners

3. Effect of notch radius

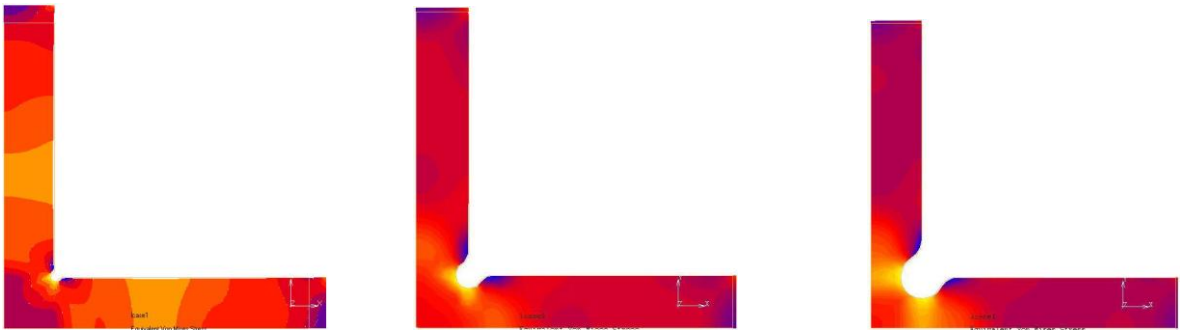

(a) Radius notch: p 2 − 1 mm (b) Radius notch: 3 p2 − 3 mm (c) Radius notch: 5 p2 − 5 mm

Fig 2.26: Von Mises stress at necking as a function of the notch radius

It is clear that a small notch still leads to necking in the arms. When the radius of the notches is increased, the necking starts in these notches. This is because the arms are reduced in width in the area where the notches are present. This area is therefore less strong and necking is more likely in that cross section.

So the notched geometry helps to increase the stress in the biaxially loaded zone, but it also weakens a certain area even more than the middle of the arms. This increases the danger of necking elsewhere than in the biaxially loaded zone.

4. Effect of number of arms:

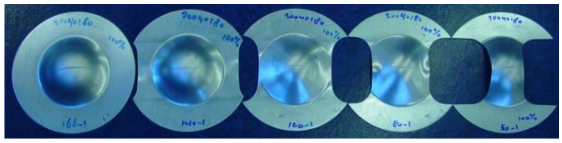

Fig 2.27: Nakazima strips used in bulge tests

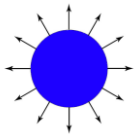

Fig 2.28: Ideal in-plane biaxial test specimen

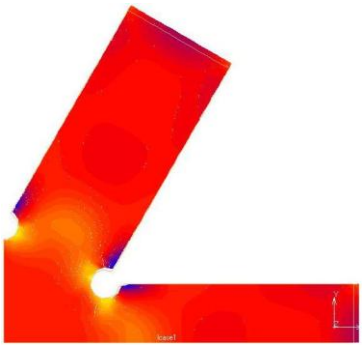

Fig 2.29: specimens with 6 arms

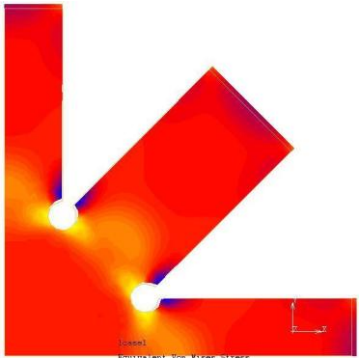

Fig 2.30: specimens with 8 arms

Figures 2.29 and 2.30 show results similar to the results found in the simulations of the specimen with four arms. So there is not significant effect of number of arms of testing specimen.

The results obtained in this study can be summarized as follows:

1. In specimens with sharp corners, necking occurs in the arms, independent of arm width.
2. Round corners decrease the stress in the corners. In a specimen with notch corners, the necking occurs in area between the notches, if the notches are sufficiently deep.
3. The number of arms does not change the localization.
4. A homogenous thickness reduction in the center of the specimen results in high stress at the edge of this area.
5. A thickness reduction in the form a bowl results in yielding, necking and damage at the center of the specimen, even under complex loading.

H. Seibert et al. (2014) [39] proposed an experimentally optimized shape of cruciform specimen.

Fig. 2.31 displays four intermediary stages beginning at the reference geometry in Fig. 10a) up to the finally chosen shape in Fig. (10d). The thickness of all the specimen tested were same.

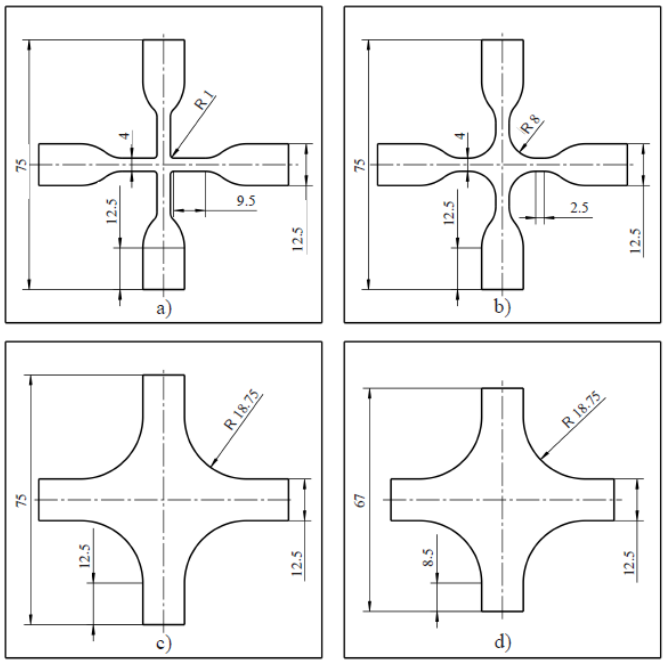

Fig 2.31: sample geometries

Rui Xiao et al. (2015) [31] proposed a shape of cruciform specimen for biaxial testing. The influence of the parameters on the test results were then calculated by the finite element method (FEM), and the optimization was carried out. Optimization results showed that thickness of central area can be decreased moderately based on a half of the original thickness, and the best value should be controlled by 40% to 50%.

Chapter 3

Design of Biaxial Fixture

The fixture is designed as a lightweight, and cheap alternative to present biaxial testing machines. However, it can only work in 1:1 ratio in the σ1- σ2 stress space.

Selection of Material

This biaxial tensile test fixture is developed for 50 kN universal testing machine. It is easily adaptable to any UTM in colleges. Now the challenge was to develop a light weight fixture which should be easy to install. And as well as it should be economical also. So for that we compared the properties of various type of steels.

AHSS

AHSS are complex, sophisticated materials, with carefully selected chemical compositions and multiphase microstructures resulting from precisely controlled heating and cooling processes. Various strengthening mechanisms are employed to achieve a range of strength, ductility, toughness, and fatigue properties.

The AHSS family includes Dual Phase (DP), Complex-Phase (CP), Ferritic-Bainitic (FB), Martensitic (MS or MART), Transformation-Induced Plasticity (TRIP), Hot-Formed (HF), and Twinning-Induced Plasticity (TWIP). These 1st and 2nd Generation AHSS grades are uniquely qualified to meet the functional performance demands of certain parts. For example, DP and TRIP steels are excellent in the crash zones of the car for their high energy absorption. For structural elements of the passenger compartment, extremely high-strength steels, such as Martensitic and boron-based Press Hardened Steels (PHS) result in improved safety performance. Recently there has been increased funding and research for the development of the “3rd Generation” of AHSS. These are steels with improved strength-ductility combinations compared to present grades, with potential for more efficient joining capabilities, at lower costs. These grades will reflect unique alloys and microstructures to achieve the desired properties. The broad range of properties is best illustrated by the famous Global Formability Diagram, captured in Figure

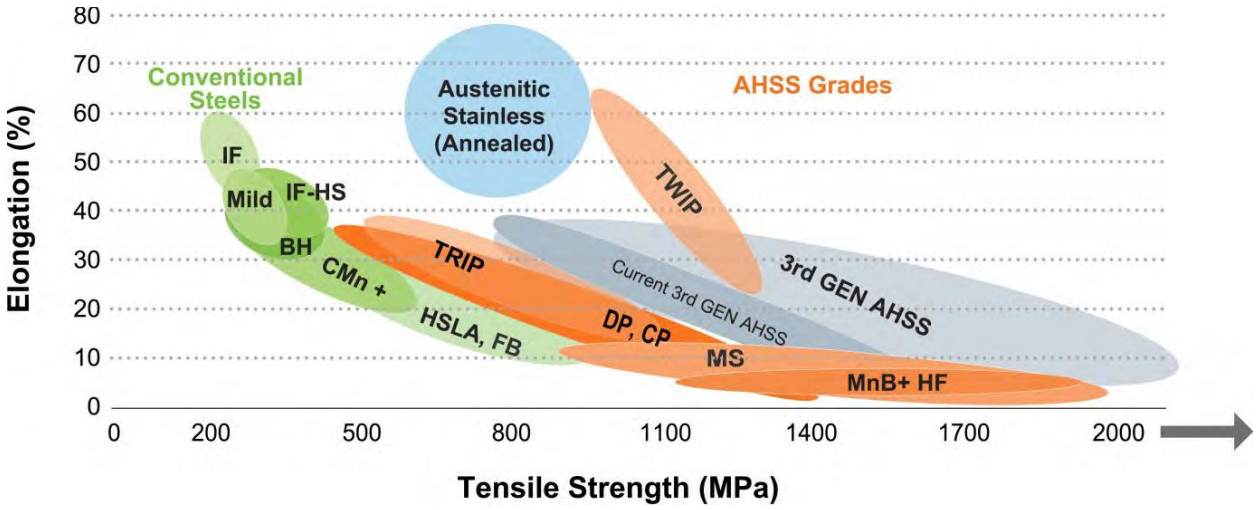

Fig 3.1: Tensile strengths of different grades of steel

Steels with yield strength levels in excess of 550 MPa are generally referred to as AHSS. These steels are also sometimes called “ultrahigh-strength steels” for tensile strengths exceeding 780 MPa. AHSS with tensile strength of at least 1000 MPa are often called “Giga Pascal steel” (1000 MPa = 1GPa). Please note another category of steels, represented with a bubble in Figure Austenitic Stainless Steel. These materials have excellent strength combined with excellent ductility, and thus meet many vehicle functional requirements. Due to alloying content, however, they are expensive choices for many components, and joining can be a challenge. Third Generation AHSS seeks to offer comparable or improved capabilities at significantly lower cost.

XX	TYPE OF STEEL	XX	TYPE OF STEEL
MILD	- Mild Steel	HSLA	High-Strength Low-Alloy
BH	Bake Hardenable	IF	Interstitial Free
CP	Complex Phase	MS	Martensitic (MART)
DP	Dual Phase	TRIP	Transformation Induced Plasticity
FB	Ferritic Bainitic	TWIP	Twinning-Induced Plasticity
HF	Hot Formed (and quenched)		

Table 3.1: Steel type designators

NO.	Steel	Grade	MIN YIELD STRENGTH MPa	MIN TENSILE STRENGTH MPa
1	Mild	140/270	140	270
2	BH	170/340	170	340
3	BH	210/340	210	340
4	DP	210/440	210	440
5	BH	260/370	260	370
6	IF	260/410	260	410
7	BH	280/400	280	400

Table 3.2: AHSS materials portfolio

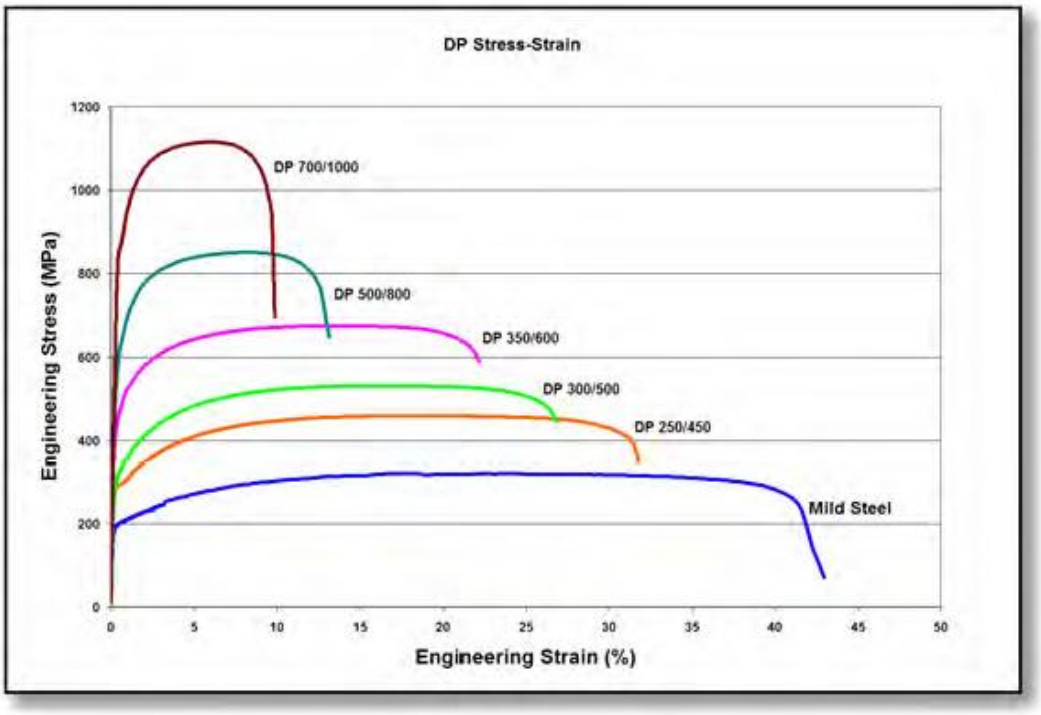

Fig3.2: Comparison between engineering Stress-Strain curves

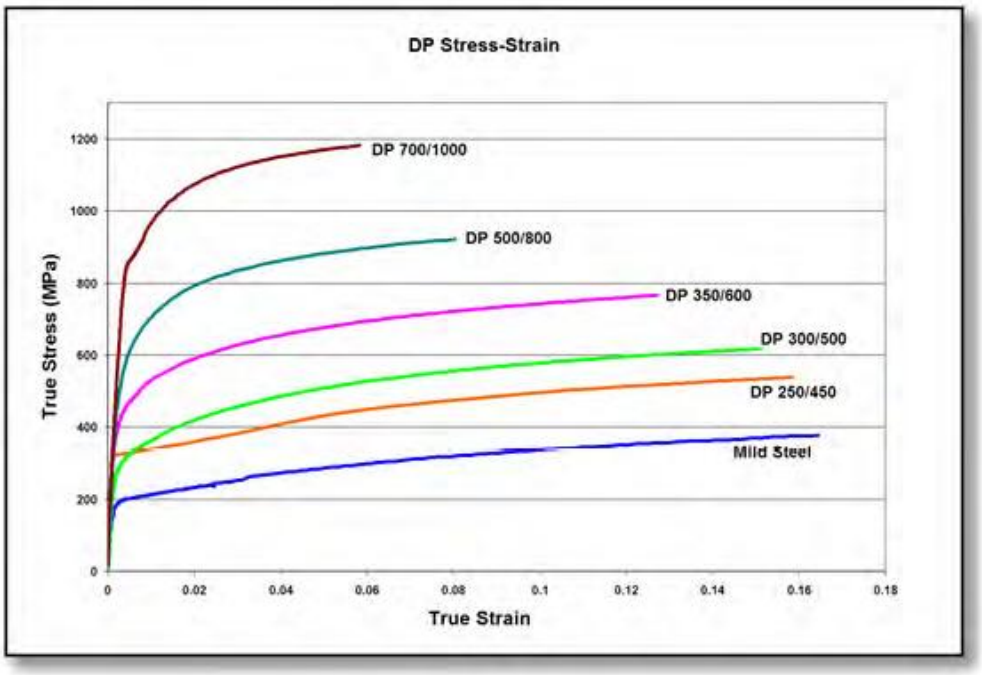

Fig 3.3: Comparison between true Stress-Strain curves

Fixture components description

The software used for the modelling is Solidworks 14.0 academic version. It is a 3D solid modelling package which allows users to develop full solid models in a simulated environment for both design and analysis. In SolidWorks, we can sketch ideas and experiment with different designs to create a 3D models. SolidWorks is used by students, designers, engineers, and other professionals to produce simple and complex parts, assemblies, and drawings. Designing in a modelling package such as SolidWorks is beneficial because it saves time, effort, and money that would otherwise be spent prototyping the design.

The fixture contains the following parts:

1) Base

The base is a solid cylinder with three mountings on top to assemble the rod and the test plate holding jigs. The entire piece is made of solid alloy.

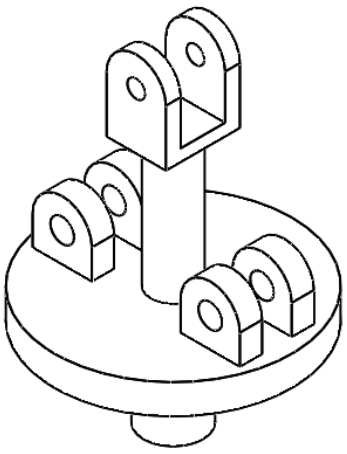

Fig 3.4: Base

2) Upper Frame

This is the primary component that distributes force in the fixture. Two arms at 30° angle to the vertical, and 60° angle between them. It is done so that the component of force in the horizontal direction on one arm is half of that applied in the vertical. As there is no force

being applied on the base, the vertical force on the upper frame gets distributed in both arms equally, and thus, a net equal force is obtained in the horizontal as well.

Slots are cut into the arms to provide mounting for rollers.

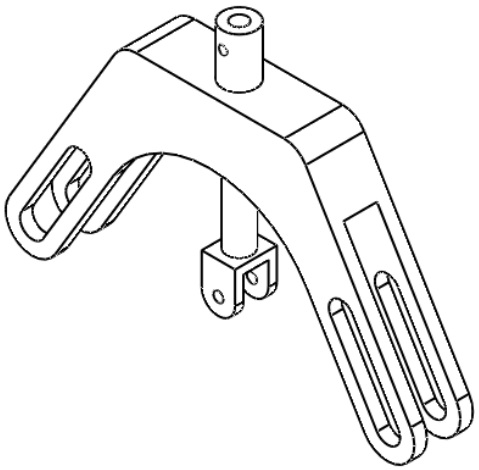

Fig 3.5: Upper Frame

3) Rod

These are the members that connect the roller to the base. They also mount the slider. As the upper frame moves upwards, the rods rotate about their respective hinges such that the horizontal displacement is half of the vertical displacement. There is only a small section of the upper frame where this can happen. However, since the motion in the fixture will be very less due to the nature of the test plates, the motion will be sufficient for our purposes.

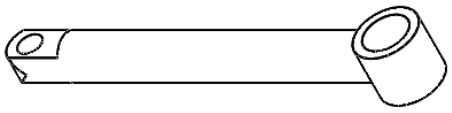

Fig 3.6: Rod

4) Roller

These are the components that are mounted in the slots of the Upper Frame. They rotate in the slot to minimize sliding and prevent friction. They translate their motion into the rods.

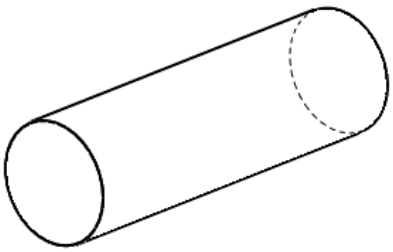

Fig 3.7: Roller

5) Slider

These are the components that mount the hinges. They have a cylindrical slot for the rod. They can slide about the rod. This gives leeway when setting up the fixture for an experiment.

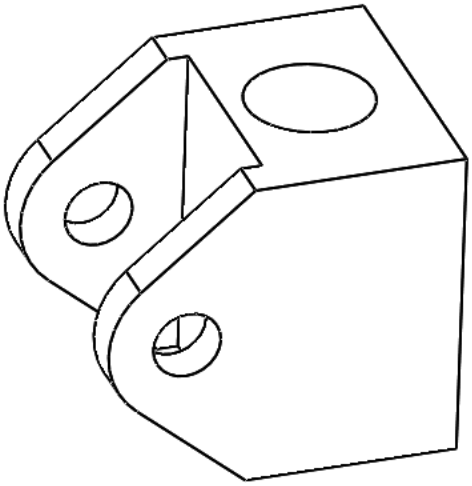

Fig 3.8: Slider

6) Hinge

These are mounted in the Sliders using a pin. They swivel about the slider to help in setting up the experiment.

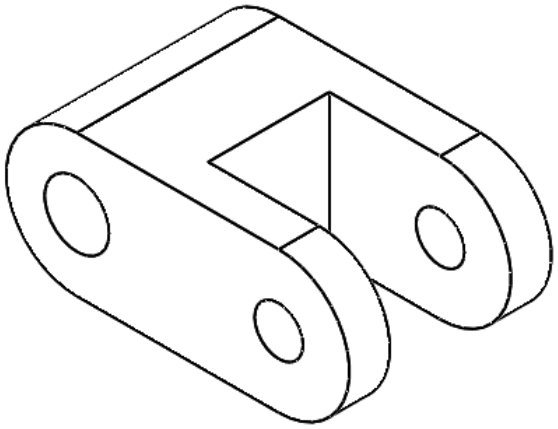

Fig 3.9: Hinge

Assembly of Fixture

In modeling phase all the components are made rigid to simulate the kinetic behavior. Deformations will be negligible and negligible concentration will be on movement of linkages.

For the desired functioning of fixture assembly we had to constrain the motion of each linkage with respect to other.

This is a 2-Dimensional linkage mechanism so each part having 3 DOF two translatory and one rotary motion.

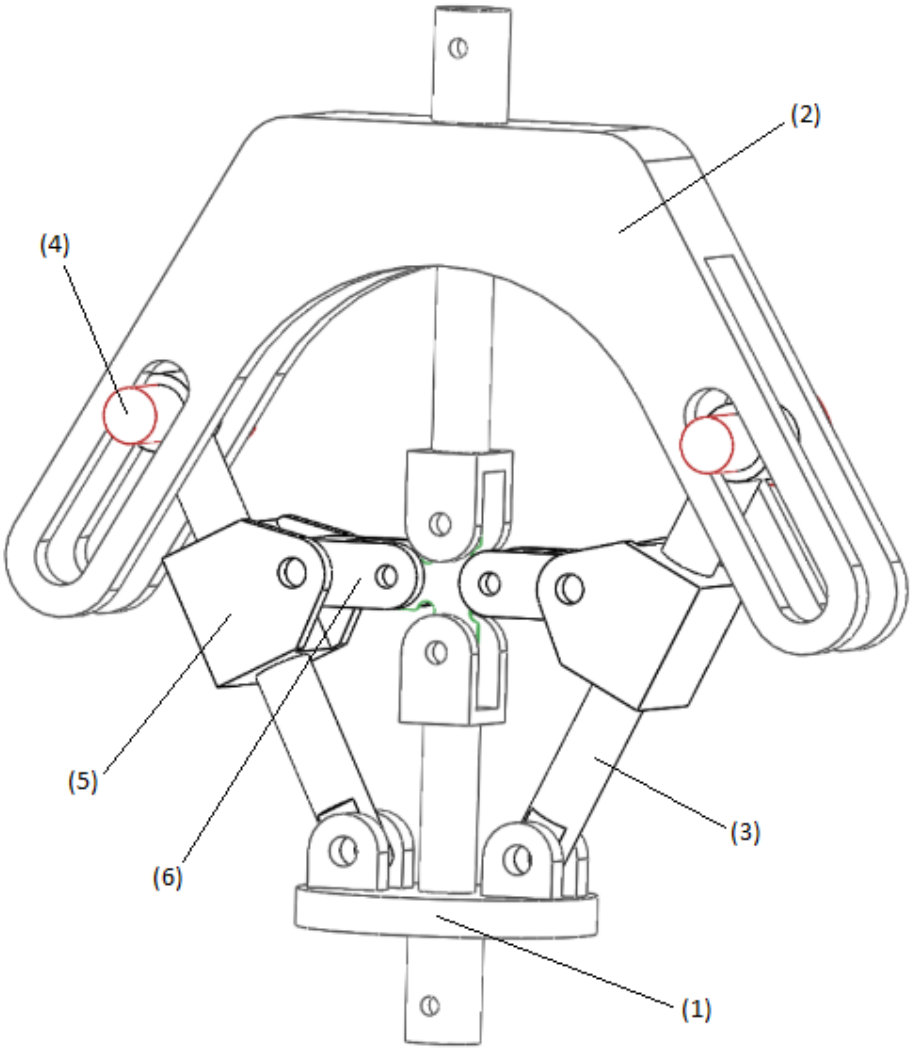

Fig 3.10: Assembly schematic of biaxial fixture

Explanation of Joints and Contacts Used in the Assembly

Revolute Joints

A Revolute- joint allows the rotation of one part with respect to another part about a common axis.

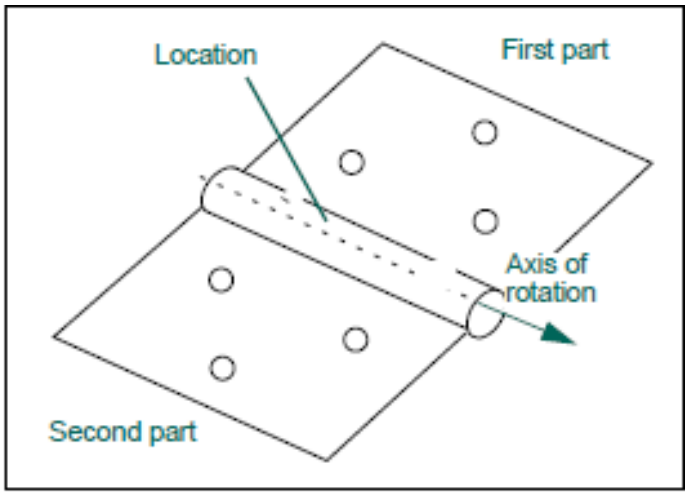

Fig 3.11: Revolute Joint

Translation Joints

A translation joint allows one part to translate along a vector with respect to another part

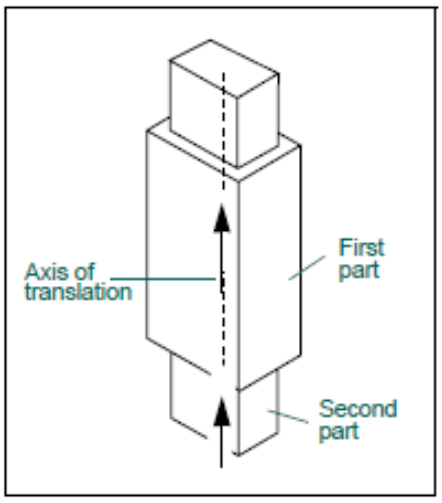

Fig 3.12: Translation Joint

Cylindrical Joints

A cylindrical Joint allows both relative rotation as well as relative translation of one part with respect to another part.

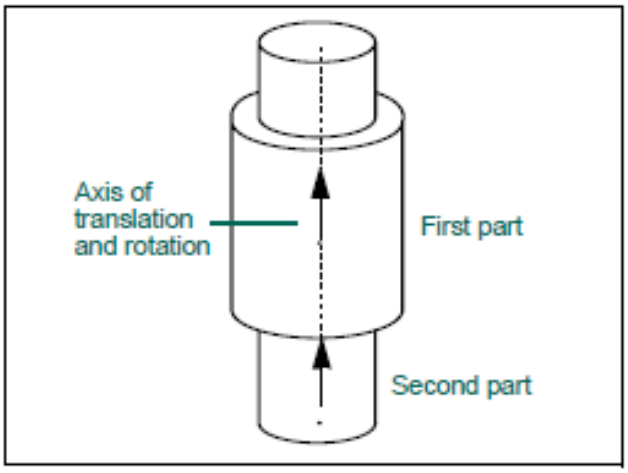

Fig 3.13: Cylindrical Joint

Fixed Joints

A fixed joint locks two parts together so that they cannot move with respect to each other.

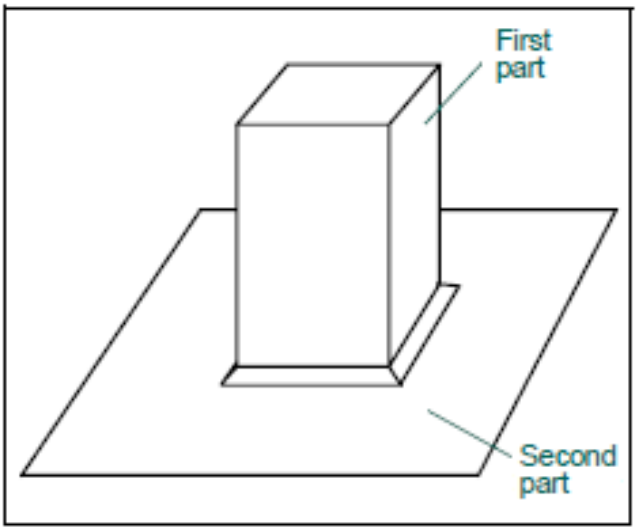

Fig 3.14: Fixed Joint

Kinematics of fixture

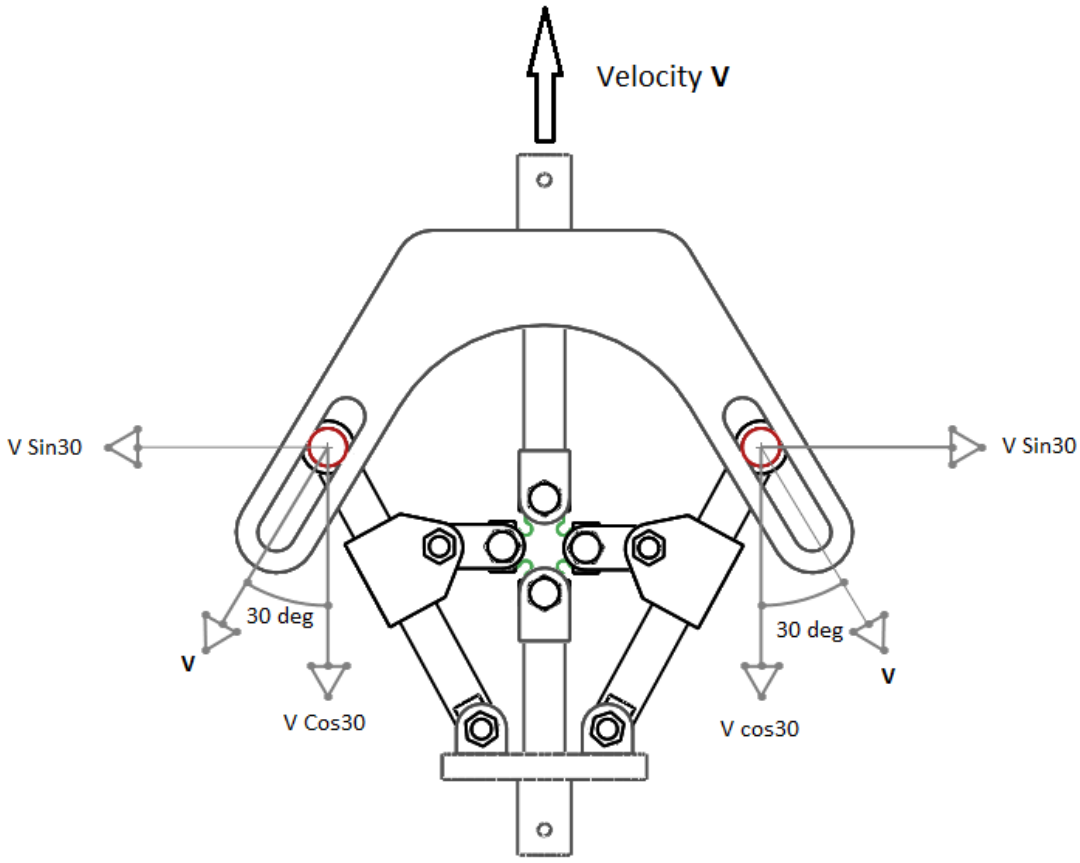

Fig 3.15: Kinematic schematic of fixture

Base (1) is fixed with the ground so all the motions of base is constrained. Two rod linkages are connected with the base at opposite sides with the help of pins. They are connected with revolute joints which are the lower pair connection.

Upper frame have only 1 DOF. It can only translate up and down with respect to Y axis. Other two motions are constrained.

Upper frame and rods are connected with the help of rollers which can translate in in the cutting slots.

They are free to rotate about their own axis. So in this rolling pair there will be pure rolling and no sliding of the surfaces which will help in reducing the friction significantly.

Slider has the 2 DOF. It can translate over the rod and can rotate about the axis of rod as well. Here is the surface contact between these two parts so we will reduce the friction by using bush bearings at fabrication level.

Hinge is connected to slider by a pin joint. So its two translatory motions are constrained, it call only revolute about axis of pin joint with respect to the slider.

Now the degree of freedom of whole mechanism can by calculated by using Grubler's Equation which is as follows:

$$F = 3(n-1)-2L-h$$

Where n is no. of links, L is no. of lower pairs and h is no. of higher pairs.

When cruciform specimen is not fixed in the fixture, Mechanism have three degree of freedom. One for upper frame and two for rods. Degree of freedom of upper frame is can be defined as independent DOF while as of rods are dependent.

When specimen will be fixed then DOF of this assembly will be negative by this Grubler equation and it will behave as rigid structure.

Working mechanism of fixture

The upper frame and base are mounted on the universal testing machine with the help of hardened pins and their respective slots. Now the base part is fixed and the upper frame is free to move as the load cell starts applying the load. The upper frame will move vertically upwards with a velocity of V. So now as per the designing of slots in the upper frame the roller will start to move in slots. Velocity of the roller in the horizontal direction then will be $V\sin30^{o}$ which is equal to V/2. So the design of fixture equally distribute the vertical force into two equal component acting in horizontal direction opposite to each other.

So when load is applied the upper frame starts moving vertically upward with a velocity V and simultaneously horizontal grips also moves apart in opposite directions in the horizontal axis with a velocity of V/2.

Cruciform Specimen and its plasticity equation of failure theory

We are considering the material behavior of cruciform specimen to be elasto-plastic. The young's modulus and the poison's ratio of the material are 70 GPa and 0.33 respectively.

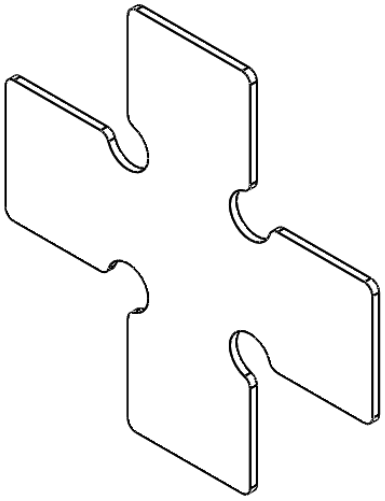

Fig 3.16: Cruciform Specimen

For the plastic behavior the type of hardening considered is isotropic in nature. The yield criteria considered is isotropic and associated flow rule is assumed.

The isotropic yield function depends upon Von Mises' Theory. It states that yielding in a ductile solid material will occur only when distortion energy density will reach a value which is equal or greater than a critical value for that ductile material.

The von mises stress in terms of stress components can be written as

$$\sigma_{VM} = \sqrt{\frac{(\sigma_{xx} - \sigma_{yy})^2 + (\sigma_{yy} - \sigma_{zz})^2 + (\sigma_{zz} - \sigma_{xx})^2 + 6(\tau_{xy}^2 + \tau_{yz}^2 + \tau_{zx}^2)}{2}}$$

The isotropic yield function is defined for plane stress condition as follows

$$\psi(\sigma_{ij}) = \sqrt{\sigma_{xx}^2 + \sigma_{yy}^2 - 2\sigma_{xx}\sigma_{yy} + 3\sigma_{xy}^2}$$

The final assembly looks as follows

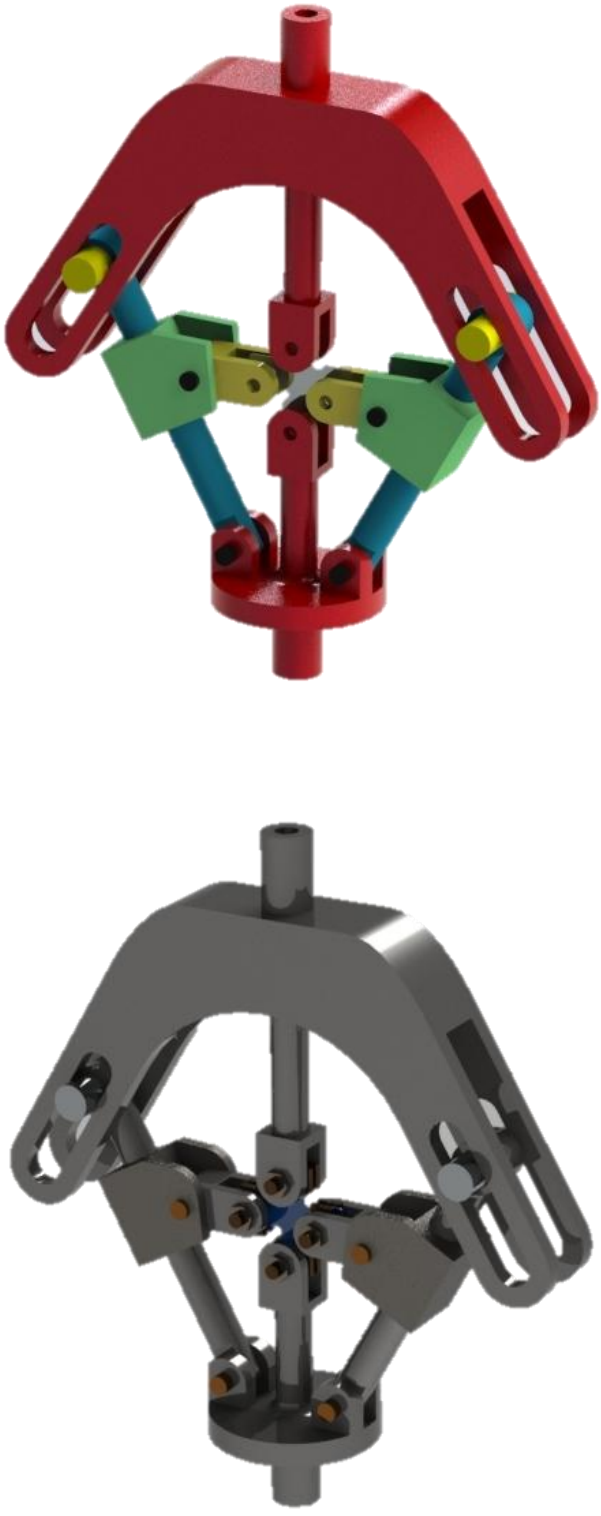

Fig 3.17: 3D Rendered models of Biaxial Fixture

Chapter 4

Computer Aided Engineering of fixture

What is CAE:

The term process simulation describes all methods by which one or more of the process parameters of a real physical process or process family is or are predicted approximately before its or their actual happening. The aim of the determination of these parameters in case of metal forming processes is usually one or more of the following:

• Checking the feasibility of the process design for producing a workpiece,

• Evaluating the product properties for service use,

• Increasing the insight about the real process in order to optimize the production sequence.

Therefore, the application of process simulation must be always more economical than the application of the real process.

The commercial programs - basically finite element programs - have such comfortable pre- and post-processors, that any student or engineer can use the programs. The successful application of these software still requires

1. The existence of a well-defined physical problem, for which a numerical analysis can provide an a solution,

2. The correct idealization of this physical problem (simplifications, assumptions, detection of governing physical phenomena),

3. The correct spatial discretization of the idealized problem (type of elements, topology of element mesh, density of element mesh)

4. The setting of correct boundary conditions

5. The use of correct material laws and parameters

6. The selection of correct numerical parameters (penalty factors, convergence limits, increment sizes, remeshing criterion),

7. The economical analysis (reasonable computational times, reasonable modeling times, reasonable storage requirements),

8. The correct interpretation of the numerical results

Finite Element Analysis

This fixture mechanism consists large no. of components. Simulating such a system not only requires capturing the correct physical behavior but also using efficient techniques of analysis. Different levels of abstraction modeling are appropriate for separate stages of the design process. Kinematics and initial sizing can be studied using a partially rigid model, while final designs may be analyzed with completely meshed flexible geometry.

Softwares used for CAE are as following

Ansys Workbench 15.0

Abaqus 6.11

ANSYS is a general purpose software, used to simulate interactions of all disciplines of physics, structural, vibration, fluid dynamics, heat transfer and electromagnetic for engineers. So ANSYS, which enables to simulate tests or working conditions, enables to test in virtual environment before manufacturing prototypes of products. Furthermore, determining and improving weak points, computing life and foreseeing probable problems are possible by 3D simulations in virtual environment. ANSYS can work integrated with other used engineering software on desktop by adding CAD, Solidworks and FEA connection modules.

ANSYS can import CAD data and also enables to build geometry with its "pre-processing" abilities. Similarly in the same pre-processor, finite element model (a.k.a. mesh) which is required for computation is generated. After defining loadings and carrying out analyses, results can be viewed as numerical and graphical.ANSYS can carry out advanced engineering analyses quickly, safely and practically by its variety of contact algorithms, time based

loading features and nonlinear material models. ANSYS Workbench is a platform which integrates simulation technologies and parametric CAD systems with unique automation and performance. The power of ANSYS Workbench comes from ANSYS solver algorithms with years of experience. Furthermore, the object of ANSYS Workbench is verification and improving of the product in virtual environment. ANSYS Workbench, which is written for high level compatibility with especially PC, is more than an interface and anybody who has an ANSYS license can work with ANSYS Workbench. As same as ANSYS interface, capacities of ANSYS Workbench are limited due to possessed license.

All the components of fixture are designed in modeling software Solidworks 2014 keeping all the aspects of designing in consideration e.g. dimensioning, compactness, mass consideration etc. and then all assembled together as described in previous chapter.

Finite Element Analysis (FEA)

FEA consists mainly three stages which are described below briefly

1. Pre processing
2. Processing (Analysis)
3. Post processing

Pre processing

In the preprocessing part of FEA we have to give all the inputs which require for the deformation and stress distributions in the component as a output.

This include the

1. Material properties
2. Finite element discretization
3. Solution parameters

Defining Material Properties

For all the fixture components High Strength Steel is employed. Mechanical properties values of HSS is assigned then within elastic limit

Young's modulus = 200 GPa

Poison's ratio = 0.3

And for the test plate initially we are considering the aluminium. After the successful development of fixture different composite material's behavior could be analyzed under biaxial loading.

Aluminium mechanical properties

Young's modulus = 70 GPa

Poison's ratio = 0.33

Meshing

Meshing is the discrete representation of a continuous geometry which is involved in the problem. Essentially, it partitions the whole space into elements over which the equations can be approximated for getting the results.

Generation of Mesh is one of the most important parameters of engineering simulation. Too many mesh elements may result in long solver runs, and few may lead to improper results. So we chose different element size for different parts of the assembly to compromise between the accuracy of results and computation time & memory for the solver. The software incorporates a variety of 3D solid elements that could accommodate any model. Tetrahedron elements are used everywhere in the model for meshing. Each part of the assembly is meshed with fully integrated continuum 4-node C3D4 three-dimensional (3D) linear tetrahedron elements.

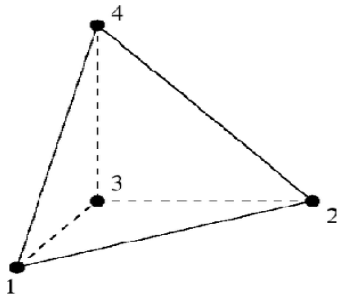

Fig 4.1: 3D Tetrahedron Meshing Element

Tetrahedral-Elements

1. Simple to automate
2. Flexible (local refinement)
3. High number of degrees of freedom
4. Elements cannot endure severe distortions

We have controlled the meshing quality by giving the different approximate global size for different parts. At the curvature sections we have given deviation factor (h/L) in between 0 to 0.1

The quality of meshing at the regions of holes, curves, fillets etc. is controlled by adaptive meshing techniques.

The finite element analysis of each component is done by Abaqus 6.11 The ABAQUS™ software. This software was chosen to perform Finite Element Analysis because of their ease with the Pre-processing part. Adaptive meshing is comparatively easy in Abaqus.

The meshed elements are shown in figures further and statistics of no. of nodes and elements also shown in the table 4.1

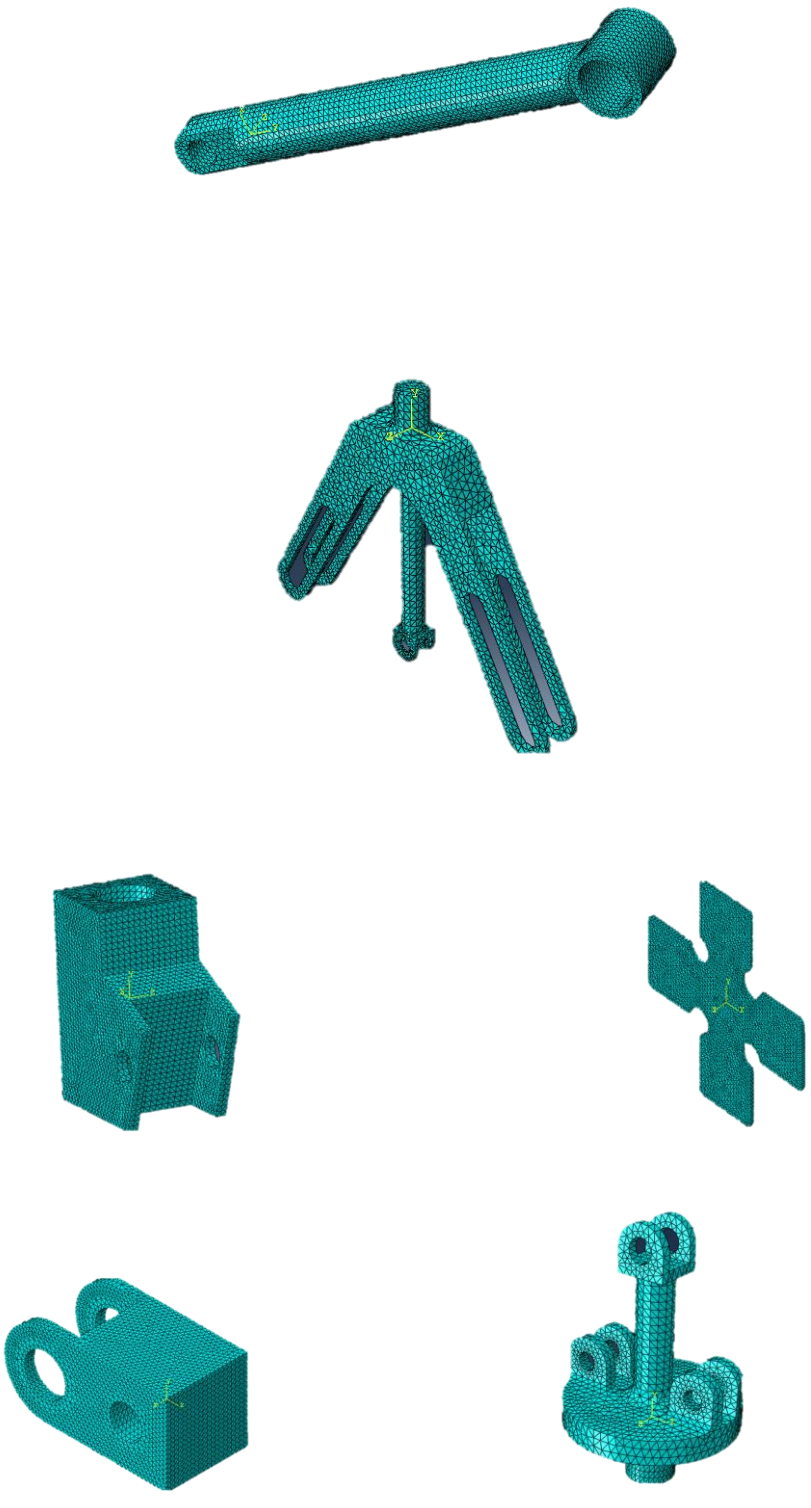

Fig 4.2: Meshed components of the fixture

NAME OF PARTS	NO. OF ELEMENTS	NO. OF NODES
BASE	7490	14029
UPPER FRAME	17500	33156
SLIDER	2789	5259
HINGE	1567	2985
ROD	2495	4995
ROLLER	1745	3318
TEST PLATE	6151	12740

Table 4.1: Meshing Statistics

Loading and Boundary Condition

We have to tell the FEA package where we want to apply loads and where we want to constraint the part or assembly. We are assuming the factor of safety 2 for loading. we will operate the fixture at 50kN load so we are considering here 100 kN load. This tensile load is applied at top of the upper frame part. The bottom of the Base part is kept fixed. The motion of the other parts of assembly is constrained with the help of suitable connector elements e.g. translational, revolute, cylindrical joints.

Processing (Analysis)

The finite element objects like stiffness, force vectors, matrices etc. are computed in the processing section, boundary conditions are enforced and the solution of the system is found. This is a background process and user do not have to deal with it. Processing time depends upon the complexity of the problem and no. of meshed elements.

Linear Equation Solver Type

DIRECT SPARSE is the algorithm method used by the solver of Abaqus software by default to solve the linear equations. This solver extract the solutions by solving multiple linear equations simultaneously with the help of matrices. Master stiffness equation is

$$\mathbf{Ku = f}$$

Where **K** is the master stiffness matrix, **f** the vector of node forces and **u** the vector or node displacements.

The equation is solved for deformations. Using the deflection values, stress, strain, and reactions are calculated. All the results can be used to plot graphic plots and charts.

Kinematic Simulation of Fixture

The kinematics simulation of fixture is done by a MBD module (Rigid Dynamics) of software Ansys Workbench 15.0

All the links of mechanism were defined with respect to each other with the help of connectors. As basic connectors used in the fixture have been described before. These connectors provide the relative motion between the linkages in constrained manner. This was very helpful in understanding the kinematic behavior of the fixture mechanism.

Complete analysis study is done on the software Ansys workbench 15.0. Two modules of this analysis software is used for this study.

1. Rigid body dynamics
2. Flexible body dynamics

Rigid Body Dynamics (Multi Body dynamics)

The converted IGES file of the fixture is imported from solidworks to ansys workbench.

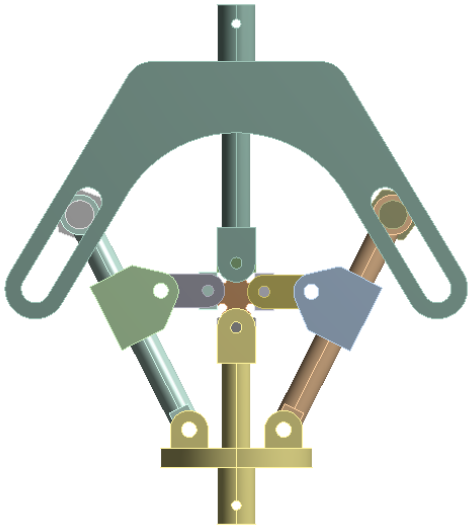

Fig 4.3: Tensile Fixture Geometry imported in Ansys Workbench

Then connections were defined between all the parts of fixture as shown further by the help of images.

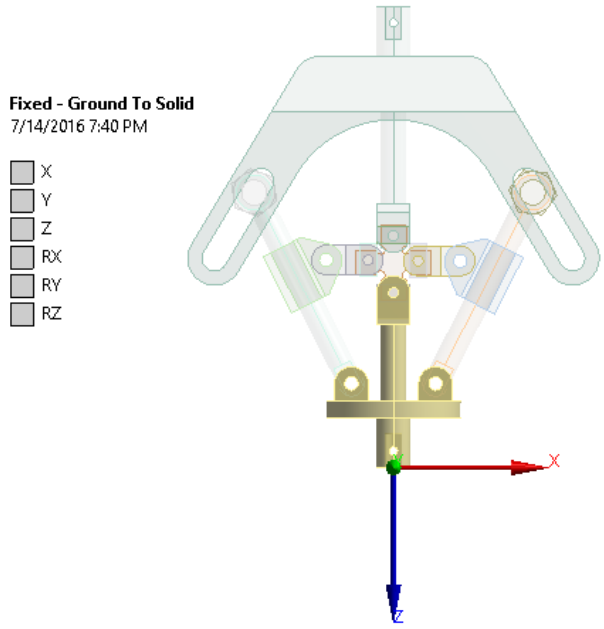

Fig 4.4: Fixed Base part

The base part will be fixed while using on the UTM machine so all the degrees of freedom of Base were constrained in the simulation shown in fig

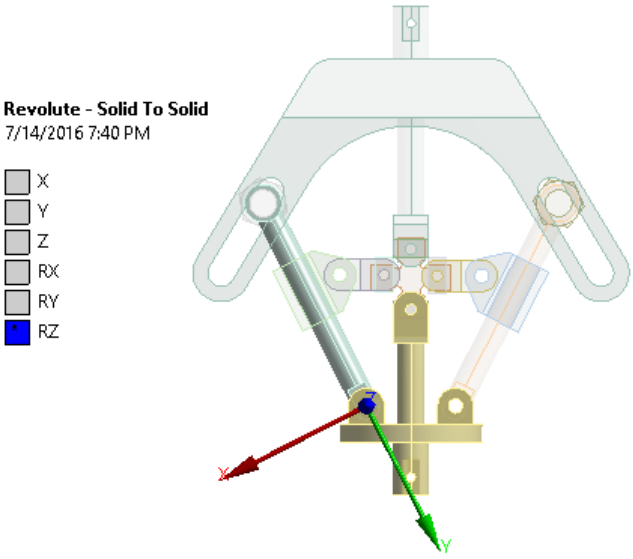

Fig 4.5: Revolute pair between the base part and rod

As we can see in fig revolute pair has been defined between base and rod. All the relative motion are constrained between them except the rotation about Z axis.

Similarly all the revolute pairs were defined which are shown in the figure below

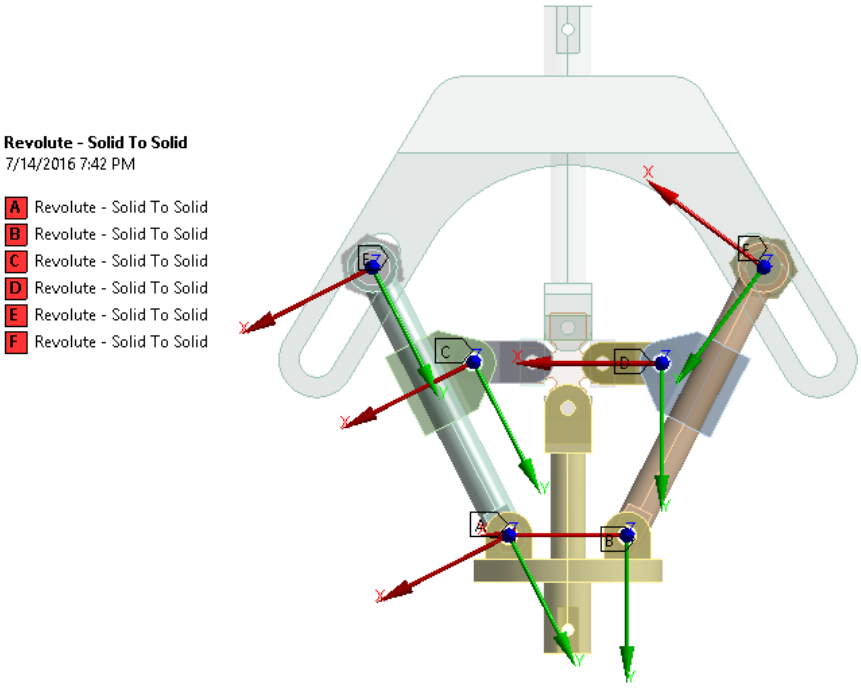

Fig 4.6: Revolute pairs defined in the fixture

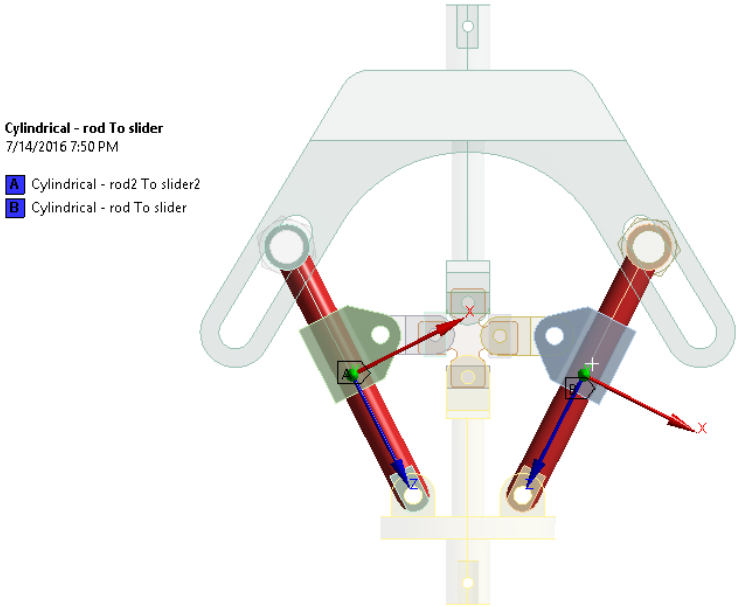

Fig 4.7: Cylindrical joints between rod and slider parts

In the cylindrical joints the slider can translate on the rods in the direction of Z axis as well as can rotate w.r.t. same axis. So these parts will help to keep the hinges in horizontal direction while they were moving on an inclined path.

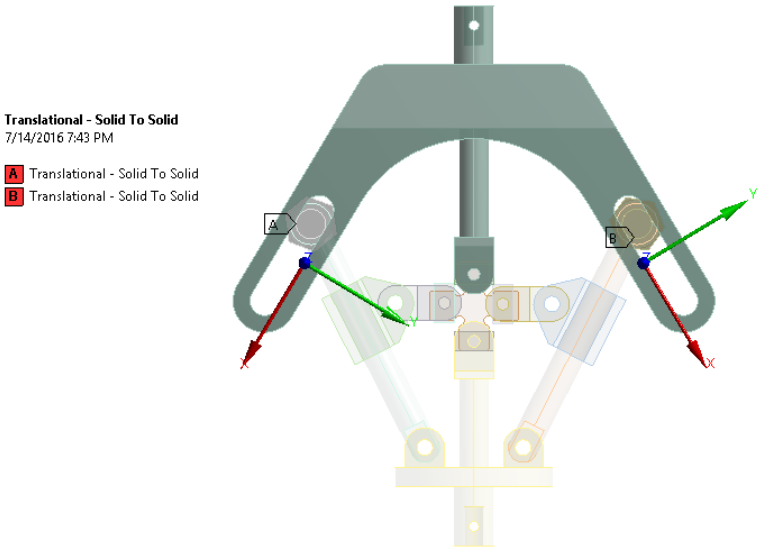

Fig 4.8: Translation motion of rollers in the slots

Translation joints are also assigned to the rollers so that they will move in the slots in the direction of X axis shown in fig.

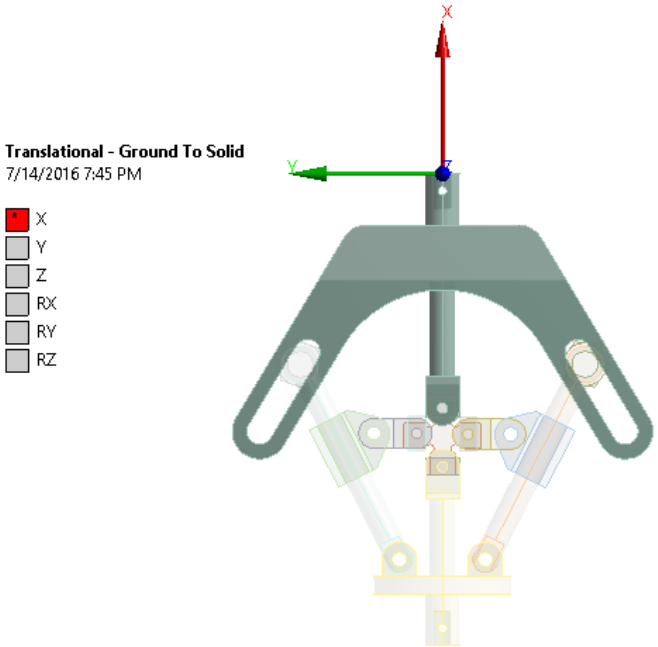

Fig 4.9: Translational joint of upper frame

A translational joint is defined to upper frame w.r.t base in the direction of X axis of local coordinate system. All other degrees of freedom are constrained in all direction.

Flexible body dynamics

Each rigid component was converted into deformable parts, assigned material properties and discretized using Finite Element Method. Deformation and stress patterns were studied then under different loading and boundary conditions. Which is described briefly further

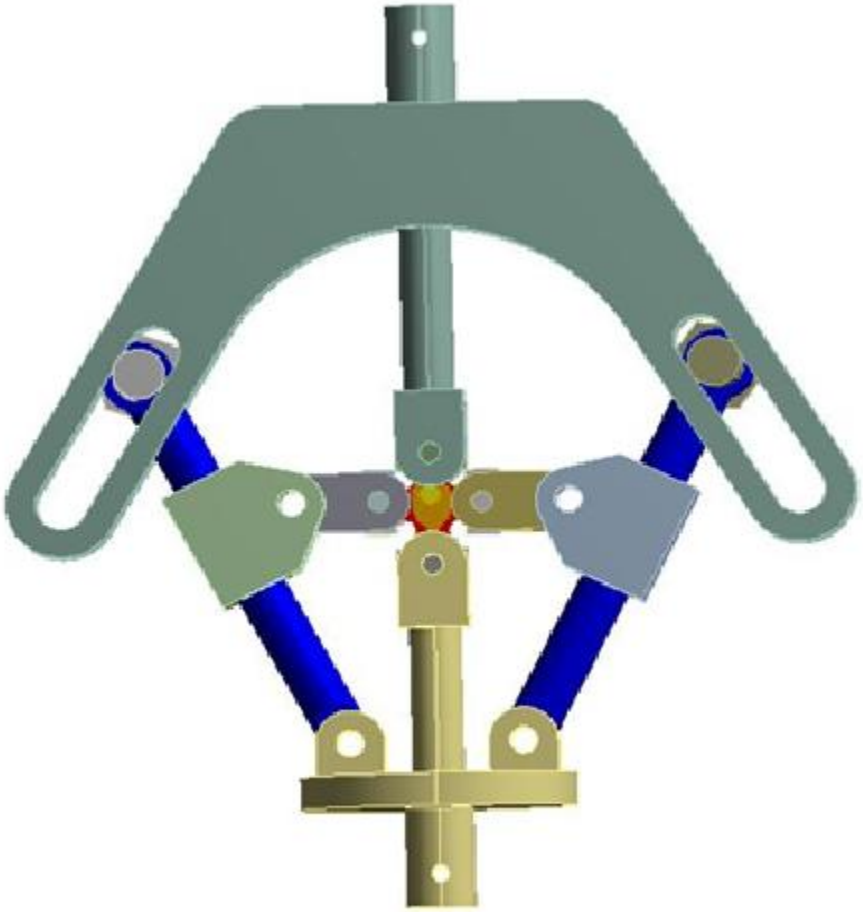

Fig 4.10: Flexible Rods

Rapid Prototyping (3D Printing)

Due to time constraint, fabrication work of actual model could not be completed so rapid prototyping was considered as an alternate option to replicate the actual model. This 3D replica will be helpful in understanding the mechanism of the biaxial fixture how it works. So below is the brief about rapid prototyping, its mechanism and details of the 3D printer used.

Rapid Prototyping and Manufacturing (RP&M) technologies have emerged for quickly creating 3D products directly from computer-aided design systems. These technologies significantly improve the present prototyping practices in industries as well as for academic purposes. 3D printing is an additive manufacturing (AM), refers to various processes used to synthesize a three-dimensional object. In additive manufacturing processing, successive layers of material are formed under computer control to create the object. These objects can be of almost any shape or geometry and are produced from digital model data 3D model or another electronic data source.

The basic process of RP&M

A part is first modelled by a geometric modeller such as a solidworks modelling software. The part is then mathematically sectioned (sliced) into a series of parallel cross-section pieces. For each piece, the curing or binding paths are generated. These curing or binding paths are directly used to instruct the machine for producing the part by solidifying or binding a line of material. After a layer is built, a new layer is built on the previous one is the same way. Thus, the model is built layer by layer from the bottom to top. In summary, the rapid prototyping activities consist of two parts: data preparation and model production.

3D Printer Used

There are several technologies available for model production based on the principle of 'growing' or 'additive machining'. We used a **Stratasys Objet30 Scholar** 3D printer as shown in figure (4.11). This 3D printer uses the material jetting mechanism and this mechanism is described further:

Fig 4.11: 3D printer used for fixture prototyping

Material Jetting

Material jetting machines utilize inkjet print heads to jet melted materials, which then cool and solidify. By adding layer on layer, the part is built. Wax materials are used with this technology. Material jetting requires support structures for overhangs, which is usually built in a different material. In this process, material is applied in droplets through a small diameter nozzle, similar to the way a common inkjet paper printer works, but it is applied layer-by-layer to a build platform making a 3D object and then hardened by UV light as shown in figure 4.12.

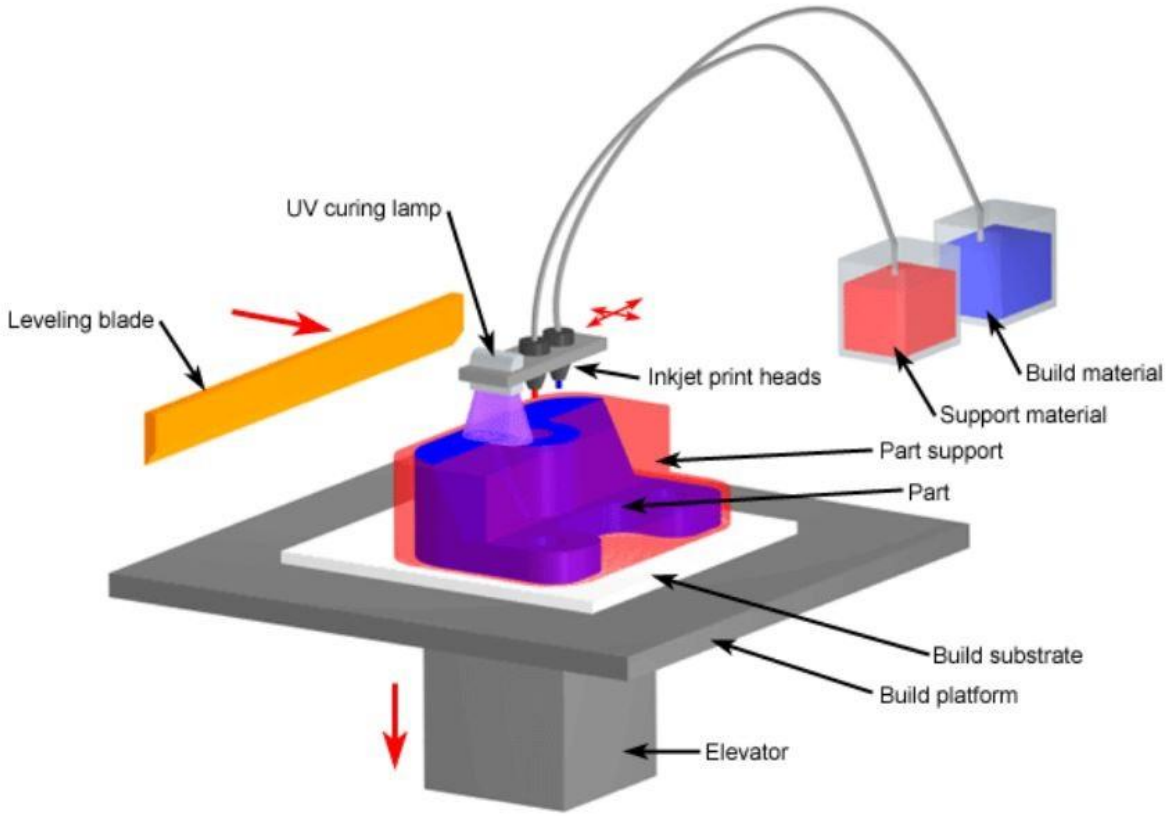

Fig 4.12: Mechanism of Material Jetting rapid prototyping

3D Printing Process

The basic process of rapid prototyping is described further with the help of flow diagram.

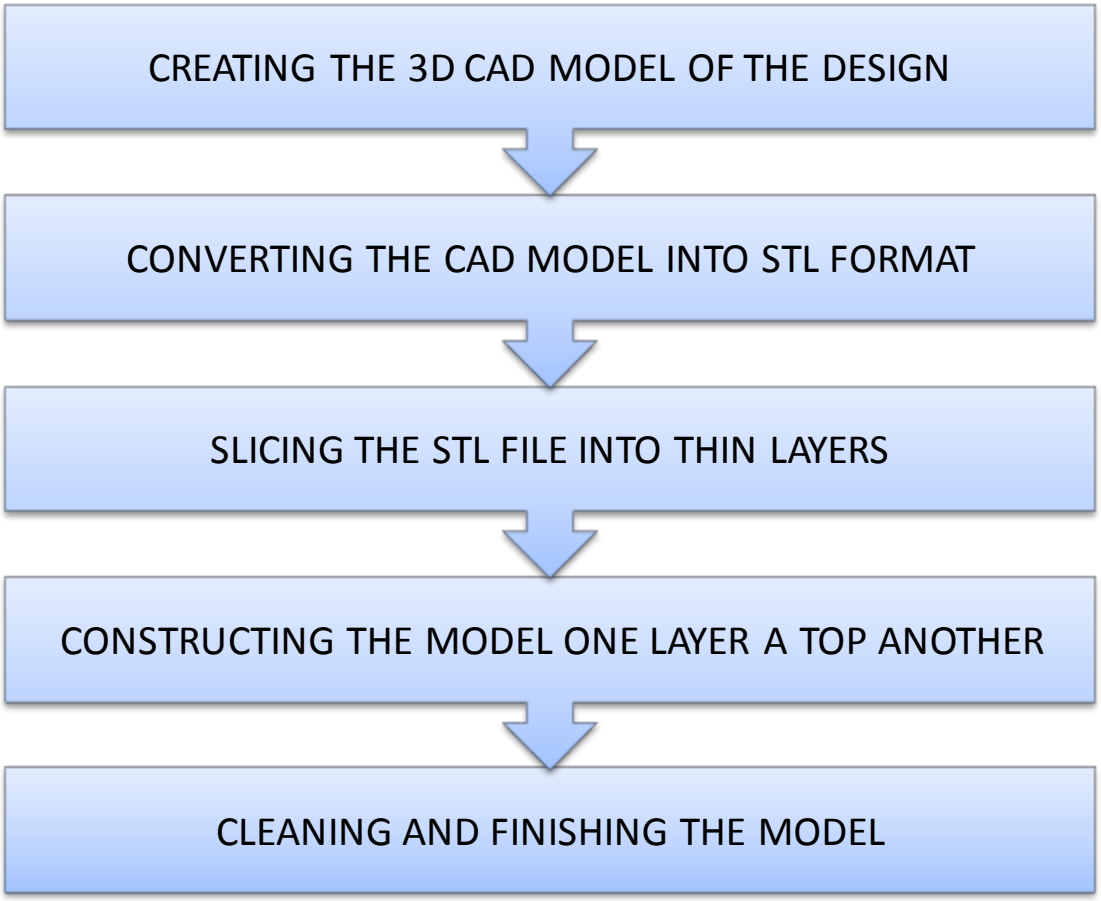

Printing of a 3D model is done from a **.STL** file. Generally, STLs are produced from a solid model obtained by conversion through a 3D modelling software.

Then STL file needs to be processed by a piece of software called a "slicer," (Objet Studio as used in our case) which converts the model into a series of thin layers and produces a G-code file containing instructions tailored to a specific type of 3D printer. This G-code file can then be printed with 3D printing client software (which loads the G-code, and uses it to instruct the 3D printer during the 3D printing process).

Printer resolution describes layer thickness and X-Y resolution in dots per inch (dpi) or micrometres (µm). Typical layer thickness is around 100 µm (250 DPI), although some machines can print layers as thin as 16 µm (1,600 DPI).

Construction of a model with contemporary methods can take anywhere from several hours to several days, depending on the method used and the size and complexity of the model. Additive systems can typically reduce this time to a few hours, although it varies widely depending on the type of machine used and the size and number of models being produced simultaneously.

Additive manufacturing can be faster, more flexible and less expensive when producing relatively small quantities of parts. 3D printers give designers and concept development teams the ability to produce parts and concept models using a desktop size printer.

Characteristics / Restrictions

- Maximal build envelope: 300 x 185 x 200 mm^3
- Minimum feature size: 0.1 mm
- Typical tolerance: +/-0.025 mm
- Minimum layer thickness: 0.013 mm

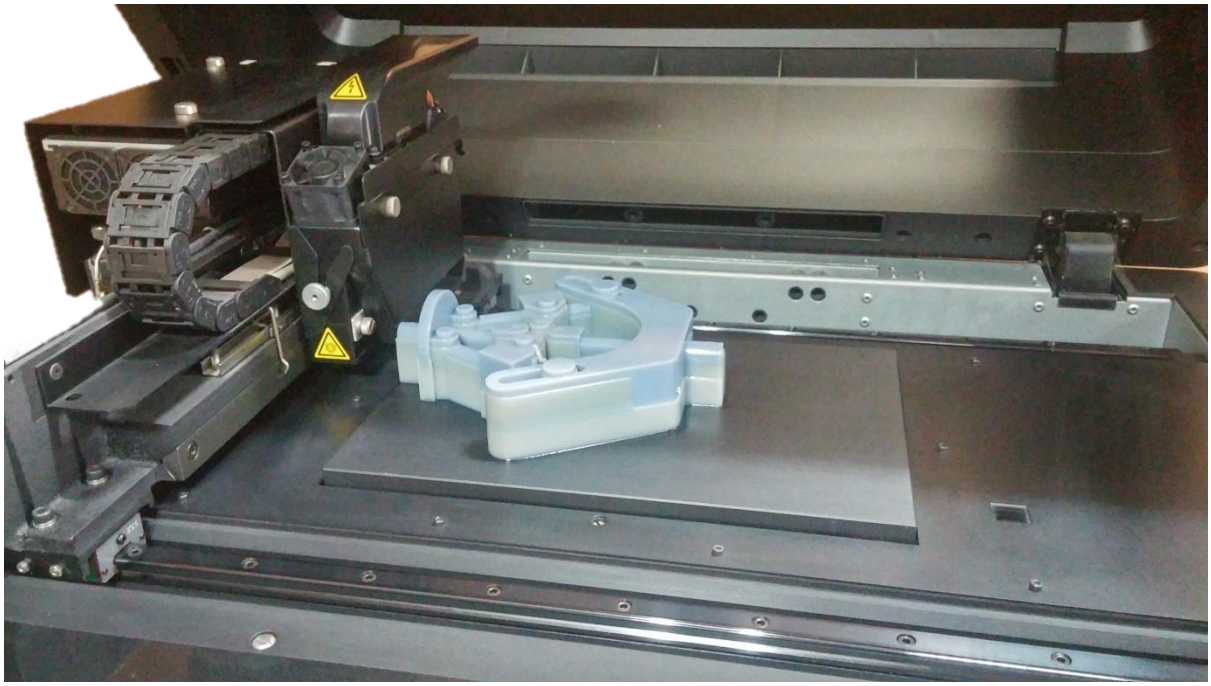

Fig 4.13: Completed 3D printed Part

Fig 4.14: Stratasys 3D printer with Cleaner

Material

There are many commercially available photopolymers. All of them are a kind of acrylate. Objet30 Scholar printer used the RGD240 grade of material provided with the printer.

Support

Because a model is created in liquid, the overhanging regions of the part (unsupported below) sag or float away during the building process. The prototype thus needs some predesigned support (Wax kind of material) until it is cured or solidified. The support can be pillars, bridges and trusses. Sometimes posts or internal honeycomb sections are needed to add rigidity to tall thin-walled shapes during the process. These additional features are built on the model parts and have to be trimmed after the model building is completed.

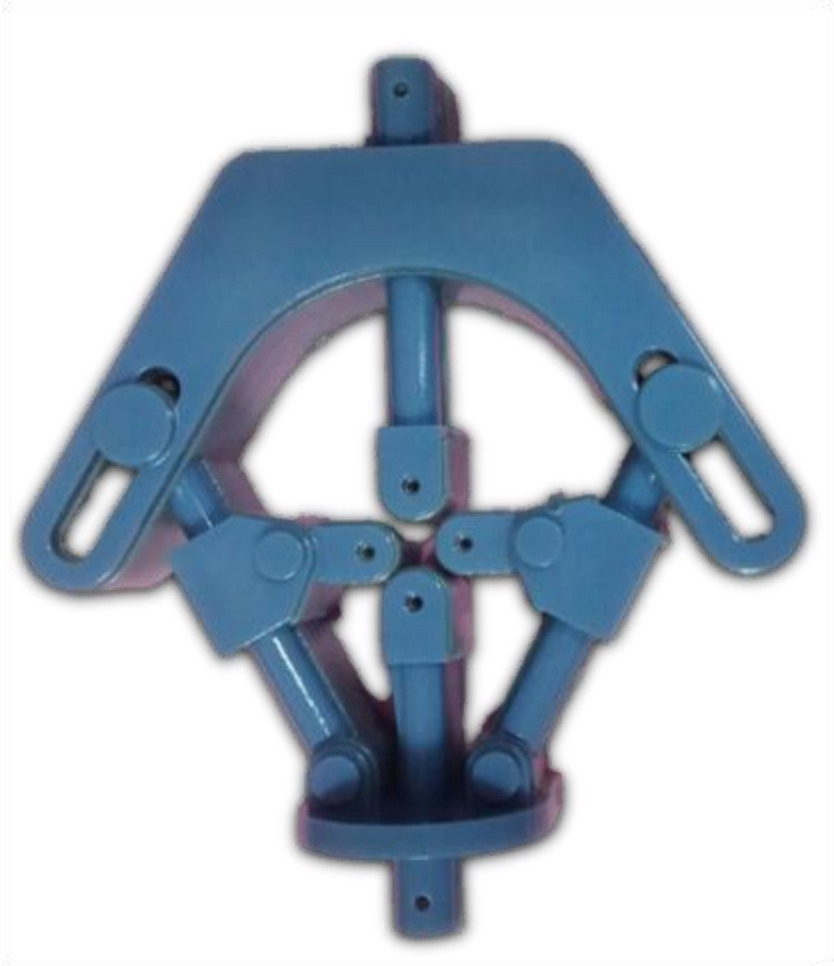

Fig 4.15: Biaxial Fixture replica by Rapid Prototyping

Job Specifications

The window shown in figure 4.16 gives the details about how much model material and support material is consumed. The number of layers in which whole job is subdivided also shown.

MATERIAL USED	MATERIAL TYPE	CONSUMPTION (GRAMS)
MAIN	RGD240	428
SUPPORT	WAX	383

Table 4.1: Material Specifications for 3D Prototyping

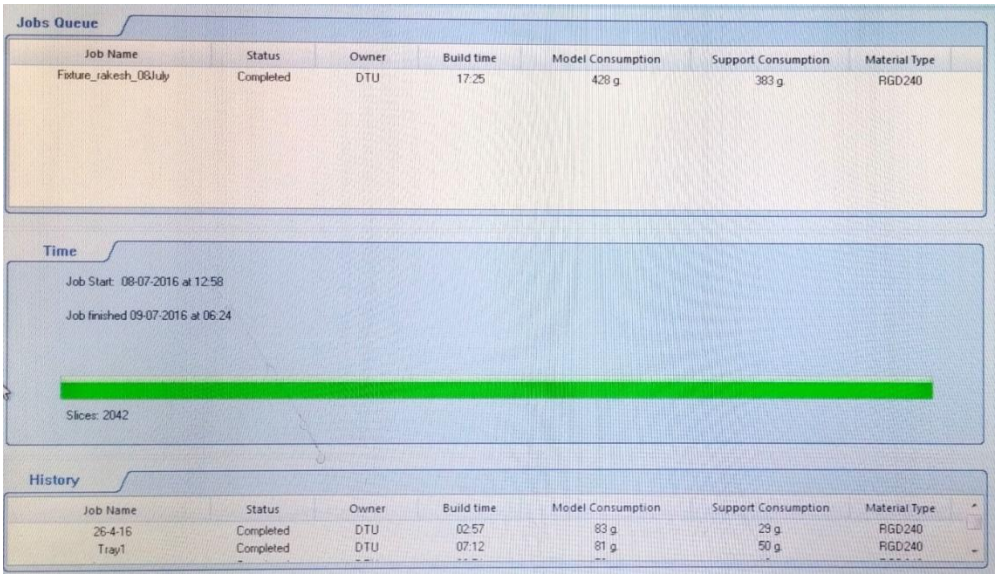

Fig 4.16: Material and layer Specifications window

Layer Thickness of Used Objet30 Scholar 3d printer

Height of The Model = 60 mm

Number of Layers = 2040

So Layer thickness = 30 µm (approx.)

General Advantages of Rapid Prototyping

- Almost any shape or geometric feature can be produced.
- Reduction in time and cost (could range 50 –90%. Wohler)
- Errors and flaws can be detected at an early stage.
- RP/RM can be used in different industries and fields of life (medicine, art and architecture, marketing)
- Assemblies can be made directly in one go.
- Material waste is reduced.
- No tooling is necessary.
- The designers and the machinery can be in separate places.

General Advantages of Rapid Prototyping

- The price of machinery and materials.
- The surface is usually rougher than machined surfaces.
- Some materials are brittle.
- The strength of RP parts is weaker in z-direction than in other.

Summary

By using Stratasys Objet30 Scholar printer we were able to replicate the fixture design successfully. A scaled (35% of actual dimensions) model was printed 3 dimensionally. And the full assembly was made directly in one go (fig 4.15).

After cleaning and finishing of the model all the joints were working properly and it can demonstrate the functional mechanism in a very simple and effective way.

Chapter 5

Results & Discussions

In previous chapter CAE was introduced. A brief description of Finite Element Analysis was given. All the boundary conditions, loading conditions, types of joints defined in analysis software package and meshing fundamentals were also described.

In this chapter results of uniaxial and biaxial testing simulation will be discussed. Firstly, the material model used for the simulation will be defined. The all properties of material used for fixture components and for Uniaxial/Biaxial testing specimen will be described. Then results of uniaxial tensile testing simulation are discussed and compared with the experimental results of aluminium specimen. After the validation of material model by uniaxial testing, results of biaxial tensile testing simulation are discussed.

Material properties

In the simulation of fixture and tensile testing two material models are used. One for the material of fixture components Structural Steel, second for the material of testing specimen Aluminium grade 1050.

Properties given to the structural steel is only elastic properties. Plastic properties are not assigned to this material because this material is used for fixture components and stresses induced in the components are only elastic and are well below the yield limit, there is no plastic deformations.

Aluminium 1050

Aluminium is assigned with elastic properties as well as plastic properties. Because in the testing specimen stresses induced will be high, they will go up to fracture point. So there will be plastic deformation as well it will attain the ultimate stress point. The plastic properties given to the aluminium is in form multilinear isotropic hardening as shown in figure (5.7). After the yielding true stress and true strain values are assigned in tabular form.

Al > Constants

Density	2700 kg m^-3

Al > Isotropic Elasticity

Young's Modulus Pa	Poisson's Ratio	Bulk Modulus (Pa)	Shear Modulus (Pa)
7.e+010	0.33	6.8627e+010	2.6316e+010

Al > Tensile Yield Strength

Tensile Yield Strength Pa
3.3e+007

Al > Multilinear Isotropic Hardening

Stress Pa	Plastic Strain mm^-1
3.3e+007	0
3.4e+007	1.e-002
3.5e+007	2.e-002
3.6e+007	3.e-002
4.5e+007	6.e-002
5e+007	8.e-002
5.5e+007	0.1
6e+007	0.15
6.9e+007	0.24

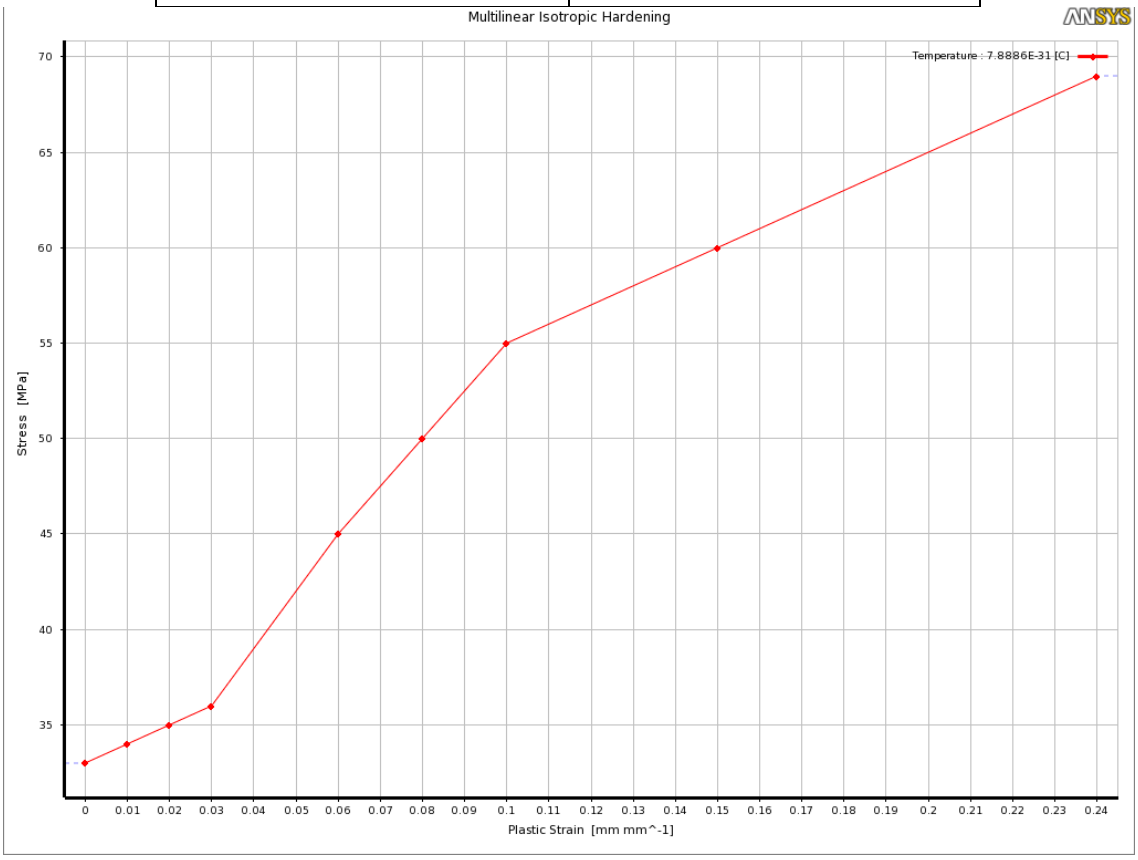

Fig 5.7: Material Properties input in Ansys (Plasticity of AL)

Al > Tensile Ultimate Strength

Tensile Ultimate Strength Pa
6.9e+007

Structural Steel

Only elastic properties were assigned to the structural steel. Because the stresses induced in the fixture parts are below the yield limit so there is no need to assign the plastic properties to the material.

Structural Steel> Constants

Density	7850 kg m^-3

Structural Steel > Isotropic Elasticity

Young's Modulus Pa	Poisson's Ratio	Bulk Modulus (Pa)	Shear Modulus (Pa)
21e+010	0.3	1.6667e+011	7.6923e+010

Structural Steel> Tensile Yield Strength

Tensile Yield Strength Pa
2.5e+008

Structural Steel > Tensile Ultimate Strength

Tensile Ultimate Strength Pa
4.6e+008

Stress and deformation contours of Each component

FEA is done of each individual component to check whether it can withstand under the loading conditions or not, also with the consideration of factor of safety.

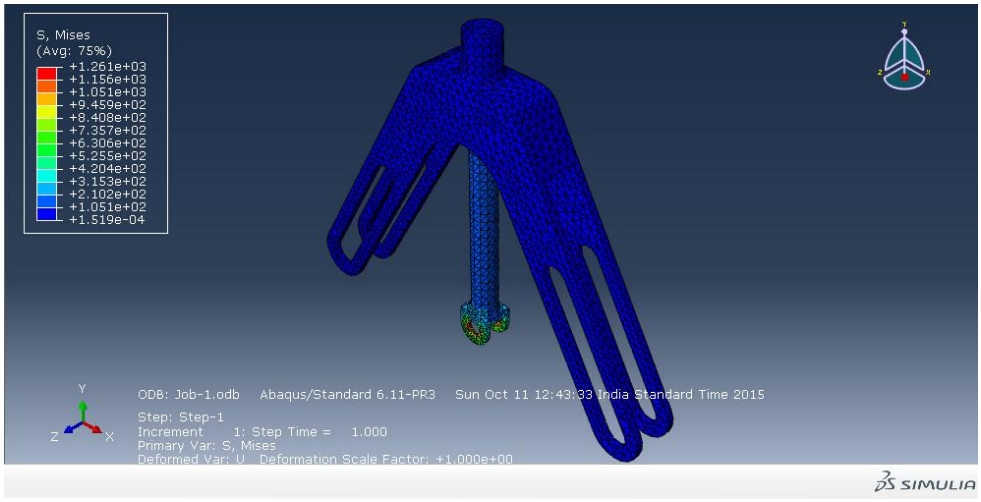

Fig 5.1: Stresses on Upper Frame

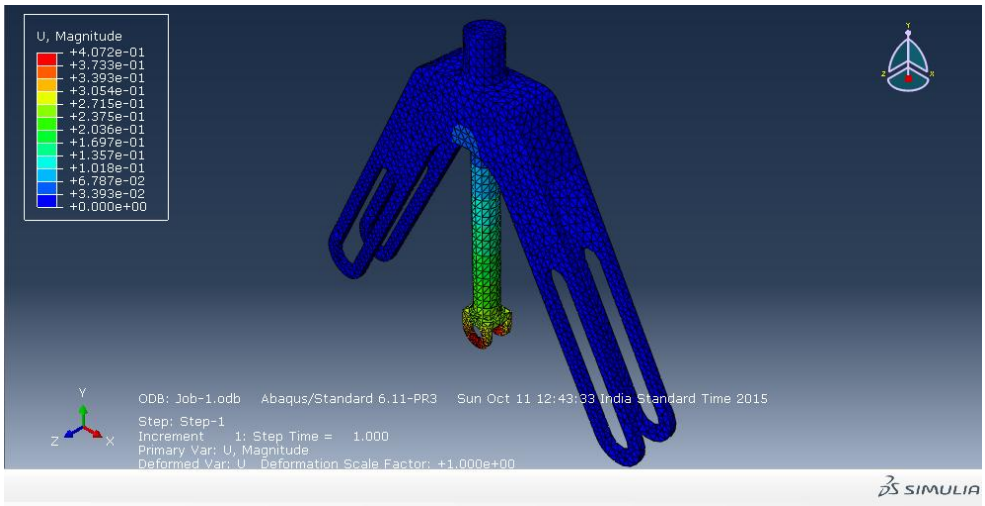

Fig5.2: Deformation in Upper Frame

Upper frame shown in Fig (5.1 & 5.2) will experience the tensile forces. And by FEA simulation we got the value 1.26 e06 Pa which is much lower than the permissible limit at which material will start yielding. So designed part can successfully hold the cruciform specimen during the tensile testing without failure.

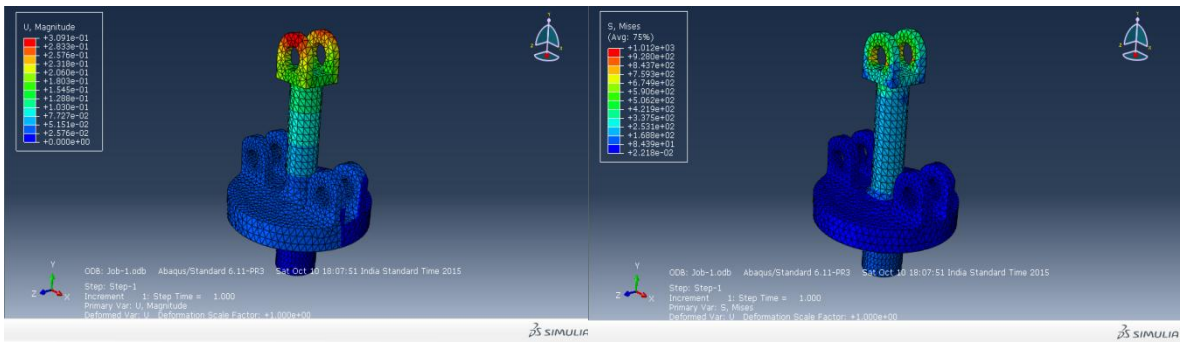

Fig 5.3: Deformation and stress of Base

Base part shown in Fig (5.3) will experience the tensile forces. And by FEA we get the value 1.012 e06 Pa which is well below the permissible limit at which material will start yielding. So designed base part will successfully hold the cruciform specimen.

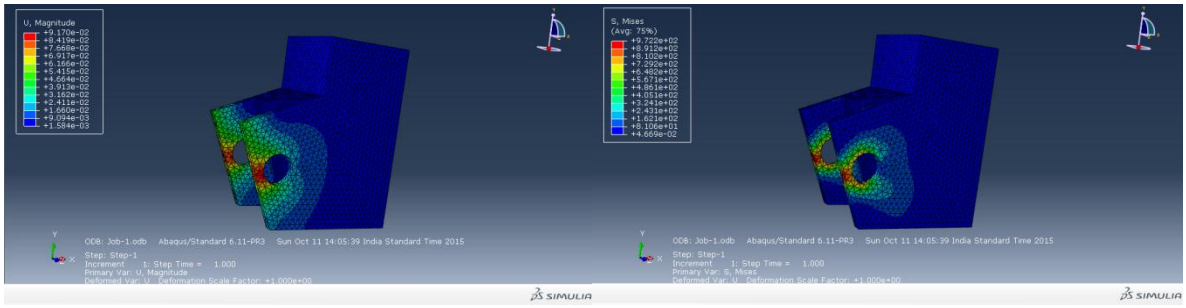

Fig 5.4: Deformation and stress of Slider

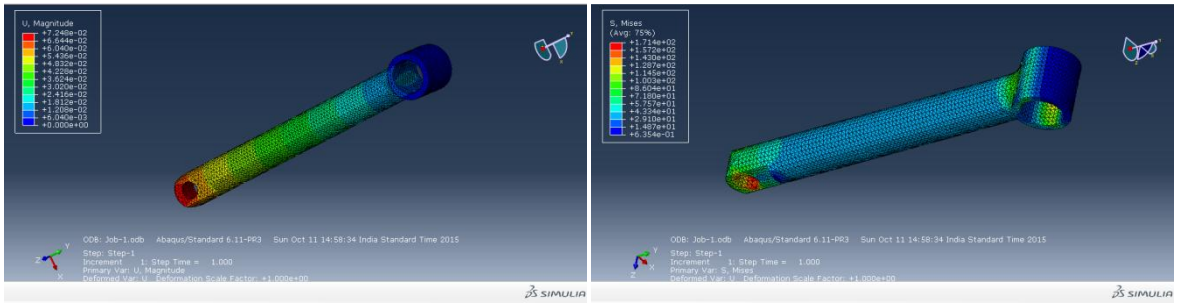

Fig 5.5: Deformation and stress of Rod

Rods (shown in fig. 5.5) connected with the base and the upper frame with the help of rollers will experience forces at both the ends. At base end it will experience tensile stress whether at the other end tensile stress as well as surface traction forces because of the

contact with rollers. As we keeping its diameter 32mm so the induced stresses will be in elastic limit and change in length will be in microns.

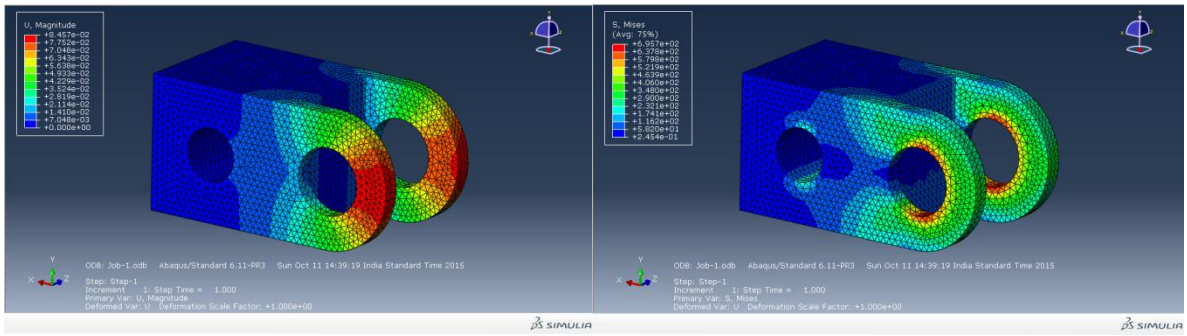

Fig 5.6: Deformation and stress of Hinge

Rollers may deform under the double shearing action of forces as they move in the cutting slots of the upper frame. After getting the results from FEA of this part, modified diameter of the roller is 32mm. Now the rollers are very much able to upholding these double shearing forces and their design will be safe.

By FEA of slider and hinge parts (shown in figures 5.4 & 5.6) we also get to know that the values of tensile stress and compressive stress due to pin are also in the permissible yielding limits.

So by doing the FEA simulation of each and every part of fixture assembly we get to know the maximum stresses and strain values they going to experience. So according to the result values we can safely design or redesign the components.

The values of the maximum Von Mises stresses and maximum deformation experienced by each component under the loading conditions is summarized below in tabular form.

PARTS	MAX DEFORMATION (MM)	MAX VON MISES STRESS (MPA)
BASE	0.309	1.012
UPPER FRAME	0.407	1.261
ROD	0.072	0.171
SLIDER	0.092	0.972
HINGE	0.084	0.696
TEST SPECIMEN	3.063	4.785

Table 5.1: Results (Deformation and Stress values) for individual components

Hence by doing the FEA of each single component we found that each designed components are safe and stresses are under the yielding limits. There will be no permanent deformations.

Uniaxial tensile test Simulation in Ansys

Uniaxial tensile testing setup is shown in figure 5.8 as simulated in ansys workbench software package. We used only two parts of the fixture Base and Upper frame. All other parts (rods, rollers, sliders and hinges) were suppressed because their contribution would be nothing on the results of uniaxial specimen. So to reduce the complexity of the model as well as simulation time remaining parts were suppressed.

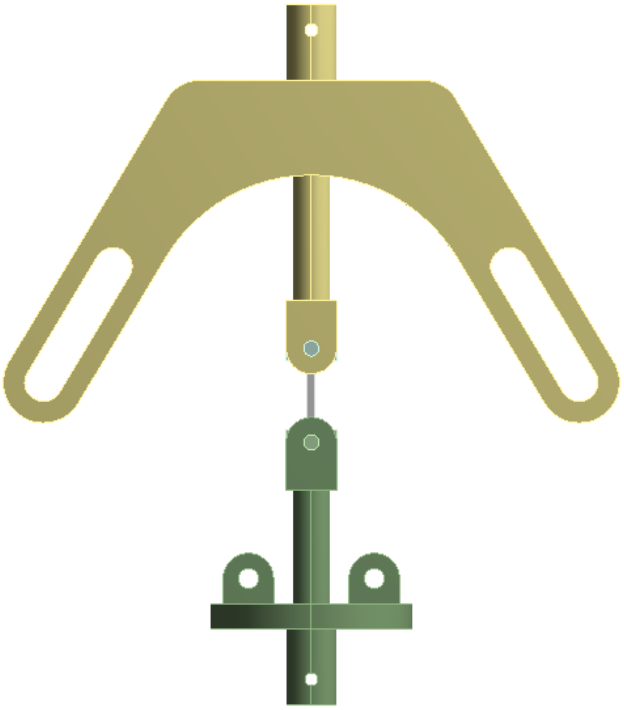

Fig 5.8: uniaxial test setup

In figure 5.9 load is shown in what way it is applied. A gradually increasing displacement was given in tabular form to the upper frame with respect to step size 1. Gradually increasing load is always better in converging the solution as compared to sudden applied in next step.

The base part was kept fixed with respect to ground. No movement is given to that as experimental condition on universal testing machine.

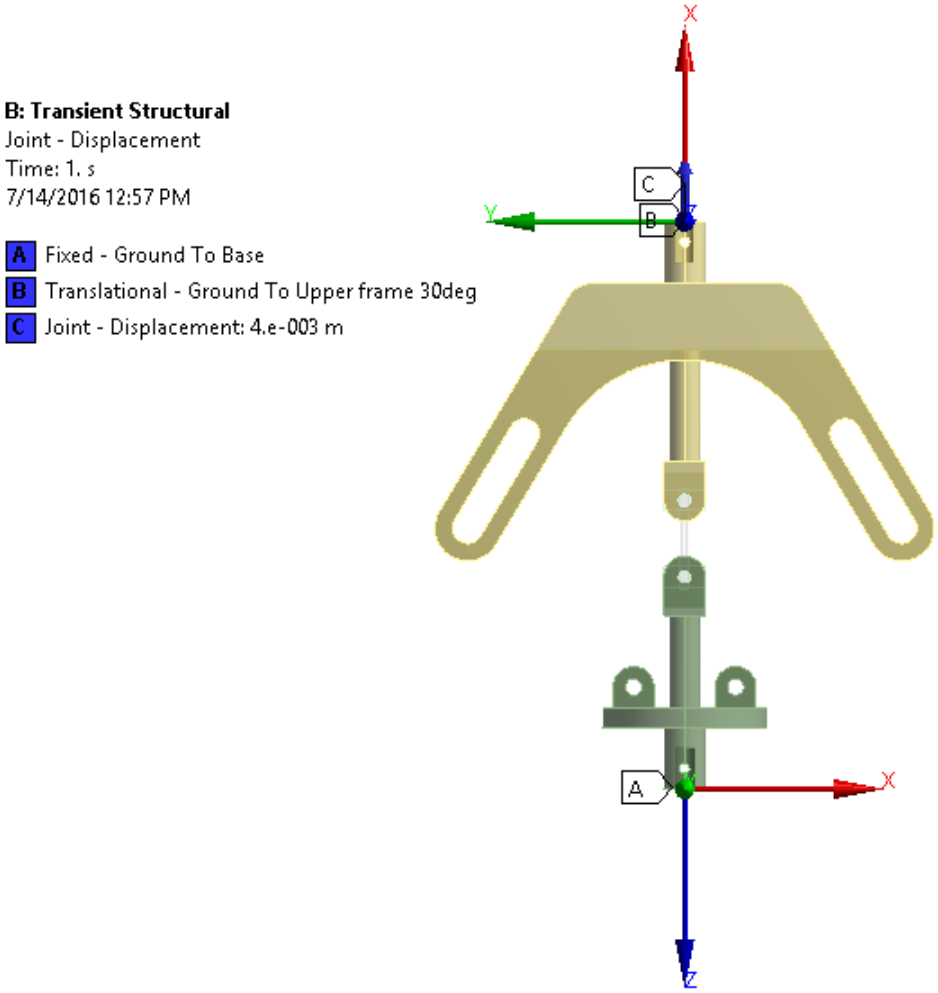

Fig 5.9: Boundary & loading conditions

The load input was given as a displacement to the upper frame. Upper frame was displaced by 4 mm in vertically upward direction. The reason of giving the input as a displacement & not giving by force is that base and upper frame are considered as rigid bodies and we cannot apply the force or pressure to the rigid bodies in ansys workbench analysis software package.

After applying the load, we simulated the setup for time period of one second for one step. It solved the setup in 198 iterations.

The results of this simulation are shown further with the help of figures.

In the figure 5.10 & 5.11 results on specimen is shown with the full setup also. The value of max equivalent Von Mises stress is 51 MPa. The critical region of the specimen for the fracture is the area shown in red color. The width of this area is kept less intentionally to focus our attention to this area only for the strength & fracture study of the material.

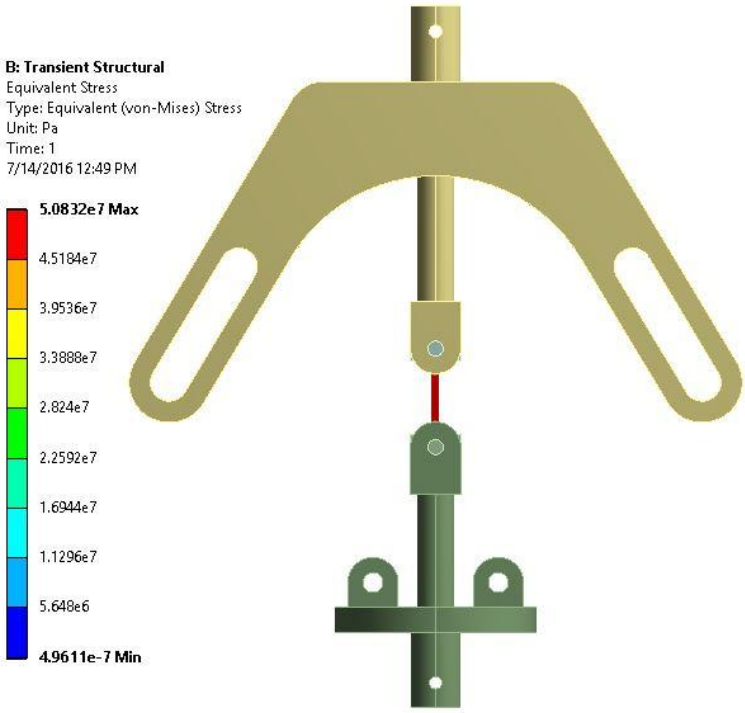

Fig 5.10: Equivalent stresses in specimen with full setup

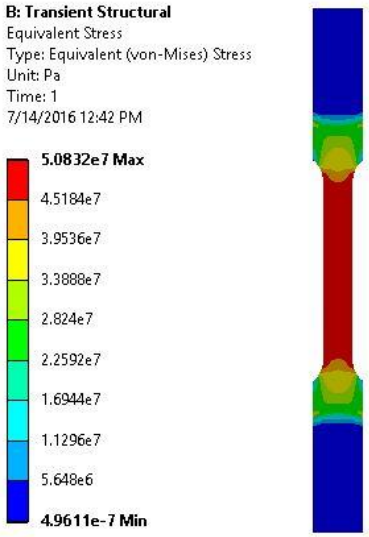

Fig 5.11: Equivalent stress in specimen

The contour plots of the equivalent elastic strain, plastic strain & total strain are also shown below in figures (5.12, 5.13 & 5.14) respectively.

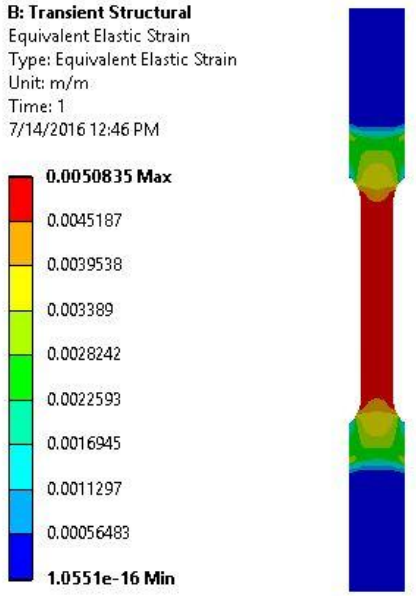

Fig 5.12: Equivalent elastic strain

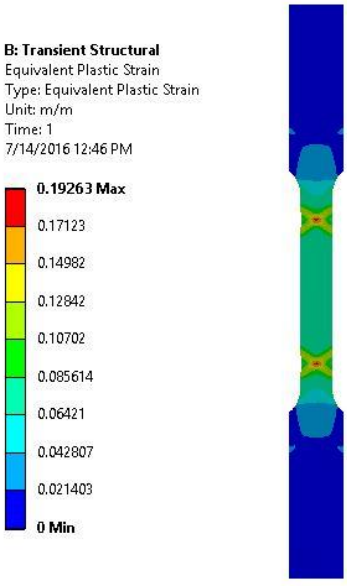

5.13: Equivalent plastic strain

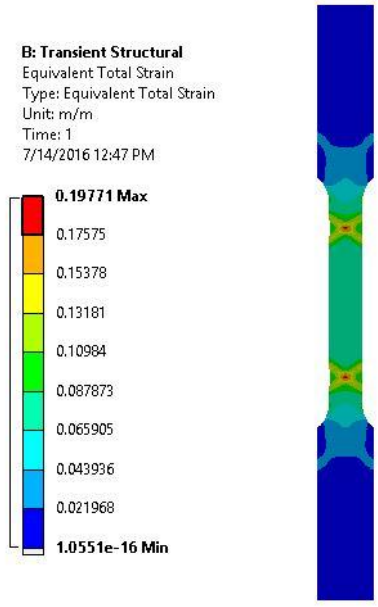

Fig 5.14: Equivalent total strain Fig

Comparison of the results of simulation and testing of uniaxial tensile testing

The results of simulation were compared to the testing results of uniaxial tensile testing of the Aluminium specimen on universal testing machine.

Experimental results

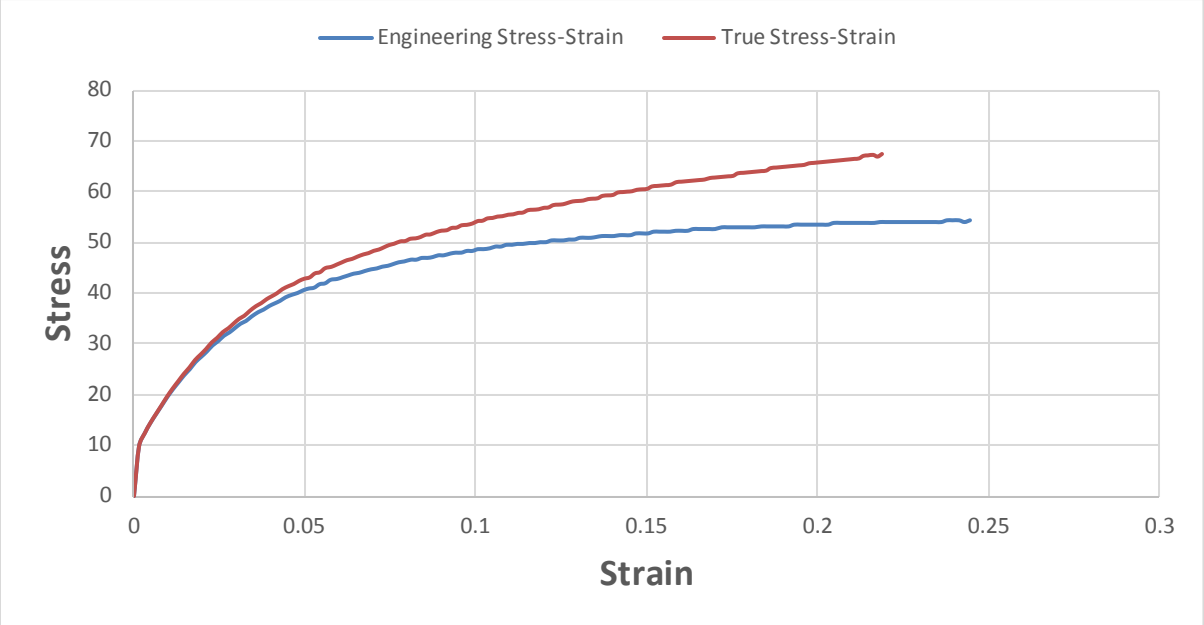

Fig 5.15: Experimental stress strain curves (nominal & true)

From testing data, we got the nominal stress strain values then with the help of those data we calculated the true stress strain values as shown in fig (5.15).

Nominal	**True**
Ultimate stress	**Ultimate stress**
54.5 MPa	68.9 MPa

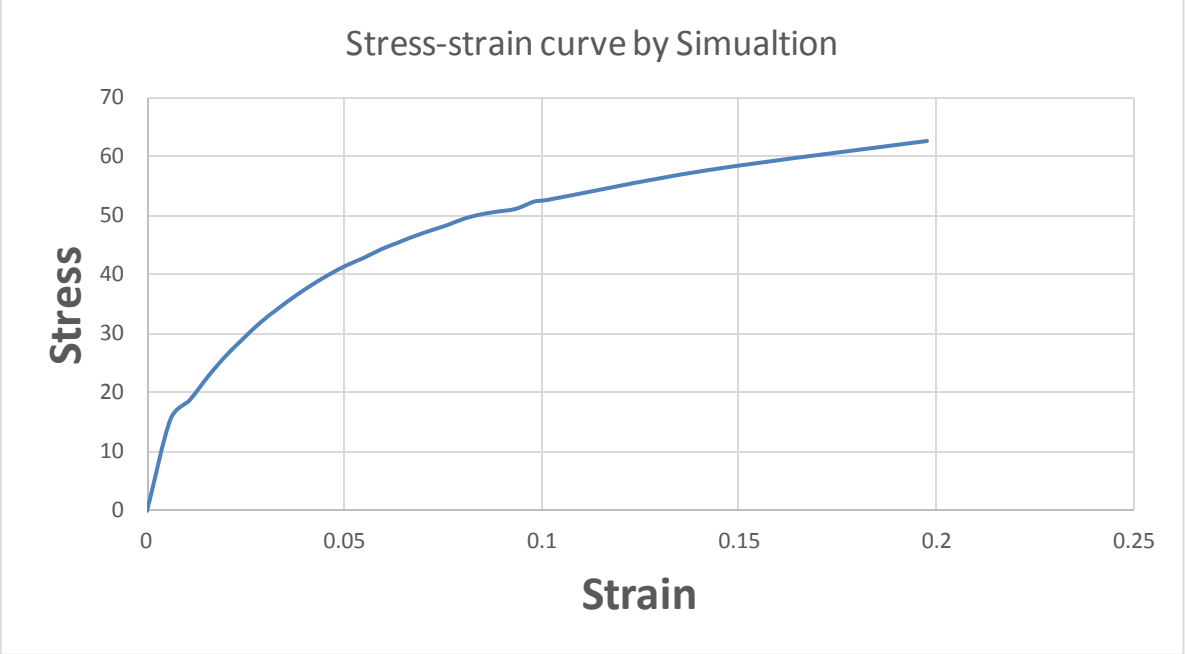

Fig 5.16: Stress Strain Curve obtained by simulation results

Stress-strain curve shown in fig (5.16) obtained by the results from the simulation of uniaxial tensile testing.

By merging these curves in a single graph we can better understand their validation.

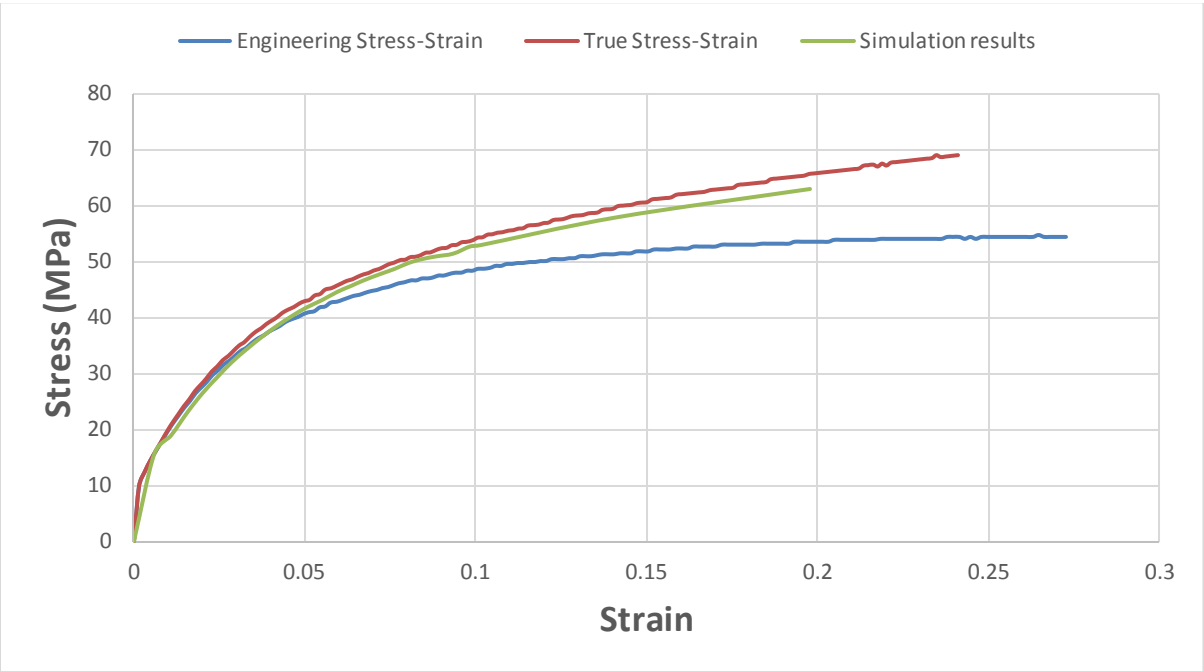

Fig 5.17: Comparison of Stress Strain curves (experimental & simulation)

Biaxial tensile testing simulation

After the validation of uniaxial tensile testing results of simulation with the testing results, we did the simulation of Biaxial tensile testing with the same material properties of Aluminium as were assigned in the uniaxial testing simulation.

Advantage of transient dynamic analysis

Transient dynamic analysis is a working module of Ansys Workbench analysis software package. In this module we can work with the both kind of bodies rigid as well as flexible simultaneously as shown in figure (5.16).

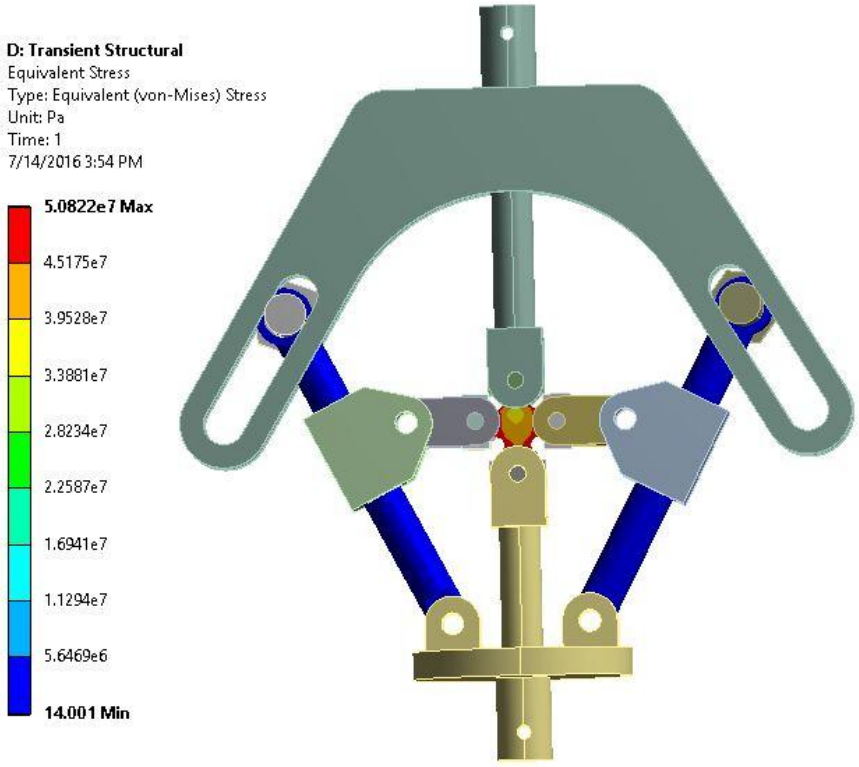

Fig 5.18: Stress contour with flexible rods only

By making certain parts flexible we can see the stress strain values on that specific part. It makes the simulation easy because less no of meshed elements & nodes will take part in result calculation and so saves our valuable time in simulation. So by using this technique figure 5.16 shows that there is no stress induced in the rods.

All the components of biaxial fixture were made flexible then (fig 5.17) and material properties of structural steel were assigned. Then at the same loading conditions we simulated the fixture. Testing specimen is assigned with Aluminium properties.

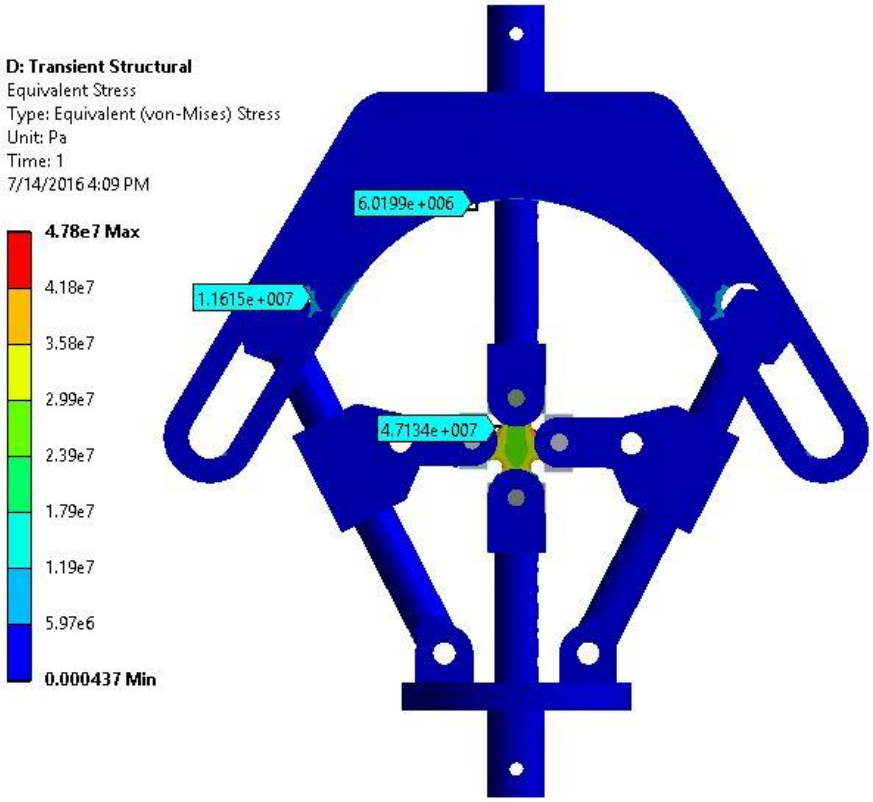

Fig 5.19: Equivalent Von Mises Stress contours of Fixture

The maximum values of stresses in the fixture components is 6 MPa & 11 MPa (shown in fig 5.17) which are very well below the yielding stress of structural steel (250 MPa). Where as in the testing specimen max equivalent Von Mises stress value 47 MPa which is above the yielding limit of Aluminium (33 MPa). So All the load is transferred to the testing specimen only.

Equivalent Elastic Strain in all fixture components is shown in figure (5.18). From the results it is evident that there is no elastic strain in the components of biaxial fixture. All the load is transferred to the cruciform testing specimen and it undergo all the deformation elastic as well as plastic depending on the loading conditions.

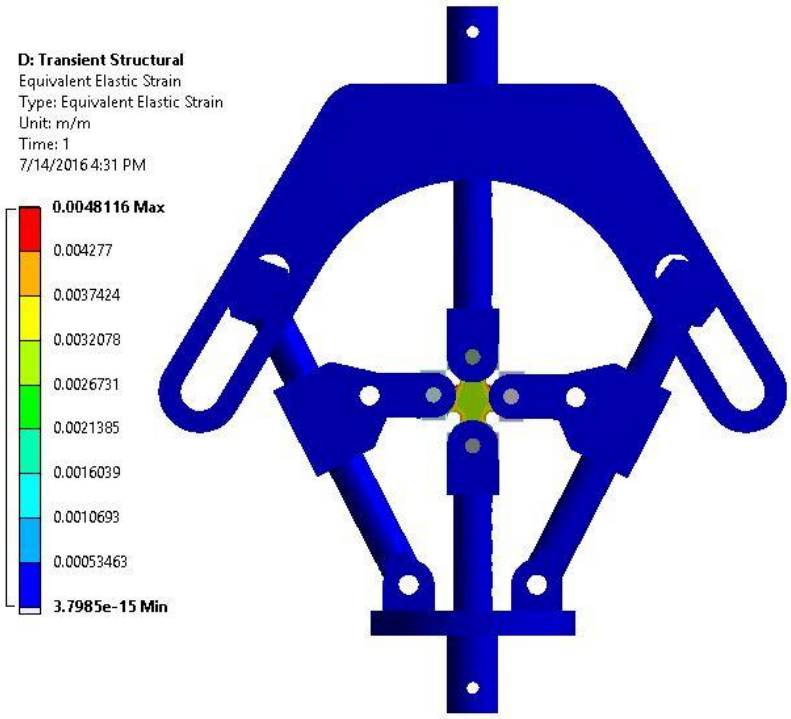

Fig 5.20: Equivalent Elastic Strain in Fixture

Stresses on cruciform testing specimen

For the biaxial tensile testing we opted a cruciform shaped specimen. Corners of the specimen were given cuts for the stress concentration in a particular region Simulations results on the cruciform testing specimen are shown further

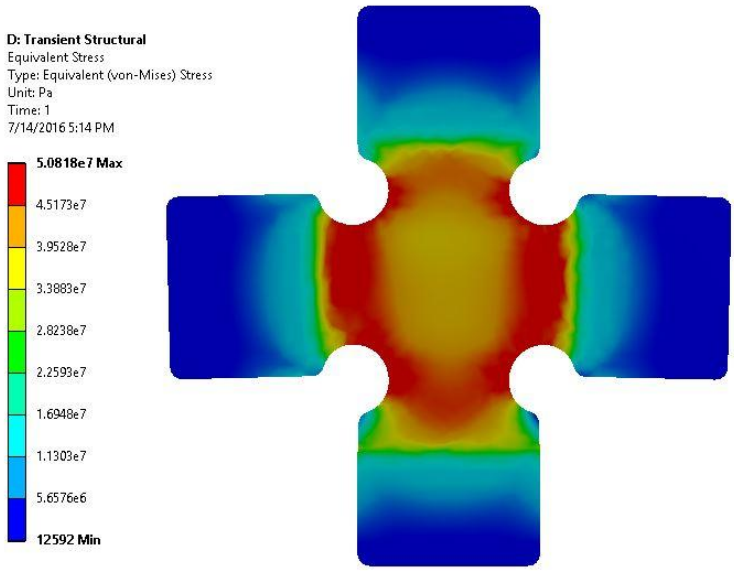

Fig 5.21: Equivalent Von Mises Stress Contour

As we can see from the stress contour (fig 5.19) the middle region is under biaxial stresses. And area shown in red color is most prominent to fracture.

The strain contours on the cruciform specimen are also shown further in fig 5.20, 5.21 & 5.22

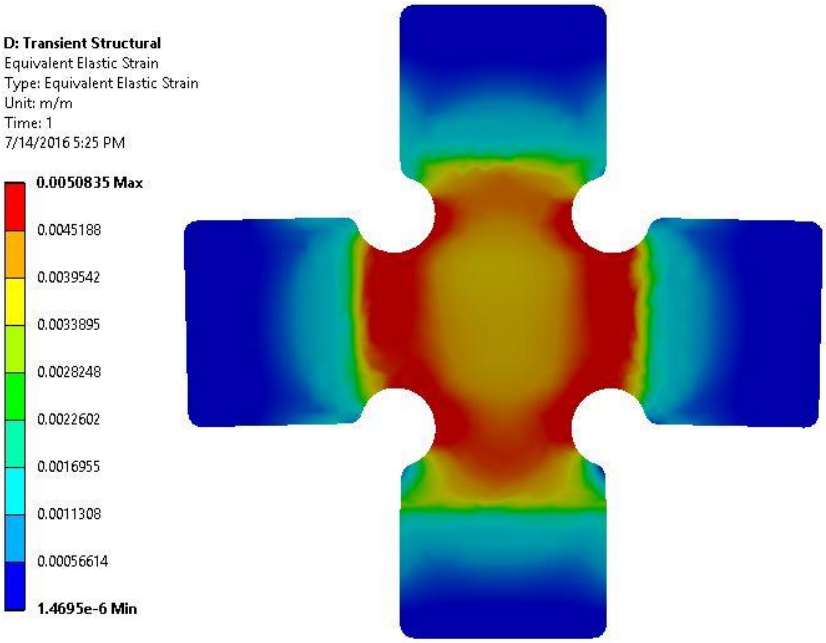

Fig 5.22: Equivalent Elastic Strain In cruciform specimen

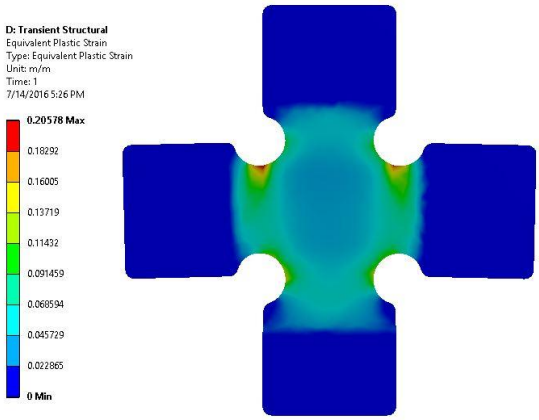

Fig 5.23: Equivalent Plastic Strain

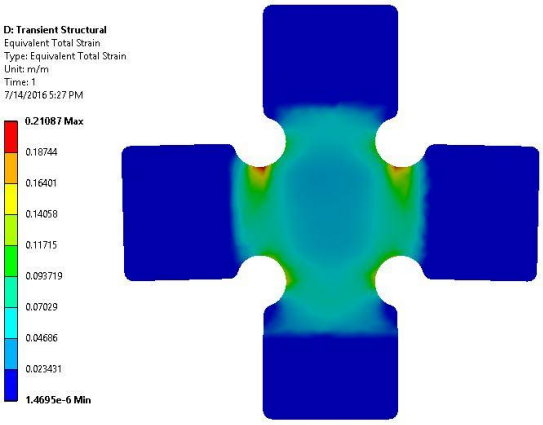

Fig 5.24: Equivalent Total Strain

Comparison of the results of uniaxial tensile testing & Biaxial Tensile testing simulation

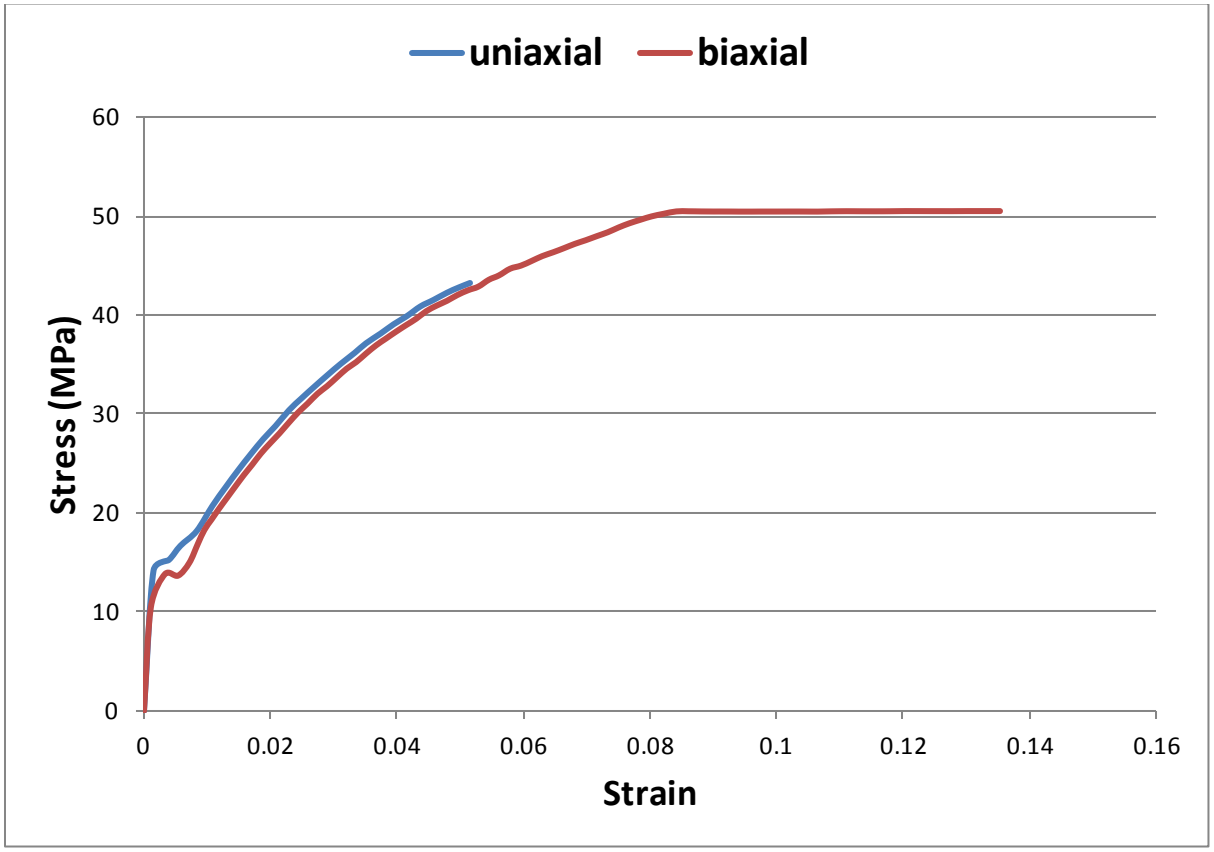

Fig 5.25: Comparison of stress-strain curves of uniaxial & biaxial tensile testing simulation

Comparison between the results of stress strain data for both tensile testing (Uniaxial & Biaxial) is shown in figure (5.25).

For the same loading condition uniaxial specimen only undergo the plastic deformation while cruciform specimen under biaxial loading deforms plastically up to fracture.

References

[1] Banabic, D. (2000). Formability of Metallic Materials, chapter 4-5. Springer- Verlag.

[2] Butuc, M., Gracio, J., and Barata da Rocha, A. (2003). A theoretical study on forming limit diagrams prediction. J. Mat. Proc. Techn., 142:714_724.

[3] Campos, H., Butuc, M., Gracio J.J.AND Rocha, J., and Duarte, J. (2006), Theorical and experimental determination of the forming limit diagram for the AISI 304 stainless steel. J. Mat. Proc. Techn., 179:56_60.

[4] Ozturk, F. and Lee, D. (2005). Experimental and numerical analysis of out-of-plane formability test. J. Mat. Proc. Techn., 170:247_253.

[5] Slota, J., Spi²ak, E., and Stachowicz, F. (2004). Investigation of biaxial stress-strain relationship of steel sheet metal. Int. J. Appl. Mech. and Eng., 9:161_168.

[6] Raghavan, K. (1995). A simple technique to generate in-plane forming limit curves and selected applications. Met. and Mat. Transactions, 26A:2075_ 2084.

[7] Foecke, T., Iadicola, M., Lin, A., and Banovic, S. (2007). A method for direct measurement of multiaxial stress-strain curves in sheet metal. Met. and Mat. Transactions, 38A:306313.

[8] Gozzi, J., Olsson, A., and Lagerqvist, O. (2005). Experimental investigation of the behavior of extra high strength steel. Soc. Exp. Mech., 45:533_540.

[9] Automotive Applications, C. (2006). Advanced high strength steel (AHSS) application guidelines. Technical report, International Iron and Steel Institute.

[10] Advanced High-Strength Steels Application Guidelines version 5.0 by World Auto Steel May 2014

[11] Gutscher, G., Wu, H.-C., Ngaile, G., and Altan, T. (2004). Determination of _ow stress for sheet metal forming using the viscous pressure bulge (VPB) test. J. Mat. Proc. Techn., 146:1_7.

[12] Liu, J., Ahmetoglu, M., and Altan, T. (2000). Evaluation of sheet metal formability, viscous pressure forming (VPF) dome test. J. Mat. Proc. Techn., 98:1_6.

[13] Ranta-Eskola, A. (1979). Use of the hydraulic bulge test in biaxial tensile testing. Int. J. Mech. Sci., 21:457_465.

[14] Rees, D. (1995). Plastic _ow in the elliptical bulge test. Int. J. Mech. Sci., 37:373_389.

[15] Josef Kana, Bohuslav Masek, Katerina Rubesova, Measuring Material Properties of Metal Foils Using Bulge Test Method, Procedia Engineering 100 (2015) 861 – 867

[16] Lee, Y.-W., Woertz, J., and Wierzbicki, T. (2004). Fracture prediction of thin plates under hemi-spherical punch with calibration and experimental veri_cation. J. Mech. Sciences, 48:751_781.

[17] Keeler, S. P.: Plastic instability and fracture in sheet stretched over rigid punches, Thesis, Massachusetts Institute of Technology, Boston, MA 1961.

[18] Hecker, S. S.: A cup test for assessing stretchability, Met. Eng. Quart. 2 (1974), 30-36.

[19] Nakazima, K.; Kikuma, T.; Hasuka, K.: Study on the formability of steel sheets, Yawata Tech. Rep. No. 284 (1971), 678-680.

[20] Hasek, V.: Research and theoretical description concerning the influences on the FLDs, Blech Rohre Profile 25 (1978), 213-220, 285-292,493-399, 617-627.

[21] M. Coleman, H.Alshehri, R.Banik, W.Harrison, S.Birosca, Deformation mechanisms of IN713C nickel based super alloy during Small Punch Testing, Materials Science & Engineering A650 (2016) 422–431

[22] J Y Jeon, Y J Kim, J W Kim, S Y Lee, Possibility to Estimate Fracture Toughness of Ductile Steel Materials from Small Punch Test Data, Procedia Engineering 130 (2015) 1029 – 1038

[23] Gronostajski, J. and Dolny, A. (1980). Determination of forming limit curves by means of marciniak punch. Mem. Sci. Rev. Metall., 77(4):570_578.

[24] Marciniak, Z., Duncan, J., and Hu, S. (2002). Mechanics of Sheet Metal Forming. Butterworth Heinemann.

[25] Marciniak, Z. and Kuczynski, K. (1967). Limit strains in the process of stretch-forming sheet metal. Int. J. Mech. Sci., 9:609_620.

[26] Demmerle, S. and Boehler, J. (1993). Optimal design of biaxial tensile cruciform specimens. J. Mech. Phys. Solids, 41:143_181.

[27] Vos, R. (2007). A computational study of biaxial sheet metal testing: effect of different cruciform shapes on strain localization. Technical Report MT 07.03, Tech. University of Eindhoven.

[28] Wu, X., Wan, M., and Zhou, X. (2005). Biaxial tensile testing of cruciform specimen for limit strain analysis by FEM. Mat. Proc. Techn., 168:181_183.

[29] Yu, Y., Wan, M., Wu, X., and Zhou, X. (2002). Design of a cruciform biaxial tensile specimen for limit strain analysis by FEM. Mat. Proc. Techn., 123:67_70.

[30] A. Smits, D. Van Hemelrijck, T.P. Philippidis, A. Cardon, Design of cruciform specimen for biaxial testing of fibre reinforced composite laminates, Composites Sci. Technol. 66 (2006) 964.

[31] Rui Xiao, Xiaoxing Li, Lihui Lang, Yangkai Chen, Yulong Ge (2015), Design of biaxial tensile cruciform specimen based on simulation optimization, *2nd International Conference on Machinery, Materials Engineering, Chemical Engineering and Biotechnology (MMECEB 2015)*

[32] Yong Y. Min W. Xiang-Dong W. Xian-bin Z.: Design of a cruciform biaxial tensile specimen for limit strain analysis by FEM. Journal of Materials Processing Technology, 123: 64-70, 2002.

[33] Gerard Quaak (2008). Biaxial Testing of Sheet Metal: An Experimental-Numerical Analysis, U/e Master Thesis May 2008

[34] Boehler, J., Demmerle, S., and Koss, S. (1994). A new direct biaxial testing machine for anisotropic materials. Exp. Mech., 34:1_9.

[35] Hannon, A. and Tiernan, P. (2008). A review of planar biaxial tensile test systems for sheet metal. J. Mat. Proc. Techn., 198:1_13.

[36] Muzyka, N. (2002). Equipment for testing sheet structural materials under biaxial loading. part 2. testing by biaxial loading in the plane of the sheet. Strength of Materials, 34:206_212.

[37] Naresh Bhatnagar, Rakesh Bhardwaj, Palani Selvakumar, Mathias Brieu, Development of a biaxial tensile test fixture for reinforced thermoplastic composites, Polymer Testing 26 (2007)

154–161

[38] M. Brieu, J. Diani, and N. Bhatnagar, A New Biaxial Tension Test Fixture for Uniaxial Testing Machine—A Validation for Hyperelastic Behavior of Rubber-like Materials, 2007 Journal of Testing and Evaluation, Vol. 35, No. 4

[39] Henning Seibert, Tobias Scheffer, Biaxial testing of elastomers – Experimental setup, measurement and experimental optimisation of specimen's shape, ResearchGate, Jan 2014

[40] Tadros, A. and Mellor, P. (1977). An experimental study of the in-plane stretching of sheet metal. Int. J. Mech. Sci., 20:121134.

[41] Xiang-Dong Wu, Min Wan, Xian-Bin Zhou, Biaxial tensile testing of cruciform specimen under complex loading, Journal of Materials Processing Technology 168 (2005) 181–183